QUANTIFYING BOTTOMLAND HARDWOOD FOREST AND AGRICULTURAL GRASSLAND EVAPOTRANSPIRATION IN FLOODPLAIN REACHES OF A MID MISSOURI STREAM

A Thesis presented to the
faculty of the Graduate
School at the University of
Missouri-Columbia

In Partial Fulfillment of the
Requirements for the Degree
M. S. Natural Resources,
Water Resources Emphasis

---

by

Keith Brown
Dr. Jason Hubbart, Thesis Supervisor
December, 2013

The undersigned, appointed by the dean of the Graduate School, have examined the thesis entitled

QUANTIFYING BOTTOMLAND HARDWOOD AND AGRICULTURAL GRASSLAND EVAPOTRANSPIRATION IN FLOODPLAIN REACHES OF A MID MISSOURI STREAM

presented by Keith Brown,

a candidate for the degree of Master of Science,

and hereby certify that, in their opinion, it is worthy of acceptance.

Dr. Jason A. Hubbart

Dr.Chung Ho-Lin

Dr. Neil Fox

DEDICATION

I would like to dedicate this thesis to my parents for their love and support throughout my life. I appreciate the willingness they have shown me in pursuing what interests me in life and I know I would not be accomplishing this today without their support and encouragement.

ACKNOWLEDGMENTS

I would like to thank my advisor, Dr Hubbart for his guidance and support throughout my thesis research and graduate courses. I appreciate his insights into the physical processes at work in my research. Furthermore, I would like to thank Dr Hubbart and all interdisciplinary hydrology members for their contributions to my thesis research, including establishing an excellent site within the Hinkson Floodplain. Special thanks are extended to Edward Bulliner and Pennan Chinnasamy for their assistance establishing and maintaining equipment in the field.

I would also like to thank my committee members, Dr Fox and Dr Lin for their support and encouragement during my thesis research. I would like to extend thanks to the University of Missouri and the Forestry department for providing me the opportunity to pursue graduate education. Special thanks to Dr Pallardy for supplying me with the Baskett area Ameriflux data. Thanks also to Dr Guinnan for maintaining Sanborn Field climate data for public use and directing me to HARC pan evaporation data. I would also like to extend thanks to Dr Larsen for assisting me with forest inventory equipment and to Dr Stephan of Lincoln University for all of her help with vegetation survey planning and plant identification.

TABLE OF CONTENTS

LIST OF FIGURES

Figure Page

LIST OF TABLES

Table Page

Quantifying bottomland hardwood forest and agricultural grassland evapotranspiration in floodplain reaches of a mid Missouri stream

Keith Brown

Dr. Jason Hubbart, Thesis Supervisor

ABSTRACT

Bottomland hardwood forests (BHF) play an important role in floodplain dynamics, particularly along urban streams where flood mitigation is critical to protecting human life and property. Enhanced evapotranspiration (ET) of riparian floodplain forests could help reduce flooding through drying of soils and improved absorption of overland flows. Quantifying BHF ET is essential for characterizing hydrological benefits of riparian forest consumptive water use. A bottomland hardwood forest (BHF) and Agricultural Grassland (AG) were instrumented with microclimate stations and WY 2012 ET was estimated six out of seven methods of ET calculation show higher rates of ET in BHF than AG, within the Hinkson Creek Floodplain. Widely applied methods of ET calculation estimated BHF ET to be from 802mm yr^{-1} (P-M) to 975mm yr^{-1} (SEB). Agricultural grassland site ET values were estimated to be 720mm yr^{-1} (SEB) and 719mm yr^{-1}(P-M). The difference of these ET estimates between the BHF and AG sites respectively yield an additional 83mm yr^{-1} to 255mm yr^{-1} of soil moisture consumed. Coupled with the increased infiltration capacity of forest soils the enhanced evapotranspiration of bottomland forests could play a role in ameliorating flood events.

CHAPTER I:

INTRODUCTION

Riparian ecosystems provide an interface between terrestrial and aquatic environments (Corenblit et al., 2009, Nilsson and Svedmark, 2002, Gregory et al., 1991). Forested riparian areas form a contiguous zone alongside stream reaches that, if managed properly, are capable of buffering streams from the inputs of sediment and excess nutrients associated with urban development and agricultural runoff, while providing corridors for movement of wildlife (Sweeney et al., 2004). Many riparian areas also function as floodplains, providing space for floodwaters to spread and slow, limiting the impacts of flooding for downstream communities (Neary et al., 2009, Tabbachi et al., 2000).

The expansion of cities to accommodate human population growth has led to habitat degradation of riparian zones in urban watersheds (Song et al., 2012, Pataki et al., 2011, Pouyat et al., 2002). Urban development typically includes removal of forest canopy and the establishment of impervious surfaces, leading to alterations in local hydrology (Kim et al., 2011, Reichold et al., 2010). Watersheds undergoing rapid urban growth often exhibit rapid runoff of storm waters and flashy hydrographs (Cea et al., 2010). Excessive stormwater runoff can lead to channel erosion (Tillinghast et al., 2011), incision (Hardison et al., 2009), pollutant transport (Berretta et al., 2007), sedimentation

of streambeds (Rossi et al., 2013) and flooding (Popovska et al., 2010, Freni and Oliveri, 2005). It has been suggested that intact floodplain ecosystems, that include mature riparian forests, may play a critical role in mitigating urban storm water overflows (Hubbart et al., 2011, Matteo et al., 2006).

Extensive reforestation of floodplains has been proposed to restore the many ecosystem services provided by riparian forests (Hubbart et al., 2011, Twedt et al., 2005, Stanturf et al., 2001). Ecosystem benefits from floodplain forests can include; flood attenuation (Hubbart et al., 2011, Neary et al., 2009, Ghavasieh et al., 2006, Tabbacchi et al., 2000,), wildlife habitat (Gwaze and Elliott, 2011, Newell et al., 2009), carbon sequestration (Yu et al., 2008, Giese et al., 2003), enhancement of water quality (Dosskey et al., 2010, Vidon et al., 2010), and establishment of recreational areas (Cole and Marion,1998). Quantification and comparison of evapotranspiration (ET) rates in a remnant bottomland hardwood forest and an old field grassland riparian area will enhance understanding of ecohydrological processes, specifically the consumptive use of water by plant assemblages.

Statement of Need

Evapotranspiration is a consumptive use of water that returns vapor back to the atmosphere from the soil surface via plant transpiration processes (Stannard et al., 2010, Wilcox et al., 2008, Huxman et al., 2005). The portion of annual precipitation that is not consumed through ET is available for streamflow, groundwater recharge and human use (Yeh and Famiglietti, 2009). Therefore, identifying accurate methods of estimating ET is

useful for watershed management and water resource planning. For example, computation of ET can allow for more accurate estimation of groundwater recharge and other variables considered in a watershed mass balance (Senay et al., 2011).

Bottomland hardwood forests have been shown to provide multiple benefits to wildlife (Sweeney et al., 2004) and are an integral part of ecological restoration of riparian corridors (Romano, 2010). Forest trees provide shade and biomass inputs to stream systems, but require adequate soil water for growth. The consumptive use of soil water by floodplain forests may impact hydrologic conditions in adjacent streams. Establishing estimated annual rates of ET for riparian floodplain forests will provide information for expected outcomes of large-scale reforestation and restoration projects occurring in the Mississippi river basin and quantify the benefits in terms of flood attenuation (Groninger, 2005). Similarly, validating the annual ET rates of bottomland hardwood forests can help to justify continued investments in riparian restoration projects and floodplain land conservation practices (Borders et al., 2006).

Currently there are few studies that compared ET of forested and formerly cropped riparian transitional grass sites in the Midwestern US urban areas. Marginally productive agricultural lands have been abandoned extensively in Eastern North America (Foote and Grogan, 2010) and the hydrological implications of reforestation have not been thoroughly investigated. Additionally, the role of riparian forest and grassland ET as a consumptive water use within growing urban watersheds has not been quantified. A quantitative assessment of forest and grassland ET, will improve understanding of the role of land cover types in urban hydrological cycles.

Another challenge to accurate estimation of ET rates is that many locations of interest only have basic (if any) climate station instruments (Lee, 2009). Determining a suitable method of ET estimation that does not require fully equipped and therefore costly climate station instrumentation will allow for ET estimation in remote or otherwise under-instrumented areas (Lee, 2009, Rosenberry et al., 2004).

Objectives

Given the preeding information, the overall objective of this study was to conduct a bookended case study to quantify annual ET for grassland and forested riparian reaches of an urban stream in the Midwestern United States (i.e. Central Missouri). Sub-objectives include a) using microclimate and soil moisture data from the sites to force multiple hourly ET models to estimate of annual ET (for the water year 2012) and assess accuracy between methods and b) surveying and analyzing the composition of vegetative communities located within BHF and agricultural grassland floodplain study sites c) making recommendations for future ET modelers investigating similar ecosystems.

Hypotheses

The three hypotheses investigated in this study were;

H_{1O}: Annual ET in the forest and agricultural grassland is equal.

H_{1A}: Annual ET in the forest and agricultural grassland is not equal.

H_{2O}: Annual ET estimates for all ET models are statistically equal

H_{2A}: Annual ET estimates for all ET model are not statistically equal.

H_{3O}: Empirically derived annual ET model estimates will equal annual ET estimates derived from physical process-based models.

H_{3A}: Empirically derived annual ET model estimates will not equal annual ET estimates derived from physical process-based models.

and

H_4: Vegetation diversity is equal between bottomland hardwood forest understory and riparian grassland plant communities.

H_{4A}: Vegetation diversity is not equal between bottomland hardwood forest understory and riparian grassland plant communities

CHAPTER II:

BACKGROUND AND LITERATURE REVIEW

Background

Bottomland Hardwood Forests

Bottomland Hardwood Forests (BHF) grow on alluvial soils alongside watercourses in the temperate climate zone of the Central and Southern USA (Hodges, 1997) and facilitate many ecologically significant processes. Of particular importance is the role that bottomland hardwood forests serve as forested riparian buffers (Hubbart et al., 2011). Relatively rapid growth rates and deep roots make riparian forest tree species ideally suited for capture and utilization of nutrient rich runoff (Cavalcanti and Lockaby, 2005). Due to the ample supply of nutrients and moisture, riparian areas are often the most productive sites for biomass accumulation within a given landscape (Morison et al., 2000, Chaney et al., 1990). Riparian trees also influence hydrologic processes (Naiman et al. 2010). For example, bottomland hardwood forests generally accompany soils characteristics such as lower bulk densities (less compaction) which allows greater infiltration of rainwater relative to grasslands, thereby reducing storm runoff into receiving water bodies (Hubbart et al., 2011, Wilcox et al., 2008, Huxman et al., 2005).

Bottomland hardwood forests in the USA have been greatly diminished in extent since European American settlement (Romano, 2010, Newell et al., 2009; Ullah et al., 2005). Many original bottomland hardwood forests were harvested for their timber value and cleared for planting (Twedt et al. 2006, Abernathy and Turner 1987). Within the lower Mississippi valley approximately 78% of the native bottomland hardwood forests have been removed and converted to agriculture since European American settlement (MacDonald et al., 1979). Re-establishment of these forests will accomplish multiple natural resource management goals (Hubbart et al., 2011; Kaplan, 2010; Borders et al., 2006, Groninger, 2005), including (but not limited to); storage of carbon in biomass and soils (Yu et al., 2008,Giese et al., 2003), establishing sinks for nitrogen inputs (Yu et al., 2008, Ullah et al., 2005), adding hydraulic roughness to floodplains thereby slowing floodwater velocity (Marian et al., 2009, Neary et al., 2009, Ghavasieh et al., 2006, Tabbacchi et al., 2000) and maintenance of habitat for rare and endangered species (Gwaze and Elliott, 2011, Newell et al., 2009).

Floodplain Forest Processes

Forested riparian areas act as a filter for sediments and nutrients suspended in runoff entering watercourses (Knight et al., 2010, Puckett, 2004). Newbold et al.(2010) reported that storm runoff from riparian buffers planted with grass and trees contained 43% less sediment, compared to runoff from tilled fields without stream buffers in Pennsylvania, USA. Sedimentation of streams can alter stream geomorphology and negatively affect water quality (Oswalt and King, 2005). Furthermore, increased

sediment deposition can impact the distribution and quality of aquatic organism habitat through bed aggradation and subsequent loss of pools (Sweeney et al., 2004).

Streams without adequate riparian forest cover often lack critical habitat components needed by many aquatic organisms (Sweeney et al. 2004). In contrast, streams flowing through intact riparian forests typically support healthy populations of aquatic organisms (Koehle and Adelman, 2007). Riparian forests improve aquatic conditions in a variety of ways. For instance, streamside trees provide direct shading of stream surfaces by reflecting or absorbing a portion of the incident solar radiation (DeWalle, 2010). Forest canopy coverage is correlated with cooler waters and higher dissolved oxygen content, both of which are also beneficial to resident aquatic organisms (Koehle and Adelman, 2007, Harding et al., 2006, Sweeney et al., 2004, Macdonald et al., 2003). Additionally, riparian forests provide direct inputs of biomass to aquatic ecosystems including leaf litter and large woody debris (Naiman et al., 2010, Wohl et al., 2010). It has been noted that where in-stream primary productivity is limited, inputs of forest detritus supplies critical nutrients maintaining aquatic food chains (Wipfli, 2005). Also, the recruitment of large woody debris from riparian forests improves aquatic habitat structure by providing refuge sites for organisms and altering fluvial processes (Wohl et al., 2010; Naiman et al., 2010). The overall stream channel geomorphology is influenced by riparian forests which slow waters and capture sediments during flood events, leading to the development of deeper soil profiles on floodplain terraces (Hodges 1997).

Floodplain forests also facilitate greater absorption of floodwaters through reduced flow velocities due to surface roughness features (i.e. tree stems, woody debris, microtopography) and enhanced infiltration through the abundant forest soil macropores. In addition to altering overland flows during flood events, bottomland hardwood forests have shown to transpire greater quantities of soil water than riparian grasslands (Scott et al., 2005). Drying of floodplain soils through riparian forest evapotranspiration could attenuate flooding intensity (Hubbart et al., 2011, Najvot and Sodhi, 2009, Thomas and Nisbett 2007). Drier antecedent soil conditions coupled to improved infiltration characteristics in riparian forests allows for greater infiltration of precipitation before overland flow into stream channels occurs (Wine and Zou, 2012, Neary et al., 2009, Tabbachi et al., 2000). Conceivably, reforestation and conservation of riparian forests for their ecosystem services, including consumptive water use through evapotranspiration, may improve flood management within urban areas (Hubbart et al. 2011, Wang et al., 2008).

Evapotranspiration

Evapotranspiration is defined as the phase change of water from liquid to vapor state, either from an exposed surface of soils or water (evaporation) or, by diffusion through plant stomata (transpiration) (El-Bourady, 2010). Worldwide, average evapotranspiration accounts for up to two thirds of annual precipitation (Fisher et al., 2004). Because ET consumes a considerable proportion of total precipitation, assessment

of local evapotranspiration rates is critical for accurate estimation of the water balance (Senay et al., 2011, Wilcox et al., 2008, Yeh and Famiglietti, 2008, Huxman et al., 2005). In some studies annual evapotranspiration rates were shown to be in excess of annual precipitation, indicating that groundwater is being accessed by plants during dry periods (Kochendorfer et al., 2011, Yeh and Famiglietti, 2008, Gazal et al., 2006). Many riparian forest tree species such as those within the *Populus* genus are considered facultive phreatophytes, with deep roots capable of accessing groundwater (Kochendorfer et al., 2011; Scott et al., 2008; Gazal et al., 2006, Naiman and Decamps, 1997). Phreatophytic trees may reduce the water table in floodplains through consumptive use of shallow groundwater. Reduction of floodplain water tables by forest ET provides a recharge zone capable of absorbing overbank flows and rainfall, thereby reducing flooding during critical storm events (Hubbart et al., 2011, Gribovski et al., 2008, Wilcox et al., 2008, Huxman et al., 2005, Tabacchi et al., 2000).

Annual ET rates are typically larger for woody species than grassland vegetation. In the San Pedro river basin of southern Arizona, Scott et al. (2008) used eddy covariance methods to estimate 746mm of annual ET in riparian Mesquite (*Prosopis velutina*) woodlands compared to 581mm of ET in adjacent riparian Sacaton (*Sporobulus wrightii)* grasslands in 2003. Gazal et al. (2006) used sap flow measurements and Penman-Monteith (P-M) equations to estimate 966mm of annual ET within a riparian Fremont cottonwood (*Populus fremontii*) forest also located within the San Pedro watershed. Kochendorfer et al. (2011) used eddy covariance methods to measure approximately 1095mm of ET in a riparian cottonwood (*Populus fremontii*) forest in central California.

In the Midwestern USA Irmak et al. (2012) implemented the Penman-Monteith method to calculate annual reference ET rate of 1003mm for well watered grass in Nebraska for the year 1993. Evapotranspiration rates for riparian grasses in the Midwestern US could conceivably approach the potential ET reported by Irmak et al. (2012), provided there are few soil moisture limitations and warm air temperatures during the growing season.

Given that ET plays a significant role in local hydrology, changes in land use, such as conversion of grassland to forest, can affect the amount of precipitation that is streamflow (Yeh and Famiglietti, 2008). When land cover is converted from low ET (typically grasses) to high ET (forest) vegetation, net water yield of streams may be reduced (Wilcox et al., 2008). Therefore, quantifying ET for various vegetative cover types within a watershed can provide information useful for informed water resource management decisions (Twine et al., 2004).

Validating the most accurate method for estimating evapotranspiration, while minimizing data requirements, is critical for providing useful information to land managers (Irmak et al., 2008, Rosenberry et al., 2004). Evapotranspiration may be measured directly through eddy covariance systems (Kochendorfer et al., 2011) or inferred through remote sensing imagery (Healey et al., 2011). Many other ET estimation methods have been developed, but all are based on the conservation of mass and energy. The primary mass and energy balance equations are described in the following section.

Evapotranspiration: The Mass Balance Equation Approach

ET equations are all fundamentally based on balance equations of mass or energy. Mass balance equations may be applied to account for the addition and subtraction of water within a system (Huggett 2007). Basic mass balance equations can be expressed as follows (Huggett, 2007):

$$\frac{dM}{dt} = M_{in} - M_{out} \quad (1.0)$$

Where $\frac{dM}{dt}$ is the change of mass (M) over time (t), M_{in} is mass input and M_{out} is mass output

Water budgets of streams and watersheds are governed by the principles of conservation of mass (mass is neither created nor destroyed) and also may be represented in the form of a mass balance equation. A watershed mass balance equation is expressed as follows (Dingman, 2002):

$$P + G_{in} - (Q + ET + G_{out}) = \Delta \frac{ds}{dt} \quad (1.1)$$

where, P is precipitation, G_{in} is groundwater flowing into the watershed, Q is streamflow, ET is evapotranspiration, G_{out} is groundwater seepage out of the watershed and $\Delta \frac{ds}{dt}$ is the change in storage over a given time period.

Assuming changes in net groundwater storage are negligible, a simplified water balance relationship is as follows (Scott et al., 2008; Gandhari and Mogaddam, 2011; Senay et al., 2011; Gribovski et al., 2008; Barros et al., 2011; Pan et al., 2012):

$$\Delta \frac{dS}{dt} = P - Q - ET \quad (1.2)$$

. The water balance equation can be rearranged and solved for evapotranspiration as follows:

$$ET = P - Q - \Delta \frac{dS}{dt} \quad (1.3)$$

This water balance equation is adequate for natural systems but in watersheds where human activities have altered hydrologic processes, other withdrawals, such as municipal and agricultural must be accounted for (Barros et al. 2011). Consumptive water uses for irrigation or municipalities are not included here. The water balance equation used here assumes that there are neither inputs of water from another watershed, nor any water drawn for consumption elsewhere (Chuanguo et al., 2010).

Pan evaporation techniques offer an additional mass balance method for estimating potential evapotranspiration (Abtew and Iricanin 2010). Although the limitations to evapotranspiration imposed by vegetative and soil resistance's to water diffusion are not addressed, pan evaporation methods provide an estimate of the maximum potential evaporation that could occur from the free surface of a water body. Climate variables such as vapor pressure deficits, wind speed and net radiation all influence evaporation rates from a free surface of water as measured evaporation pan (Masoner et al. 2008) and are also common forcings in many ET models. Many evapotranspiration models also include the additional resistances to movement of water across soil particles and plant tissues (Irmak et al., 2008) resulting in ET estimates that

are below potential free surface (pan) evaporation. Coefficients have been developed to model actual crop evapotranspiration from pan evaporation rates, but empirical data for forests and other non-agricultural plant communities is limited (Abdel-Waheb and Snyder, 2008)

Pan evaporation measurements require a standardized pan (US class A pan dimensions: 1.21m diameter, 0.254m height) filled with water to a measured depth and equipped with an adjacent precipitation gauge to quantify atmospheric inputs (Lim et al., 2012). Measurements of pan evaporation rates supply an estimate of free surface evaporation through application of the principles of mass balance on a small scale. Pan evaporation is calculated with the following equation (Abtew et al., 2010):

$$E_{pan} = D_{t-1} - D_t + R - L \pm \boldsymbol{\varepsilon} \quad (1.4)$$

where, D_{t-1} is the previous days measured depth(cm), D_t is the current day's measured depth (cm), R is the rainfall over the pan (cm), L is other losses from bird and animal sources (cm), and $\boldsymbol{\varepsilon}$ accounts for other errors (advected heat sources, wind obstruction, and windblown sediment accumulations).

Determining watershed scale ET is challenging when lacking sufficient data for difficult to measure variables such as groundwater seepage and storage (Senay et al., 2011). For instance, Zhu et al.(2011) showed that river stage influences groundwater depths, potentially confounding the mass balance accounting of these variables within floodplain systems. In addition to the difficulty of comprehensive groundwater and

streamflow measurements, accurate precipitation data must be collected over the entire watershed to perform an accurate mass balance analysis. Heterogeneity of precipitation, vegetation, soils, land uses and underlying geology within a watershed make it very difficult to make generalizations over a wide area (Volpi et al., 2012, Qiuhong et al., 2007). In locations with few climate stations isolated precipitation measurements may not be spatially representative of the entire watershed (Wagner et al., 2012), especially in areas with diverse topography or frequent convective storms. In many cases it may be beneficial to use surface energy balance equations (or some derivation thereof), to find ET rates and scale them up to the watershed level in order to achieve closure of the watershed mass balance equation.

Evapotranspiration: The Surface Energy Balance Approach

Evaporating surfaces exhibit lower temperatures than similar dry surfaces under the same environmental conditions, due to the removal of latent heat (energy) by water (Maes et al., 2011). The latent heat (λ) absorbed during the vaporization of water is used to break the hydrogen bonds found in liquid water, converting the water molecule to a gas (Drozdov and Vrostikov, 2000).

The relationship of ET to fluxes of both energy and mass within a system is evident, given that the latent heat (λ) required for the vaporization of water is expressed in units of energy (Joules) over mass (Kg) (Jacobs et al., 2002). Evapotranspiration rates can be estimated by isolating the latent heat energy occurring within a closed system with

known energy inputs (net radiation). This method is known as the surface energy balance equation. A simplified version of the surface energy balance equation is expressed as follows (Amiro, 2009):

$$\lambda E = R_n - G - H \quad (1.5)$$

where λE is the latent heat flux, R_n is the net radiation, H is the sensible heat flux and G is the ground heat flux (with all fluxes expressed in W m^{-2}).

Plant Transpiration

Latent heat energy is absorbed as both evaporation from free water surfaces and transpiration of water from within the stomata of plants (Maes et al. 2011). Plants take advantage of the cooling effect of evaporation by using the transpiration of water through stomata to maintain viable surface temperatures of leaves, during photosynthesis (Šír et al., 2008, Nicotra et al., 2007). During plant transpiration incident beam solar radiation that would otherwise result in increased plant surface temperature, evaporates water from the stomata surface, cooling the leaf. Leaf cooling occurs as energy is consumed to sever hydrogen bonds, initiating the water molecules to undergo phase change from liquid to vapor (Drozdov and Vostrikov, 2000). The transpiration of water from the leaf surface also creates the declining water potential gradient necessary to transport water and solutes up through the plant tissues against the force of gravity (Bond and Kavanagh, 1999;

Domec et al., 2010). During transpiration water is pulled by the forces of cohesion and adhesion, moving from high water pressure regions of the plant to replace vapor lost from the leaves by evaporation (Tyree and Sperry, 1988).

In addition to available energy, plant transpiration is also limited by the supply of moisture in the soil (Fisher et al 2005), the atmospheric vapor pressure deficit (McNaughton and Black, 1973) and by the resistances within the plant tissue itself (Steppe and Lemeur, 2007, Warring and Running, 1978). During dry weather or when soil moisture is limited plant leaf stomata may (partially) close to prevent excessive water loss (Jennerette et al., 2009, Gazal et al., 2006, Herbst, 1995). Plant leaf stomata are a critical site for both transpiration and photosynthesis (Domec et al., 2010). When stomata are open water vapor is lost to the atmosphere and CO_2 molecules diffuse in (Taiz and Zeiger 2006, Monteith 1970). Carbon dioxide molecules that enter the stomata are carboxylated upon contact with the moist surfaces ultimately providing the carbon atoms necessary for photosynthesis (Woodrow et al., 1990). Although all plants need CO_2 from the atmosphere to grow, when soil moisture is limited both transpiration and photosynthesis are reduced by the closure of leaf stomata.

Evapotranspiration Measurement and Modeling

Numerous models have been developed to estimate or measure evapotranspiration on a variety of spatial and temporal scales (Irmak et al. 2004). Small scale physical models examine the mass flux of water exiting stomata of leaves (Bond and Kavanagh 1999). At a larger scale, remote sensing technology may be utilized to apply surface energy balance calculations to estimate regional level latent heat flux (El Bourady et al. 2005). Although satellite data can provide inputs needed to calculate the surface energy balance (using infrared images to quantify sensible heat flux), data resolution may be coarse and stand or ecosystem level ET measurements by this method lack refinement necessary for small scale watershed ET estimation (Maes et al. 2011).

Other ET models such as the Priestley-Taylor and McNaughton-Black equations require varying amounts of physical and empirically derived climate variables for a given site. Temperature based ET equations such as the Blainey–Criddle , or Hargreaves and Sammani methods provide estimates of evapotranspiration using only daily mean air temperature (Irmak et al. 2004). However, those methods may be less accurate under cloudy conditions or on days with strong winds (Irmak et al. 2004). Evapotranspiration methods using measured climate variables from the site of interest such as the surface energy balance, are preferable to those which ignore critical variables (i.e. lack of wind speed or net radiation inputs in Blainey-Criddle) or substitute empirically determined values from other sites as is common in many reference ET calculations (Irmak et al.

2012, Rosenberry et al. 2004). Additional ET equations such as the Penman-Monteith method feature a combination of physically measured and empirically derived model forcings which typically supply accurate ET estimates (Akinbile and Sangodoyin 2011, Attarod et al., 2009, Lee, 2009, Fisher et al. 2005).

Highly accurate ET measurements can be calculated by eddy covariance analysis of wind vector velocity and water vapor concentration (Gu et al., 2012, Kochendorfer et al. 2011). This is possible through advancements in technology that allowed for high frequency measurement of vapor flux by infrared gas analyzers and sonic anemometers (Fisher et al. 2005). However, these systems are costly and vapor flux is difficult to quantify when air is still, as is common at night (Fisher et al. 2007).

This study will seek to provide a comparison of a suite of Evapotranspiration models using commonly measured climate variables and widely available empirical variables. The data inputs of the ET models examined range from mostly empirical (Easy Penman-Monteith, McNaughton-Black), to more physically based (Surface Energy Balance, Bowen ratio energy balance). Other methods include a combination of empirical and measured physical data. Ordered by increasing model complexity, these combination empirical/physical based ET models include: Priestley-Taylor method (based on net radiation, air temperature and an empirical coefficient), Penman-Monteith method (based on a combination of physical and empirical values) and Shuttleworth-Wallace method (calculated using several physical and empirical based data inputs). The ET equations mentioned above will be described fully later in the methods portion of this text.

CHAPTER III:

METHODS

Study Site Description

Climate stations were installed in a second growth riparian bottomland hardwood forest (BHF) and a riparian agricultural grassland (AG) floodplain (elevation 593m ASL) next to Hinkson Creek on University of Missouri property (Figure 1). Hinkson Creek is located between the Glaciated Plains and Ozark natural divisions and is classified as a Missouri Ozark border stream (Thom and Wilson, 1980). The Hinkson Creek Floodplain study site is located within the city limits of Columbia, Missouri, USA (Population 108,000:US Census, 2011). Although the immediate vicinity of the study site is only lightly developed, the watershed surrounding the study location includes some of the most high density urban areas within the Hinkson Creek drainage area (Hubbart et al., 2010). The study area reach (38°55'39"N, 92°21'05"W) of Hinkson Creek floodplain is nested between two permanent hydroclimate gauge sites that are part of a series of five nested gauge stations installed to monitor conditions in the Hinkson Creek Watershed (HCW) in 2008 (Figure 2) (Hubbart et al., 2011).

Records from Sanborn Field climate station in Columbia, Missouri (3 km distance from study site), recorded average annual air temperature of 14°C, and annual

precipitation averaging 980mm, over the past 30 years (Hubbart et al., 2011). Winter continental air masses yield approximately 508mm of snowfall annually (Nigh and Schroeder 2002). On average the wettest months are from March through June when maritime tropical and continental tropical air masses converge on the region. The growing season lasts an average of 215 days (Nigh and Schroeder 2002).

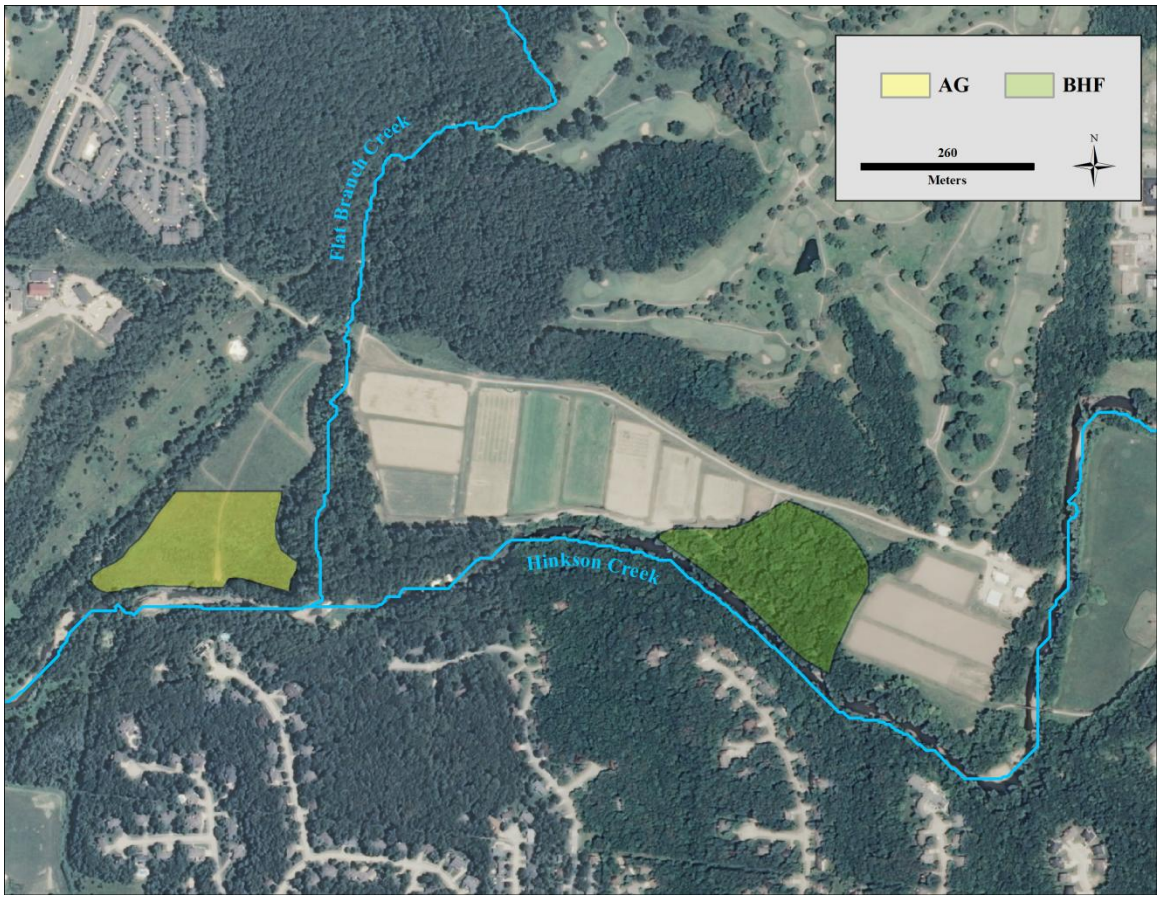

Figure 1. Aerial view of the study site with the Agricultural Grassland (AG) and Bottomland Hardwood Forest (BHF) Hinkson Creek Floodplain sites delineated, Columbia, Missouri.

Vegetation Community

The formerly cropped Agricultural Grassland (AG) site is dominated by gramminoids with an abundance of Johnsongrass (*Sorghum halepense*), and tall fescue (*Festuca arundinacea*). There is also a minor component of forbs including goldenrod (*Solidago giganteana*), and Ironweed (*Vernonia altissima).*

The Bottomland Hardwood Forest (BHF) is composed of tree species including Silver maple, (*Acer Saccharinum)*, Eastern cottonwood, (*Populus deltoides*), Boxelder (*Acer negundo*), American elm (*Ulmus Americana*), Black walnut (*Juglans nigra*) and Sycamore (*Platanus occidentalis)* (Table 3). The total basal area of the forest stand (within a fixed area plot of 80mx80m ~6400m^2) was measured as 22.71 m^2 $hectare^{-1}$ in 2010, with Eastern cottonwoods dominating the larger diameter classes (Hubbart et al., 2011). Forest composition is characteristic of a site pioneered by Cottonwood trees undergoing forest succession, with a senescent overstory and an increasing component of more shade tolerant species in the smaller size classes (Hodges, 1997).

Past and Current Site Management

The agricultural grassland (AG) site is a formerly plowed agricultural field which has been left fallow for several decades. Although row crop production has ceased, the grassland field is still mowed periodically to prevent woody vegetation establishment.

This form of management is typical for small riparian fields in the Midwestern US that are marginally productive and are too small or wet to be profitably farmed with modern equipment (Cope et al. 2011).

The forest site trees were primarily established in a period from 1930's to the 1950's (Hubbart et al., 2011). The channelization of Hinkson creek early in the 20th century (Figure 4) reduced the hydraulic connectivity and sediment delivery of the creek to the forest stand and may have diminished subsequent regeneration of Eastern cottonwood trees due to a lack of acceptable mineral substrate available for germination of this light seeded tree species (Stella et al., 2011). The current disturbance regime of the BHF is typical for a riparian forest including episodic flooding and occasional windthrow events (Almquist et al., 2002; King and Antrobus, 2001).

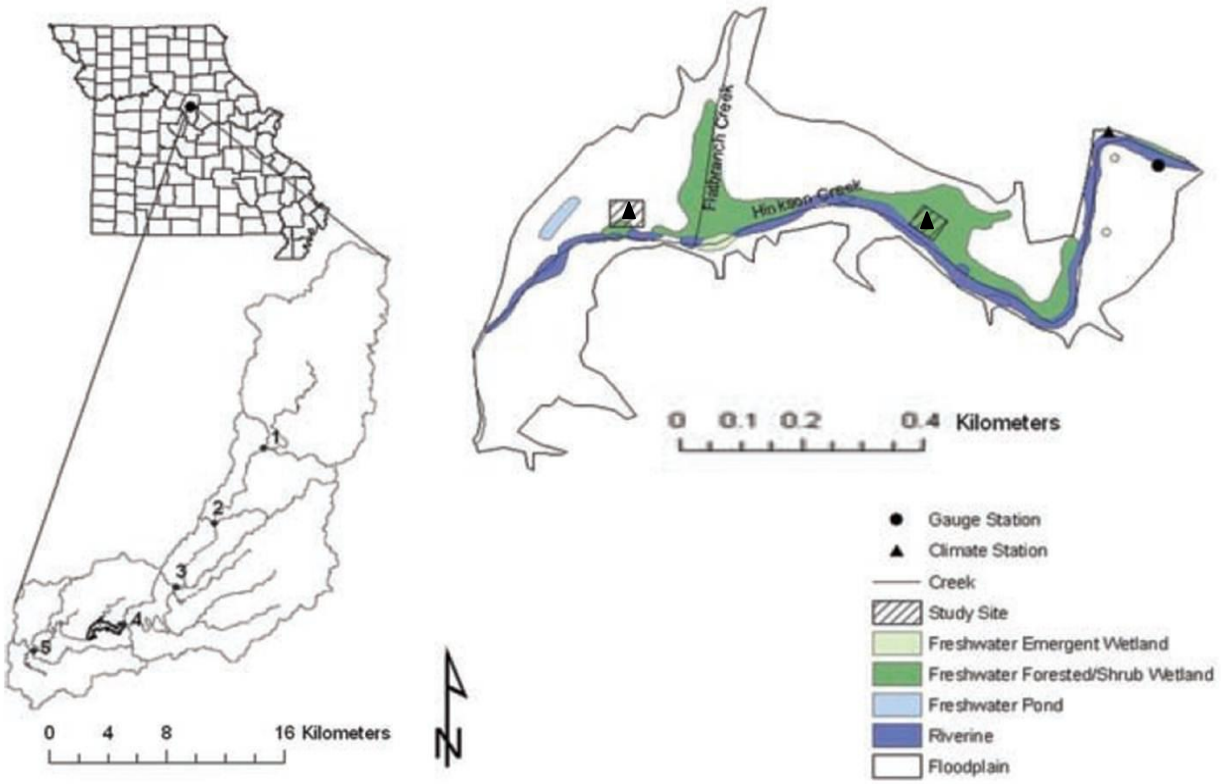

Figure 2.Study location Map: The Hinkson Creek Floodplain nested design forest and grassland sites with the Hinkson Creek watershed delineated. Columbia, Missouri. Reprinted with permission from Hubbart et al., (2011).

Soils

Alluvial soils underlying the site are fertile and well drained. The soils are predominately Haymond silt loams, with slopes of 0-3% (Young et al. 2001,NRCS Nov. 12th , 2011.http://websoilsurvey.nrcs.usda.gov) and the landscape position of the AG and BHF sites is floodplain and floodplain steps subject to frequent to occasional inundation

(Hodges, 1997). Flooding has been observed on this portion of the Hinkson Creek floodplain during spring runoff in 2010 and 2013 (Figure3).

Figure3. Photographs of floodwaters flowing over Hinkson Creek Floodplain, Columbia, Missouri. May 31st 2013

Haymond silt loam is a coarse-silty, mixed superactive, mesic fluventic entrudept, comprised of silty alluvium and classified as a very deep well drained soil. Hubbart et al. (2011) reported average soil infiltration rates of 38cm^{-hr} (BHF) and 23 cm $^{-hr}$ (AG) measured with double ring infiltrometers. Additionally, Hubbart et al. (2011) recorded maximum soil infiltration rates of 126 cm hr^{-1} in the BHF site and postulated that rapid infiltration may be occurring in the forest site due to preferential flowpaths created by tree roots penetrating into the subsoil.

Hinkson Creek has been channelized within this portion of the floodplain (Hubbart et al., 2011), and the current stream channel is less sinuous than the pathway observed in historic photographs (Figure 4.). The channelization of Hinkson creek

promotes efficient downstream drainage, thus reducing the probability that overbank flows will deliver inputs of fresh alluvium to floodplain soils for all but the largest streamflow events (Oswalt and King 2005).

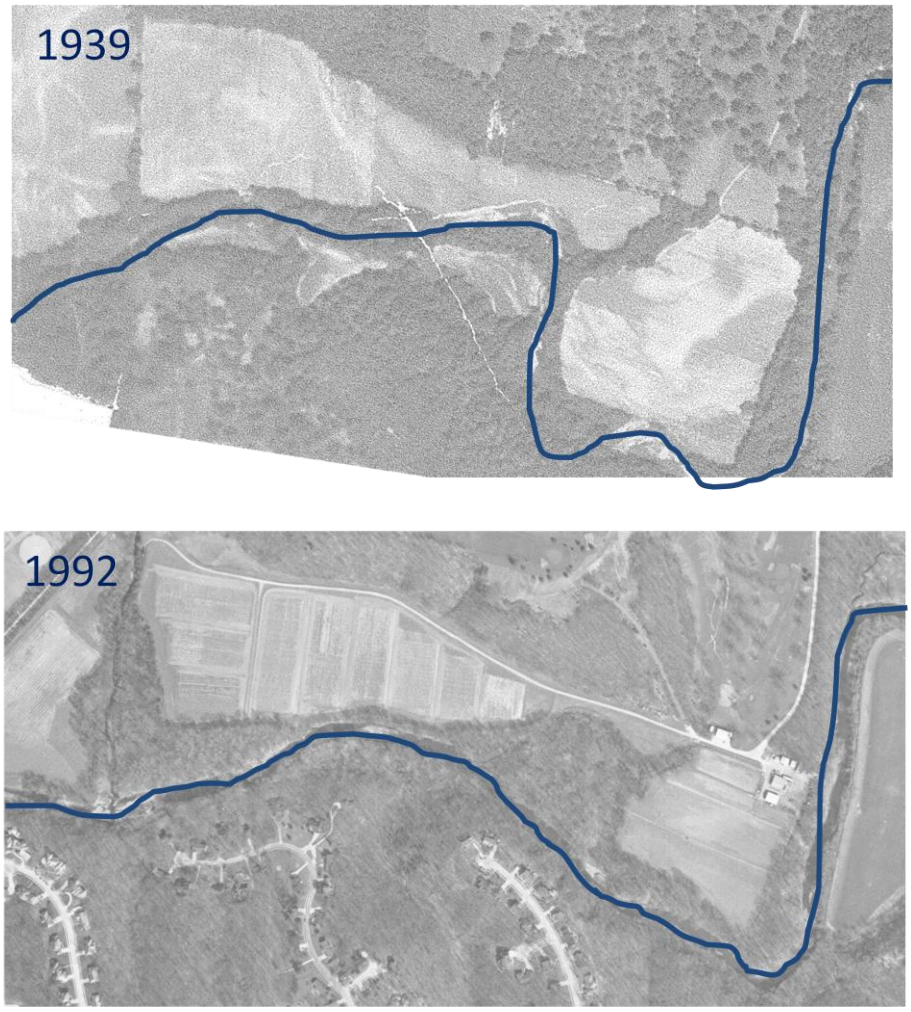

Figure 4. Sample historic and modern aerial photographs of the Hinkson Creek Floodplain, Columbia, Missouri, showing signs of channelization. Reprinted with permission from Hubbart et al., (2011).

Vegetation Survey and Forest Stand Inventory

Vegetation Survey

Vegetation surveys consisting of multiple transects were conducted in the grassland and forest sites of the Hinkson Creek floodplain, Columbia, Missouri during July 2011. Vegetation composition was examined by systematic point sampling (Krebs, 1989) along several parallel transects (Chahouki et al. 2012). The vegetation survey was conducted as follows: six consecutive north-south transects were established with each transect beginning 15m west of the last. Transect sampling was done this way in both the forest and grassland sites of the Hinkson creek floodplain. A $1m^2$ PVC plastic frame was placed on the ground to delineate a vegetation sampling quadrat (Ramsey et al. 2006) every 15m along each north to south transect (Figure 5) (for a total of 6 plots per transect and 36 plots total for BHF and AG sites respectively). Within each 1m quadrat ground cover percentages were occularly assessed (Xiao-Bing et al., 2005, Popham et al., 1987) for the following characteristics: total vegetation, mineral soil, woody litter, leaf litter, moss and other (rocks or trash) (Krebs, 1989). The $1m^2$ PVC plastic frame was marked every 10cm of length to aid in visual estimation of species coverage. Total vegetation percent coverage values over 100% were observed in some quadrats, made possible because we took into account vertical stratification of foliage (Kershner et al., 2004). All groundcover plant species found in each quadrat were identified to species (or genus) level and the percentage of quadrat total vegetation coverage occupied by each species estimated visually. Unknown plant species were sampled and later identified with the aid

of a dichotomous key (Steyermark 1963) and expert advice from Dr Kirsten Stephan (Lincoln University). After completion of the vegetation survey, results were analyzed to identify which site had greatest quantities of the following: total plant species, total plant families, native species, gramminoids, Asters and woody plant species.

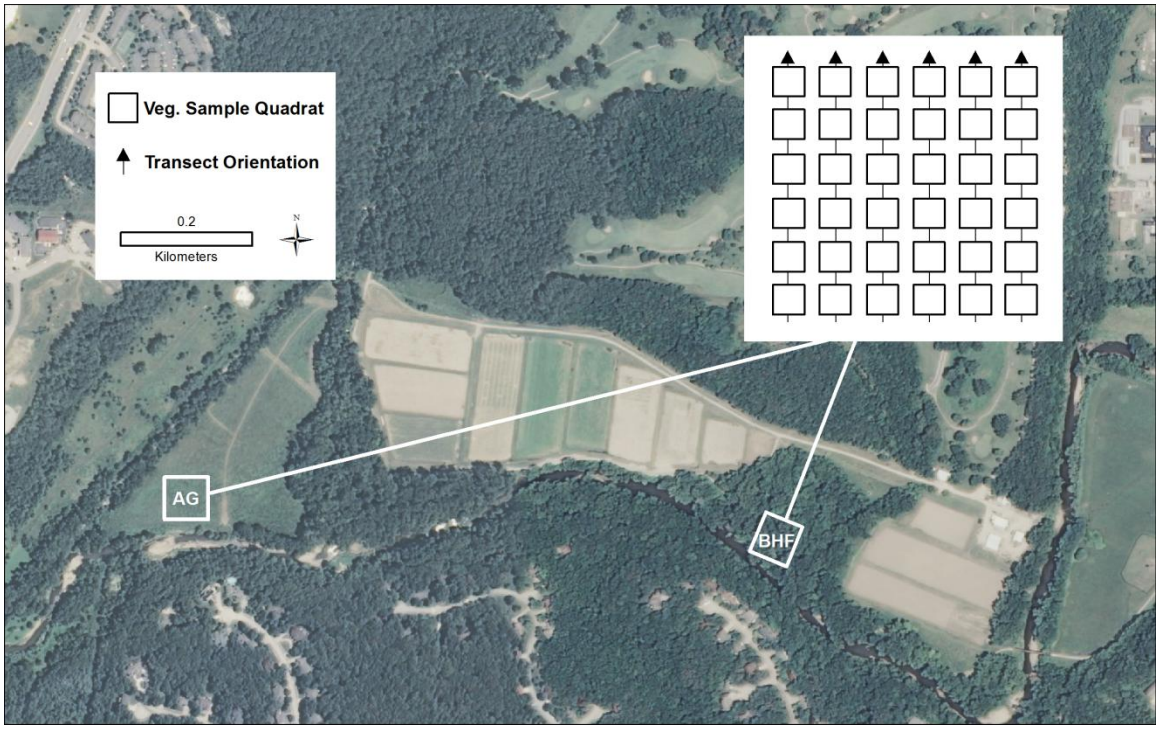

Figure 5. Vegetation survey sampling plot locations within the BHF and AG sites of the Hinkson Creek floodplain, Columbia, MO

During the growing season (mid-April to late November 2012), bi-weekly vegetation heights measurements were collected in the grassland site. Vegetation height was measured at each of the nine grassland site plot (Figure 6) centers. The fixed location piezometers used as vegetation height plot centers were established for other research and were located 40m apart (40m spacing both east-west and north-south) in a 3x3 grid

arrangement. Maximum vegetation height was measured 1m to the north, east, south and west of each plot center and the values averaged per plot. The mean of the average vegetation height of the nine plots was then calculated for use as a data input for evapotranspiration model calculations. The understory vegetation height of the BHF was measured once on August 18th 2012 (using the same procedures as in the AG site) to examine maximum seasonal growth of the forest understory.

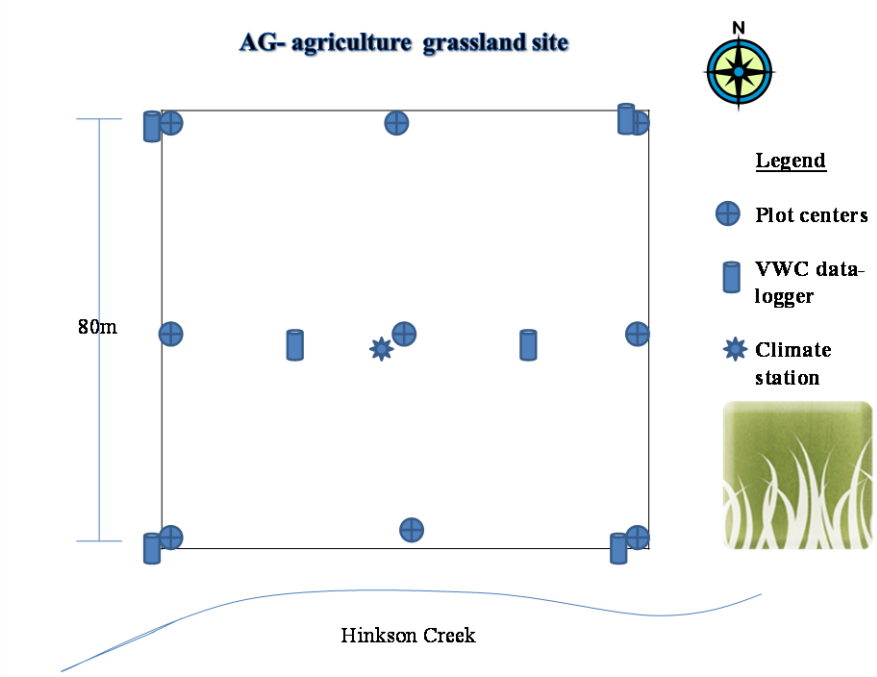

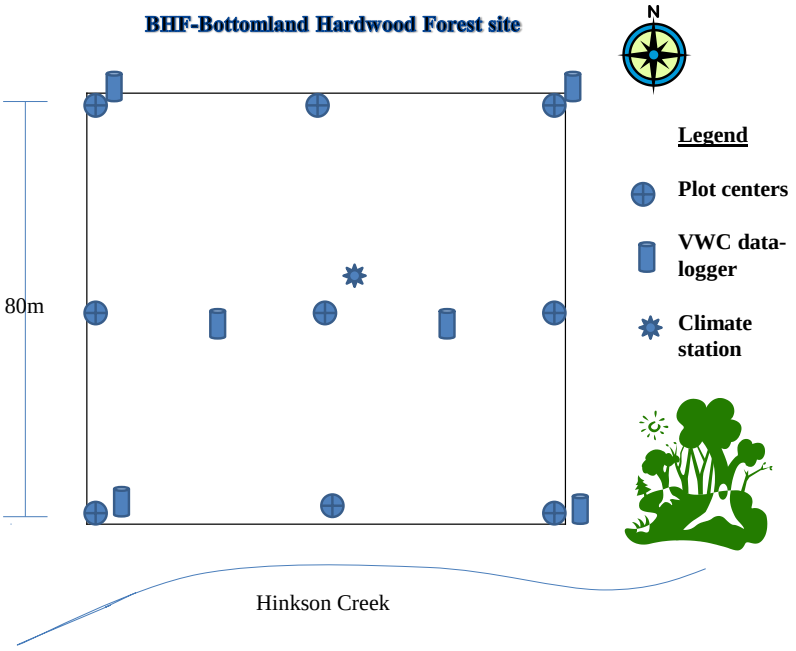

Figure 6. Site Maps with vegetation height and or canopy coverage plot centers,with climate instrument locations. Hinkson Creek Floodplain AG and BHF sites.

Forest Stand Inventory

Forest inventory measurements were collected within the Bottomland hardwood forest, July 2012. Variable radius plots were established visually using a 2.296 m^2hectare^{-1} factor prism (10ft^2acre^{-1} in English standard units), with plot centers systematically located 1m north of each of the BHF piezometers (Figure 6) (piezometers were established in fixed location for other research purposes and are arranged in a 3x3 pattern

with each approximately 40m from the last) for a total of nine plots. Limiting distances to borderline trees were measured based on diameter at breast height and individual trees of insufficient size were rejected from the plot roster (Husch et al. 2003). The trees located inside each variable radius plot were identified to the species level.

Plot tree diameters were measured in inches at 1.3m height and values were subsequently converted to centimeters. Forest basal area was calculated for each plot by summation of the number of trees tallied in the plot, multiplied by the factor of the prism (2.296 $m^2 hectare^{-1}$). Forest stand basal area was calculated by averaging the nine plots to find the mean (Husch et al., 2003).

Live tree heights were measured for all plot trees in July 2012. Tree heights were calculated by using a clinometer for occular estimation of slope percent to the living tree top, which was multiplied by the horizontal distance (m) from the observation point to tree base (Husch et al. 2003). The product of this calculation yields live tree height in meters. Forest stand canopy height was estimated by taking the mean of all measured tree heights and this value was used in subsequent ET calculations as BHF vegetation (canopy) height.

Forest canopy coverage percent was measured bi-weekly during the 2012 growing season from April 5th onward on the same dates vegetation heights were measured in the grassland (final measurements were collected November 9^{th} 2012 and were used to model the fall portion of the previous year's canopy coverage). A spherical densiometer Model-C was used to estimate canopy coverage to the north, east, south and west of each of the

nine BHF plot centers (Figure 6). The total percent of unobstructed sky reflecting on the densiometer was recorded during each reading for later use calculating percent canopy coverage with the following formula (Jennings et al., 1999):

$$C = 100 - (S * 1.04) \quad (1.6)$$

Where, C is the percent canopy coverage and S is the amount of unobstructed sky observed using densiometer (Jennings et al. 1999).

The canopy conductance term used in equations modeling forest evapotranspiration were set to vary with changes of forest canopy coverage percentage. Canopy conductance maximized for the period of complete foliation. The microclimatological data was used in conjunction with vegetation height and canopy coverage measurements to estimate dates of leaf-fall in forest (Delpierre et al., 2009; Vitasse et al., 2009) and senescence in grassland site plants, (Suyker and Verma, 2001). Given that canopy conductance is highly correlated with leaf area, stomatal conductance terms used within the forest evapotranspiration equations were reduced proportionately at the onset of leaf –fall (Brodribb and Holbrook, 2003).

The canopy conductance values used in ET models were collected from empirical data found in published sources based on vegetation type (forest grassland etc). Canopy conductance values for species dominant within a location were chosen because they are likely to comprise the majority of leaf area for each site (i.e. *Populus deltoides* for the forest and So*rghum halepense* for the grassland).

Evapotranspiration Parameters

Annual ET for the BHF and AG sites were modeled using Microsoft Excel^{TM} software for the period From October 1st 2011 to September 30th 2012 (e.g. water year 2012). The Seven methods of ET calculation used in this study include; Surface Energy Balance (Fisher et al., 2007), Penman-Monteith (Irmak et al., 2008), Priestley-Taylor (Jacobs et al., 2002), Easy Penman-Monteith (Komatsu et al., 2006), McNaughton-Black (Fisher et al., 2004), Bowen Ratio Energy Balance (Odhiambo and Savage 2009), Shuttleworth-Wallace (Fisher et al., 2004). The ET equations used in this study require varying inputs of climate data as listed in Table 1.

Table 1. Data inputs required for each of seven equations used for estimating Hinkson Creek Floodplain , Columbia, Missouri, forest and grassland ET.

	$R_{incoming}$	T_{air}	RH %	T_{soil}	Θ_{soil}	V_{wind}	Z_{veg}	$C_{stomata}$
Surface Energy Balance	X	X	X	X	X			
Penman-Monteith	X	X	X	X	X	X	X	X
Priestley-Taylor	X	X		X	X			
Easy Penman-Monteith		X	X					X
McNaughton-Black		X	X					X
Bowen Ratio Method	X	X	X	X	X			
Shuttleworth-Wallace	X	X	X	X	X	X	X	X

$R_{incoming}$, Incoming Solar Radiation(Wm^{-2}); T_{air}, Air Temperature(°C);RH, Relative Humidity(%);T_{soil}, Soil Temperature(°C);Θ_{soil},Soil Volumetric Water Content(%);V_{wind}, Wind velocity(ms^{-1}); Z_{veg}, Vegetation Height(m); $C_{stomata}$, Stomatal Conductance(mm s^{-1})

Meteorological Stations

Microclimate stations were deployed in July of 2011. For the current work data were collected from October 1st 2011 through September 30th 2012 (WY 2012). The current study used climate and soil moisture data measured and recorded during water year 2012 to compute forest and grassland ET rates. The grassland (AG) climate station was located 49m distance north of Hinkson creek, with no interference from surrounding trees or structures (the nearest trees were at least 100m from climate station). The BHF climate station is positioned, 53m north of Hinkson creek (Figure 5).

Each climate station was equipped with two soil temperature probes located at 15 and 30cm depth and a pair of air temperature/ relative humidity sensors at 1.5 and 2.5 m above ground respectively (Figure 7). These sensors were connected to Decagon data loggers recording at 30 minute intervals. The temperature and vapor pressure differences between the 1.5m and 2.5m air temperature/relative humidity sensors provide data describing gradients of sensible heat and vapor pressure. Each station also includes an anemometer, a pyranometer and a tipping bucket precipitation gauge at 2.5m above ground connected to an Onset data logger recording data at 30 minute intervals (Table 2).

Figure 7. Photographs of the (AG) grassland and (BHF) forest Climate Stations located in the Hinkson Creek Floodplain, Columbia, Missouri, USA.

Volumetric Water Content (VWC) was measured for the period of September 31st 2011 through October 1st 2012 (Figure 6). Measurement depths of 15, 30, cm were chosen to correspond with soil temperature measurement depths. Soil volumetric water content (VWC) was measured through electrical capacitance using Decagon 10HS sensors with data recorded and logged at half hour intervals in a Decagon EM50 data logger. Soil characteristics of the site were previously quantified by Hubbart et al., (2011). The WY 2012 soil VWC data was used as forcing data for estimating soil heat flux (G) terms. Additionally, soil bulk density values reported for the site by Hubbart et al., (2011) were used as data inputs in soil heat flux calculations.

Table 2. Instrumentation of microclimate stations and soil moisture sites used in ET calculations Hinkson Creek Floodplain, Columbia, Missouri.

Instrument	Variable sensed
Hobo Onset S-WCA -M003 Wind Speed and Direction	Wind speed(m/s) , Wind direction(0-360°)
Hobo Onset S-LIB- M003 Silicon Pyranometer sensor	Incoming shortwave radiation (W/m²)
Hobo Onset S-THB- M002 Temp./RH sensor (12-bit) (RS3 Solar Radiation Shield)	Air Temp. (°C), Relative Humidity (%)
Hobo Onset S-TMB-M006 Smart Temp. Sensor (12-bit)	Soil Temp. (°C) , 15cm, 30cm depth
Hobo Onset S-RGB -M002 Rain Gauge (0.2mm)	Precipitation (mm)
Hobo Onset U30 Cellular Data Logger U30-GSM	Data storage
Decagon Devices EM50 ECH20 Logger Model EM9079	Data storage
Decagon Devices 10HS Soil Moisture Sensor	Soil Volumetric Water Content (%)

Modeling Evapotranspiration

The surface energy balance provides the basis for many equations for estimating ET. This study will utilize ET equations with varying levels of complexity and examine whether ET equations which rely on more empirically derived data perform as well as equations which operate exclusively on measured climate variables. The following sections will describe several methods which have been shown to be effective for estimating ET.

Surface Energy Balance Equation

The Surface Energy balance provides a standard method of quantifying the conservation of energy for a given system (Fisher et al. 2008). Provided that there is negligible change in energy storage within a system, the surface energy balance may be

solved to isolate the latent heat flux, which may then be divided by the latent heat of evaporation and the density of water to yield a length of water evaporated within the system over the time period (Jacobs et al., 2002).

Within the surface energy balance equation the net radiant energy (R_n) is equal to the sum of the latent energy flux (λE), sensible heat flux (H), ground heat flux (G), the heat energy stored within the system (S), minus any advective energy entering the system (A) and metabolic energy consumed by organisms (M). This relationship assumes that there is negligible net change in heat storage within the system (i.e. the change in heat storage will not be significant on a daily basis). The surface energy balance equation is expressed as follows (Maes et al., 2011, El Bourady, 2010, Jacobs et al., 2002, Fisher et al., 2007, Jen-Ling et al., 2007, Ibanez et al., 1998; Herbst, 1995):

$$R_n = \lambda E + H + G + S - A - M \quad (1.7)$$

This equation can be solved for the λE term as follows (Jacobs et al., 2002):

$$\lambda E = R_n - G - H - S + A + M \quad (1.8)$$

Where λE is the latent heat flux, R_n is the net radiation, H is the sensible heat flux and G is the ground heat flux, S is the stored heat energy in the system, A is the advected energy entering the system and M is the metabolic energy consumed by organisms with all fluxes expressed in W m^{-2}.

Net radiation (R_n) can be computed as follows (Maes et al., 2011):

$$R_n = R_{in}(1-\alpha) + \varepsilon L_{in} - \varepsilon\sigma T_s^4 \quad (1.9)$$

where, R_{in} is the incoming shortwave radiation, α is the albedo of the surface (specifically reflectivity within the visible spectrum), $\boldsymbol{\varepsilon}$ is the emissivity of the surface (an empirically derived dimensionless value from zero to one, representing the surfaces' capacity to emit electromagnetic radiation of all wavelengths), L_{in} is the incoming longwave radiation, σ is the Stefan-Boltzmann constant ($5.67X10^{-8}$W $m^{-2}K^{-4}$) and T_s is the temperature of the surface (Kelvin).

Sensible heat (H), term can be calculated using the following method (Ibanez et al., 1998):

$$H = \left(gHa * C_p\right) * \left(T_{air\ below} - T_{air\ \ above}\right) \quad (2.0)$$

Where, gHa is the boundary layer conductance for heat, Cp is the specific heat of water (29.3J $mol^{-1}C^{-1}$), T air above and T air below are the air temperature measurements taken at the higher and lower levels respectively.

Ground heat flux (G), in Wm^2, can be determined empirically through computation of the difference of temperature between two sensors placed in the soil at set depths. The equation used for calculating G is a modification of Fourier's law for heat transport and is represented as follows (Weber et al., 2007)

$$G = -C\left(\frac{\partial T}{\partial z}\right) \quad (2.1)$$

where, G is soil heat flux density, the conduction of energy per unit area in response to a temperature gradient (Wm^{-2}), C is soil thermal conductivity ($Wm^{-1}K^{-1}$), $\partial T/\partial z$ defines the temperature gradient within the measured vertical (z) distance. In practice, it is not feasible to measure the temperature difference between two infinitely close layers. Consequently, soil heat flux can be calculated as per Muerth and Mauser (2012):

$$G \approx -C\left(\frac{T_2 - T_1}{z_2 - z_1}\right) \tag{2.2}$$

The distance between z_2 and z_1 is generally small but sufficient to allow measurable temperature difference. The negative sign before C makes the soil heat flux positive when heat travels downward into the soil. For small depth changes, soil thermal conductivity depends not only on mineral composition (particularly quartz content), but also on the volumetric water content, porosity, and temperature. Cosenza and Tabbagh, (2003) observed linear dependence of thermal conductivity on soil water content and porosity varying one of the variables respectively. A polynomial formula was proposed by Cosenza and Tabbagh, (2003) by fitting to a whole set of published experimental data for porosity ranging from 0.4 to 0.6, soil solid thermal conductivity ranging from 2 to 5 $Wm^{-1}K^{-1}$ and volumetric soil water content from 0.1 to 0.4:

$$C = (0.8908 - 1.0959n)C_s + (1.2236 - 0.3485n)\theta \tag{2.3}$$

Where, C_s is thermal conductivity of solid particles, n is porosity, and θ is volumetric water content.

Estimating solid grain conductivity requires quantifying soil quartz content. Quartz usually has very high thermal conductivity compared to other soil components. It is generally assumed that only crystalline forms of quartz in sand contribute to the high thermal conductivity, whereas silicate material in silt and clay has similar conductivity as other soil materials (Peters-Lidard, 1998). Therefore, a median percentage of 25% was chosen as the quartz content corresponding to the sand portion of the silt loam soil (Fisher and Binkley, 2000) which comprises the floodplain alluvium which the current work is comprised of (Young et al 2001). About 5% of the soil layer is organic material as reported on the SSURGO soil map (Young et al. 2001) and the rest of the constituents were defined as general soil minerals. Thermal conductivity of soil solids calculated by the mean was 3.84 $Wm^{-1}K^{-1}$, which is comparable to the value of 3.2 $Wm^{-1}K^{-1}$ of silt loam fitted by de Vries model (Ochsner et al., 2001). Soil moisture content of the upper 15 cm was monitored at the associated meteorological stations and mean porosity was assumed to be 0.50 as per the findings of Hubbart et al., (2011).

Investigations have shown that few systems in nature are truly closed, and it is possible that energy may enter from outside of the system (Huggett, 2007). An accurate surface energy balance equation must account for advected energy (A), and the storage of energy within the system (S) particularly if a study is conducted over the course of minutes or hours (Jeng-Lin et al., 2007). Although stored and advected energy may be

present within a system over short time periods, these fluxes are not always of a magnitude to be critical components of the surface energy balance (Amiro, 2009). Over the duration of an annual study, change in storage of energy in vegetation (S) and advection of energy from outside sources (A) tends to average out and these terms are often disregarded (Jacobs et al. ,2002). If the S and A terms are assumed to be insignificant over the time period in question, the simplified Surface Energy Balance equation solved for latent heat flux is as follows (Amiro, 2009):

$$\lambda E = R_n - G - H \tag{2.4}$$

The latent heat of vaporization term (λE) of the surface energy balance equations yields depth of water per time (m s^{-1}) when divided by the latent heat of vaporization (λ=44KJ mol^{-1}) and the density of water at 20°C (ρ_w=1000kg m^{-3}) as follows (Jacobs et al., 2002):

$$E = \frac{\lambda E}{\lambda \rho_W} \tag{2.5}$$

Penman-Monteith Equation

The Penman- Monteith (P-M) method of estimating Evapotranspiration (ET) is widely considered to be one of the most accurate ways to predict ET, due to the rigorous climate data requirements (Attarod et al., 2009, Lee, 2009, Irmak et al., 2008). The P-M method is referred to as a combination method because it incorporates the surface energy balance equations modeled by Penman (1948) with the aerodynamic resistance equations

of Monteith (1965) into one model that requires commonly measured weather data (Allen, 2005). By integrating the temperature, wind speed and radiation components of the climate for a given site, P-M can supply an accurate estimate of ET. Descriptive information about the vegetative canopy (i.e. vegetation height, and species stomatal conductance) is used as model inputs estimating the structural and biological resistances to evaporation of water vapor into the atmosphere. Penman-Monteith also incorporates the affects of vapor pressure deficits and wind speeds to determine the conductance of vapor into the air (Jacobs et al., 2002). The Penman -Monteith method is commonly expressed in the following equation (Abetew et al., 2010, Otles and Gutowski, 2005):

$$LE = \frac{\Delta(R_{n-}G)+\rho_a\, c_p\, (e_s-e_a\,)/r_a}{\Delta+\gamma(1+\frac{r_s}{r_a})} \qquad (2.6)$$

where Δ is the slope of the saturated vapor pressure curve, R_n is net radiation (Wm^{-2}), G represents the flux of heat stored in the ground (W m^{-2}), ρ_a signifies the mean air density at constant pressure (kg m^{-3}), c_p the specific heat of dry air (29.3 J $mol^{-1}C^{-1}$), e_s is the mean saturated vapor pressure (kPa), e_a is the mean ambient vapor pressure(kPa), r_a is the aerodynamic resistance (s m^{-1}), r_s is the bulk surface resistance (s m^{-1}) and γ is the thermodynamic psychrometric constant (0.067 kPa C^{-1}).

In the P-M method, atmospheric resistance (r_a) is calculated using the following relationship:

$$r_a = \frac{\ln\left[\frac{z-d}{z_o}\right]\ln\left[\frac{z-d}{z_{ov}}\right]}{k^2 U} \quad (2.7)$$

With z as the height (m) where the wind speed U was measured (m s^{-1}). The zero plane displacement height, d (m), is approximated via the relationship $d=0.67_{zveg}$, where, z_{veg} is the vegetation height (m). The roughness length z_o (m) is estimated through the equation $z_o = 0.1z_{veg}$. The roughness length for water z_{ov} (m) is estimated as; $z_{ov} = 0.1z_o$ and k is the Von Karmen dimensionless constant of 0.4 (Jacobs et al., 2002).

The P-M method of ET estimation uses comprehensive climate data inputs and is applicable in diverse locations throughout the world (Lee, 2009). Unfortunately, many sites lack the instrumentation to supply the data required for computation of Penman-Monteith and considerable effort has been made to find suitable alternative methods of ET estimation that require fewer climate station inputs (Lee, 2009).

Priestley-Taylor Equation

A primary driving force for evapotranspiration is the intensity of solar radiation (Twine et al., 2004). Simplified ET computations incorporating select additional variables have been shown to be effective for some climates (Irmak et al., 2003). For example, in locations that are not water limited and have mild air temperatures, the rate of ET can be modeled primarily by the intensity of incoming solar radiation (Irmak et al., 2003). Under such conditions it may be assumed that the local air mass is homogenous and air moving into the site will have vapor pressure equal to that which is found in the boundary layer. When this occurs, evapotranspiration increases only with additional

radiation and subsequent warming of the local air parcel to accommodate greater vapor pressure deficits (effectively moving up the saturation vapor pressure curve into higher temperatures and larger vapor pressure deficits). Consequently, the effective boundary layer may extend beyond the leaf surface and the Penman-Monteith equation may be simplified by removing variables that relate to vapor pressure deficit and surface roughness.

The Priestley-Taylor method is applied using the assumptions above where ET is estimated using only net radiation and mean temperature (Irmak et al., 2003). This is accomplished in part by inserting an empirically derived stabilizing coefficient (α), which can be adjusted for vegetation type, and height, or soil moisture conditions (Fisher et al., 2007, Priestley and Taylor, 1972). A standard value for the dimensionless coefficient α is 1.26, which is based on the assumption that the aerodynamic term (which is not included in the Priestley Taylor Equation) accounts for 26% of the available energy (Rosenberry et al., 2004). The Priestley –Taylor method is expressed in the following equation (Jacobs et al., 2002, McNaughton and Black, 1972, Priestley and Taylor, 1972):

$$\lambda E = \alpha \frac{\Delta}{\Delta+\gamma} (R_n\text{-G}) \tag{2.8}$$

Where α is an empirically determined stabilizing coefficient, Δ is the slope of the saturation vapor pressure curve, γ is the thermodynamic psychrometric constant (0.067 kPa C^{-1}), R_n is net radiation (Wm^{-2}), and G is the flux of heat into the ground (Wm^{-2})

Simplified Easy Penman-Monteith Equation

The Simplified 'Easy' Penman-Monteith equation (Komatsu et al., 2006) assumes that plant stomatal conductivity exerts greater control on transpiration rates than atmospheric stability. Consequently, wind speeds and atmospheric conductance are not considered. The 'Easy' Penman-Monteith equation, (hereafter referred to as the Easy Penman-Monteith or Easy P-M), was shown to be useful for quantifying transpiration in coniferous forest sites in Japan (Komatsu et al. 2006). Within a mature forest almost all of the incoming solar radiation is absorbed by the canopy and it can be assumed the transpirative flux of water vapor is nearly equal to total evapotranspiration. The equation is expressed as follows (Komatsu et al., 2006).

$$E = G_c \frac{D}{p_a} \tag{2.9}$$

where, E is the transpiration rate (mol $m^{-2}s^{-1}$), G_c is the respective plant canopy conductance ($m^{-2}s^{-1}$), p_a is the atmospheric pressure (kPa) and D is the vapor pressure deficit (kPa).

McNaughton-Black Equation

The McNaughton-Black ET equation, which was developed from research performed in coastal Douglas fir (*Psuedotsuga menzisii*) forest in British Columbia, Canada (McNaughton and Black, 1973), is a simplified version of the Penman-Monteith method that assumes soil moisture is not limited (Fisher et al., 2005). The McNaughton-Black ET equation requires stomatal resistance data pertaining to the vegetative

community and the vapor pressure deficit of the air surrounding the plant canopy and is expressed as follows (Fisher et al., 2004, McNaughton and Black, 1973):

$$\lambda E = \frac{c_p \rho D}{\gamma r_{cs}} \quad (3.0)$$

Where c_p represents the specific heat of air at a constant pressure (29.3 J $mol^{-1}C^{-1}$), ρ is the density of air (mol m^{-3}), D is the air water vapor pressure deficit (kPa), γ is the psychrometric constant (0.067 kPa C^{-1}), and r_{cs} is the bulk stomatal resistance of the plant canopy (s m^{-1}).

Bowen Ratio Energy Balance Equation

The ratio of sensible heat transfer to latent heat flux was first described by Bowen (1926) and is commonly referred to as the Bowen ratio (β) (Amiro, 2009). This relationship may be incorporated into the surface energy balance to provide the Bowen ratio energy balance (BREB) (Odhiambo and Savage, 2009). The BREB can be solved to find the flux of latent heat energy as follows (Ibanez et al., 1998):

$$\lambda E = \frac{R_n - G}{1+\beta} \quad (3.1)$$

Where R_n is net radiation (Wm^{-2}), G is the flux of ground heat (Wm^{-2}), and β is the Bowen ratio. β is the dimensionless ratio of sensible heat (H) (W m^{-2}) to latent heat

energy (λE)(W m^{-2}):

$$\beta = \frac{H}{\lambda E} \tag{3.2}$$

Where the atmospheric boundary layer is assumed to have equivalent resistances for heat and water vapor the Bowen ratio is calculated as follows (Ibanez et al. 1998, Herbst 1995):

$$\beta = \gamma \frac{\Delta T}{\Delta e} \tag{3.3}$$

Where, $\Delta\, e$ represents the change in ambient water vapor concentration (kPa) over time, $\Delta\, T$ is the change in air temperature over time (C^{-1}) and γ is the psychrometric constant (°C^{-1}).

The Bowen ratio energy balance (BREB) method has been shown to be accurate in locations where there are not large fluctuations of advected heat energy (Ibanez et al., 1998). Advected energy flux has been observed during nighttime periods (Kochendorfer et al., 2011; Fisher et al., 2007) and is assumed to occur during daylight hours primarily along borders of land use types (e.g. Air from a warmer field enters a forest canopy driven by winds). When modeling ET with the Bowen ratio energy balance precautions should be taken to situate air temperature and relative humidity sensors centrally within a land use type to ensure that there are minimal influences from outside sources.

Shuttleworth-Wallace Equation

In some instances it is desirable to partition evapotranspiration into the evaporative and transpirative components. This approach may be useful for computing ET if there are large areas of exposed soil within the study area, or if there are seasonal variations in extent of the vegetative cover (Zhang et al., 2011). The Shuttleworth-Wallace model of estimating ET method may be applied to make this distinction through computation of the evapotranspiration rates of the soil and plant canopy independently (Shuttleworth and Wallace, 1985). The Shuttleworth Wallace model is an adaptation of the Penman–Monteith equation and is expressed as follows (Fisher et al., 2005, Shuttleworth and Wallace, 1985):

$$\lambda E = C_c PM_c + C_s PM_s \tag{3.4}$$

Where λE is latent heat energy (W m^{-2}), C_c and C_s are unit-less coefficients that model resistances to diffusion of water vapor from the plant canopy and soil surface respectively (described below). PM_c Represents the latent heat energy available for transpiration from the plant canopy (W m^{-2}), and PM_s describes the latent heat energy from soil surface evaporation (W m^{-2}). PM_c And PM_s are calculated as follows (Fisher et al., 2005):

$$PM_c = \frac{\Delta(R_n - G) + (\rho_a c_p (e_s - e_a) - \Delta r_{ca} G)/(r_a + r_{ca})}{(\Delta + \gamma\left(1 + \frac{r_{cs}}{r_a + r_{ca}}\right))} \tag{3.5}$$

$$PM_s = \frac{\Delta(R_{n-}G)+(\rho_a\, c_p\, (e_s-e_a\,)-\Delta r_{sa}\,((R_{n-}G)-G))/(r_a+r_{sa})}{(\Delta+\gamma\left(1+\frac{r_{ss}}{r_a+r_{sa}}\right))} \quad (3.6)$$

Where $r_{ca}$is boundary layer resistance of vegetation, r_{sa} is aerodynamic resistance between the soil and canopy layer, r_{ss} is the soil resistance and other variables are as previously outlined for Penman-Monteith (equation. 2.4).

C_c and C_s are coefficients that model the combined resistances to the diffusion of water vapor through the atmosphere, plant canopy and soil surface. The coefficients are calculated through the following equations:

$$C_c = \frac{1}{(1+\frac{R_cR_a}{R_S(R_C+R_a)})} \quad (3.7)$$

$$C_s = \frac{1}{(1+\frac{R_sR_a}{R_p(R_s+R_a)})} \quad (3.8)$$

Where,

$$R_a = (\Delta + \Upsilon)r_a \quad (3.9)$$

and Δ is the slope of the saturation vapor pressure curve, Υ is the thermodynamic psychrometric constant (C^{-1}), and r_a is the atmospheric resistance to water vapor diffusion.

$$R_s = (\Delta + \Upsilon)r_{sa} + \Upsilon r_{ss} \quad (4.0)$$

Where r_{sa} is the resistance from the soil to atmosphere and r_{ss} is the resistance to vapor diffusion within the soil.

$$R_c = (\Delta + \Upsilon)r_{ca} + \Upsilon r_{cs} \quad (4.1)$$

Where r_{ca} is the resistance from the canopy to the atmosphere, and r_{cs} is the resistance from the soil layer to the canopy.

Model Parameters

Climate and vegetation data for the 2012 water year were used as inputs for model calculations parameritized in Excel software (Microsoft Corporation ^{R}). Climate data were digitally archived from the agricultural grassland and bottomland hardwood forest sites at half hour intervals and reduced to hourly temporal resolution by calculating the mean of the readings taken on each hour and half hour prior to model calculation (i.e. averaging the reading for 9:00am and 9:30 am for the 9:00am value used in ET calculations).

Vegetation characteristics including AG vegetation height and BHF canopy percent coverage were collected bi-weekly throughout the 2012 growing season. Bi-weekly readings were introduced into the model calculations by interpolating linear relationships between readings. For example: where a mean AG vegetation height of 0.406389 m was measured in April 20th 2012, followed by a mean measurement of 0.526344 m May 3rd , values were interpolated exhibiting a growth increment of

0.000384m hr^{-1}. The hourly change in vegetation height between measurements were interpolated using the following equation:

$$ht_n = ht_{n-1} + \left(\frac{(ht_i - ht_f)}{t(ht_f) - t(ht_i)}\right) \quad (4.2)$$

where ht_n is the calculated vegetation height, ht_{n-1} is the previous calculated vegetation height, ht_i is the initial vegetation height measurement, ht_f is the final height measurement and $t(ht_f)$-$t(ht_i)$ is the time passed between the initial and final measurements (in number of one hour increments).

Although vegetation growth does not occur uniformly over time, the above estimation method was assumed superior to a bi-weekly step increase and the grassland vegetation height was modeled in this way for the 2012 water year. The bottomland hardwood forest mean canopy height value (measured July 2012) was used as a fixed vegetation height in forest ET models. The forest ground cover vegetation height was not modeled in this study and prior research has shown that understory vegetation transpires much less than the forest canopy (Komatsu et al., 2006).

Percent canopy coverage measurements and visual observation were used to estimate dates of leaf emergence and senescence within the deciduous bottomland hardwood forest. Forest canopy stomatal resistance was adjusted seasonally based on leaf presence and phenological state (using linear interpolation methods similar to those described Eq. 4.2). Forest stomatal resistance values were increased incrementally during autumn based on the observed decrease in percent canopy coverage measurements

(Figure 8). During the dormant season forest stomatal resistance (r_s) was increased to a maximum value of 200 s m^{-1}, to reflect the resistances to the diffusion of water across the waxy cuticle of the dormant buds (Koch and Ensikat, 2008). Following the vernal equinox, forest r_s values were gradually decreased inversely with leaf growth (with measured increases in forest canopy coverage serving as proxy for leaf growth), ultimately reaching an annual minimum of 5.3 s m^{-1} during summer months.

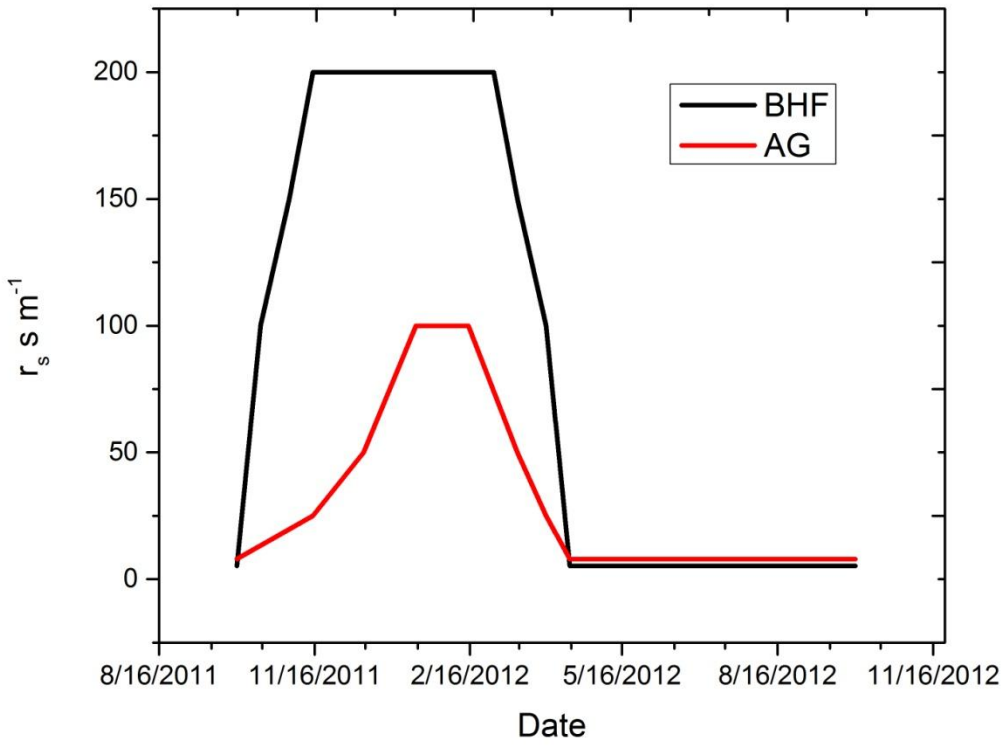

Figure 8 . Modeled seasonal variations in stomatal resistance for Hinkson Creek Floodplain BHF and AG sites.

Stomatal resistance for the AG site was also modeled with seasonal variations based on vegetation height and senescence. A summertime minimum r_s of 8 s m^{-1} was used for the grassland. During winter the AG grassland was occupied by sparse cool season grasses overtopped by a thatch of dead vegetation and the r_s was increased incrementally to a maximum value of 100 s m^{-1} (Figure 8).

Incoming solar radiation values from the AG site were used as inputs to calculate net radiation at canopy level for the BHF due to a lack of instrumentation at that height. Although the same incoming radiation data were used, variations in forest and grassland albedo values resulted in different net radiation outputs. Grassland albedo varied from a summer value of 0.25 (Federer et al., 1996) to a wintertime maximum of 0.30. The modeled differences in grassland albedo were assigned to account for the seasonal color change observed with dormancy of vegetative material (Twine et al., 2004). Forest albedo was fixed at 0.22 for the entire water year in accordance with findings of researchers who reported little or no seasonal variation of albedo in deciduous forests (Eccel et al., 2005, Rauner, 1976).

Understory forest anemometer data (2.5m) was transformed to estimate mean canopy height (27.9m) wind speeds for use in BHF ET models. Attenuation of wind velocity under forest canopies has been widely reported (Sypka and Starzak 2013, Wang 2012). Typically, wind speed decreases exponentially with increasing distance below a closed canopy. Empirical relationships have been established that estimate canopy height wind speed from anemometer readings taken near ground level. For the BHF this data

transformation was accomplished using an attenuation coefficient based on crown density *a*, (a dimensionless attenuation coefficient of 0.4 was chosen based as an average of summer and winter values within the forest canopy) (Cionco et al., 1972). Forest canopy wind speed $u(z)$ was calculated as follows:

$$u(z) = u(h)\exp[a(\frac{z}{h} - 1)] \quad (4.3)$$

Where, $u(h)$ is wind speed at measurement height in m s^{-1}, z is canopy height in m, and h is measurement height in m.

In addition to transformations of input data, some ET model estimates required post-processing as well. While the magnitude of nighttime evapotranspiration rates have been a subject of debate within the research community (Fisher et al., 2007), it is common practice to remove excessive negative latent heat values or erroneous nighttime transpiration rates during post-processing. In the current study ET values were removed from Penman-Monteith, Priestley-Taylor and Bowen ratio methods of ET calculation for time steps when R_{in} was less than 3W m^{-2} (this threshold was chosen as slightly more selective than Jacobs et al. (2002), who classified R_{in} less than 5Wm^{-2} as nighttime values to be removed from the dataset).

Data Analysis

Cumulative annual hourly evapotranspiration data were used to compare the water use of the forested and grassland reaches of the study site. Additionally, annual

floodplain ET was compared to annual reference ET calculations from the nearby Sanborn field (38°56'27"N, 92°19'17") climate station and eddy covariance ET measurements from Baskett Research and Education Area (BREA) (38°77'44"N, 92°22'50"). Growing season ET was also be compared to Pan evaporation measurement data reported at the Horticulture and Agroforestry Research Center (HARC) (39°10'22"N, 92°45'37"W) during the months of April to September 2012.

Analysis of variance (ANOVA) analysis were used to compared linear relationships between sites and methods of ET estimation. This is typically achieved by constructing an ANOVA table for simple linear regression. An example ANOVA regression table is provided below (Table 3).

Table 3: Summary of Statistics ANOVA table

Source of Variation	Degrees of freedom	Sum of Squares	Mean Square	f
Regression	1	SSR	SSR	SSR/S^2
Error	$n-2$	SSE	$S^2=SSE/n-2$	
Total	$n-1$	SST		

Provided: SSR =Sum of Squares Regression: Degree of variation accounted for by linear relationship, SSE=Sum of Squares Error: Degree of unaccounted for variation, and SST=Sum of Squares Total: SSE and SSR total (Devore, 2012).

This study explored the significance of the variation between the nested forest and grassland site ET rates. Secondarily, the variations between methods of ET estimation were examined. The data collected in this study was analyzed through completion of regression analyses (ANOVA) (Medieros et al., 2012), t-tests (Akinbile and Sangodoyn, 2011), Tukey multiple comparison test (Xixi et al., 2007), descriptive statistics and graphing (time series inquiries). Linear regressions were used to compare mean values of distinct ET methods (Temesgen et al., 2007). Evapotranspiration outputs were regressed against microclimate variable values to identify ET model sensitivity to various forcings (La Torre et al., 2011). Mathematically modeled data values were used to replace aberrant and missing data. Suitable models of data interpolation (as described in previous sections) were selected as needed for data estimation.

CHAPTER IV:

RESULTS

WATER YEAR 2012 CLIMATE

The climate in Mid-Missouri was relatively warm and dry during the current study. Climate records from Sanborn Field on the University of Missouri Campus (approximately 3km distance from Hinkson Creek floodplain study location), reported a total of 739.17 mm of precipitation during the period from October 1st 2011 to September 30th 2012 (WY 2012). Average air temperature at Sanborn Field were 15.6 °C, with maximum readings of 40.5°C and a minimum of -11.8°C during WY 2012 (Table 4).

Daily precipitation at Sanborn Field during WY 2012 ranged from a minimum of 0mm to a maximum of 45.5mm, with a standard deviation of 6.3mm. The average maximum daily wind velocity at Sanborn field was 7.7 ms^{-1}. Sanborn Field records show that daily incoming solar energy averaged 15.2$MJm^{-2}day^{-1}$, and ranged from 0.7$MJm^{-2}day\text{-}^{1}$to 29.4$MJm^{-2}day^{-1}$ during WY 2012 (Table 4). Daily vapor pressure at Sanborn Field averaged 1.2kPa and went as high as 2.6kPa during the study period. Vapor pressure deficits as high as 3.4kPa and as low as 0 kPa were recorded in Sanborn Field climate records during WY 2012. A mean daily vapor pressure deficit of 1kPa was reported for Sanborn Field (Table 4).

Table 4. Descriptive statistics of WY 2012 climate, Sanborn Field, Columbia,MO.

	Precip mm day^{-1}	Air temp °C	Windspeed (max) ms^{-1}	Rin MJ m^{-2}day^{-1}	Ea kPa	VPD kPa
Mean	2.0	15.6	7.7	15.2	1.2	1.0
Max	45.5	40.5	16.7	29.4	2.6	3.4
Min	0.0	-11.8	3.4	0.7	0.2	0.0
St.Dev.	6.3	9.9	2.4	8.2	0.6	0.8

FLOODPLAIN MICROCLIMATES

Bottomland Hardwood Forest Microclimate

The average air temperature for the Hinkson Creek floodplain BHF during WY 2012 was 14.4°C (Table 5). Air temperatures in the forest reached a maximum of 38.0°C and fell as low as -11.6°C during WY 2012 with a standard deviation of 10.5°C. Relative humidity within the forest ranged from a minimum value of 21% to as high as 100% with a mean value of 73%. Ambient vapor pressure within the forest was as high as 7.6 kPa and as low as 0.2kPa with a mean value of 1.4kPa. Vapor pressure deficits in the BHF were as high as 4.6 kPa and as low as 0kPa, with an average value of 0.6 kPa (Table 5). Maximum wind velocities within the forest were 3.06 m s^{-1} at the 2.5m measurement height. Mean wind velocity was 0.34ms^{-1}. A maximum forest net radiation of 785 Wm^{-2} was calculated. At times forest net radiation was negative (as low as -106 Wm^{-2}) and the average value was 68Wm^{-2}.

The climate records from Sanborn field in Columbia, MO show a total of 739.2mm of precipitation fell during the period from October 1st 2011 until September 31st 2012 (WY 2012). The Hinkson Creek Floodplain AG and BHF precipitation records contained erroneous data due to equipment failure, avian activity and clogging with leaves during critical rainfall events. The Hinkson creek floodplain is located less than 5km from Sanborn field and these records served as proxy precipitation measurements for the forest and grassland sites.

Forest soil moisture in the top 30cm of the pedon ranged from as low as 11.5% volumetric water content (VWC) to as high as 38.0% VWC during WY 2012, with a mean value of 31.2% VWC (Table 5). Forest soil temperatures to 30cm depth averaged 14.04°C. Maximum forest soil temperature at this depth was 25.3°C and the minimum was 2.1°C with a standard deviation of 6.9°C (Table 5).

Grassland Microclimate

During water year 2012 air temperatures recorded at the grassland site reached a maximum of 41.06°C, a minimum of -11.99°C (Table 5). The average grassland air temperature was 14.6°C, with 11.0°C of standard deviation within the WY 2012 microclimate dataset. Grassland relative humidity ranged from 22% to 98%, with a mean value of 71%. Grassland vapor pressures were measured as low as 0.17kPa and as high as 3.35kPa (Table 5). Average grassland vapor pressure during WY 2012 was 1.34kPa. Vapor pressure deficits within the grassland averaged 0.72kPa, and reached as high as

5.97kPa. Negative vapor pressure deficits were calculated for periods of WY 2012. The minimum grassland vapor pressure deficit value for WY 2012 was -0.77kPa. Wind speeds in the grassland ranged from zero to 6.8 ms^{-1}. Mean grassland wind velocity was 1.0 ms^{-1}, and there was 0.9 ms^{-1} of standard deviation within the WY 2012 data set (Table 5). Net radiation was as high as 750 Wm^{-2} in the grassland and as little as -105Wm^{-2} during WY 2012. Mean grassland net radiation was 57Wm^{-2} during the study period.

Grassland soil moisture to 30cm depth was as great as 39.9% VWC and as low as 25.7% VWC during WY 2012 (Table 5). Soil water content of the grassland site averaged 32.5% VWC in the top 30cm of the profile during the measurement period. Soil temperatures to 30cm depth averaged 13.85°C during WY 2012 at the grassland site (Table 5) Grassland soil was subjected to diurnal and seasonal patterns of warming and cooling, with temperatures dropping as low as 0.87°C and as high as 27.02°C during the year that data was recorded.

Table 5. Descriptive statistics of Hinkson Creek Floodplain microclimate, WY 2012

AG	Ts °C	soil ϴ	Ea kPa	RH	Ta °C	VPD kPa	usp ms^{-1}	Rnet Wm^{-2}
Mean	13.9	32.5	1.3	0.7	14.6	0.7	1.0	56.6
Max	27.0	39.9	3.3	1.0	41.1	6.0	6.8	750.8
Min	0.9	25.7	0.2	0.2	-12.0	0.0	0.0	-104.2
St Dev	7.3	4.2	0.7	0.2	11.1	1.0	0.9	196.4
BHF	**Ts °C**	**soil ϴ**	**Ea kPa**	**RH**	**Ta °C**	**VPD kPa**	**usp ms^{-1}**	**Rnet Wm^{-2}**
Mean	14.0	31.2	1.3	0.7	14.4	0.6	0.3	68.4
Max	25.3	38.0	7.6	1.0	37.9	4.6	3.1	784.9
Min	2.1	11.5	0.2	0.2	-11.6	0.0	0.0	-106.1
St Dev	6.9	4.6	0.7	0.2	10.5	0.8	0.5	205.8

Where Ts°C is soil temperature in Celsius, Soil Θ is soil volumetric water content(%), Ea kPa is ambient vapor pressure in kilopascals, RH is relative humidity, Ta°C is air temperature in Celsius, VPD kPa is vapor pressure deficit in kilopascals, usp ms^{-1} is wind speed in meters per second, Rnet Wm^{-2} is net radiation in Watts per square meter.

VEGETATION SURVEY RESULTS

Bottomland Hardwood Forest Understory Vegetation

Vegetation survey results from July 2011 indicated that the bottomland hardwood forest understory was dominated by live vegetation (82.9% of ground coverage) (Figure 9). Leaf litter covered 10.8% of the forest floor and woody litter (sticks, twigs and logs) comprises an additional 2.6% of ground coverage. Bare mineral soil was exposed on 3.3% of the ground area in the BHF (Figure 9). Forest understory vegetation height was measured on August 16th 2012 as a record of growing season maximum, the average of which was 1.1m.

A total of 25 species from 16 separate plant families were detected in the BHF understory (Table 6). A majority, (88%), of the plant species examined are native to Missouri. Woody plants accounted for 21% of the total number of understory species detected (Table 6). The forest understory vegetation was dominated by Stinging nettle (*Urtica dioca*), Ground ivy (*Glechoma hederacea*), and Wild rye (*Elymus virginica*) (Table 7). Tree seedlings accounted for a minor component of the total woody species found. Boxelder (*Acer negundo*), Sycamore (*Platanus occidentalis*) and Red oak

(*Quercus rubra*) seedlings comprised a combined total of 0.21% of the overall forest vegetative cover (Table7).

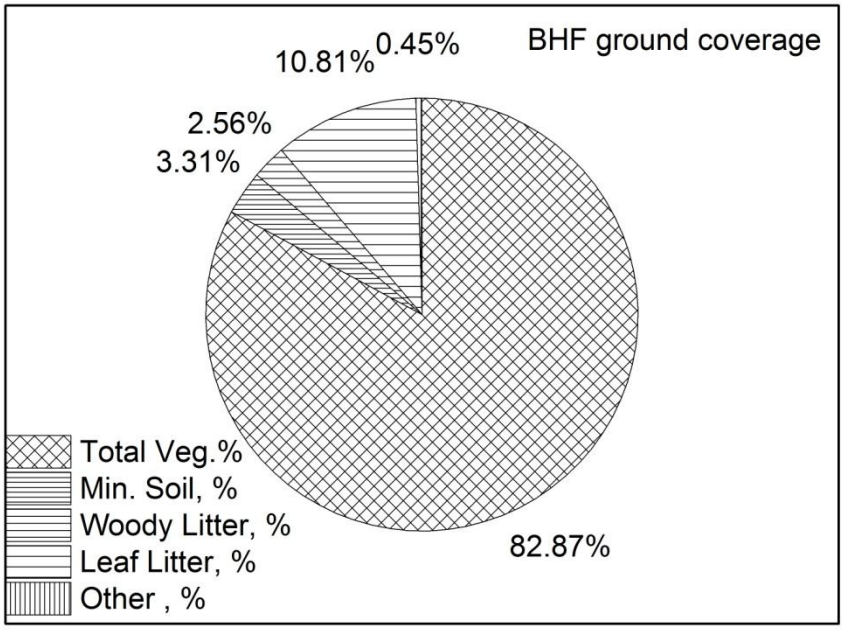

Figure 9. Ground cover composition of Hinkson Creek Floodplain Bottomland hardwood forest site- July 2011.

Table 6. Comparison of Hinkson Creek Floodplain BHF and AG vegetation

	BHF	**AG**
% Native	88	70
% Woody	21	3
% Graminoid	13	24
% Fabaceae	4	13
% Asteraceae	17	27
Total # Species	25	30
Total # Families	16	12

Table 7.. Ground cover species composition Hinkson Creek floodplain BHF- July 2011

Bottomland Hardwood Forest- BHF		
Species - Common name	**Family**	**% Veg.**
Urtica Dioica -Stinging nettle	Urticaceae	35.2
Glechoma Hederacea -Ground ivy	Lamiaceae	31.6
Elymus Viginicus -Wild rye	Poaceae	14.1
Amphicarpaea Bracteata -American hogpeanut	Fabaceae	8.6
Polygonum Hydropiperoides -Swamp smartweed	Polygonaceae	5.3
Verbesina Alternifolia -Yellow ironweed	Asteraceae	3.7
Pilea Pumila -Clear weed	Urticaceae	3.0
Impatiens Capensis –Jewelweed	Balsaminaceae	2.8
Rudbeckia Laciniata- Cutleaf coneflower	Asteraceae	1.8
Humulus Japonicus -Japanese hops	Canabaceae	1.8
Polygonum Virginianum –Jumpseed	Polygonaceae	1.4
Poa spp.- Grasses	Poaceae	0.8
Parthenocissus Quinquefolia -Virginia creeper	Vitaceae	0.35
Boehmeria Cylindrica -Smallspike false nettle	Urticaceae	0.25
Acer Negundo –Boxelder	Aceraceae	0.15
Smilax Spp. -Green briar	Smilaceae	0.14
Ammannia Coccinea -Scarlet Toothcup	Lythraceae	0.10
Dioscorea Villosa -Wild yam	Dioscoraceae	0.10
Euonymus Fortunei -Winter creeper	Celestraceae	0.08
Lycopus Spp. -Bugle weed	Lamiaceae	0.08
Bidens Bipinnata -Spanish needles	Asteraceae	0.06
Platanus Occidentalis -American sycamore	Platanaceae	0.03
Quercus Rubra -Red oak	Fagaceae	0.03
Symphyotrichum Cordifolium -Blue Wood Aster	Asteraceae	0.03
*Carex Frank*ii or *Carex Spp.*	Cyperaceae	0.01

Grassland Vegetation

The grassland site had 49.35% ground coverage by live vegetation in July 2011 (Figure 10). Leaf litter accounted for 41.39% of grassland ground area, with mineral soil and other (in this case rock) comprising 4.82% and 4.43% of the remainder respectively (Figure 10). It should be noted that the grassland site had been mowed several weeks prior to initiation of the vegetation survey in July 2011 and the leaf litter and live vegetation coverage percentages listed here may not represent ground cover conditions during WY 2012 during which the site was not mowed at all.

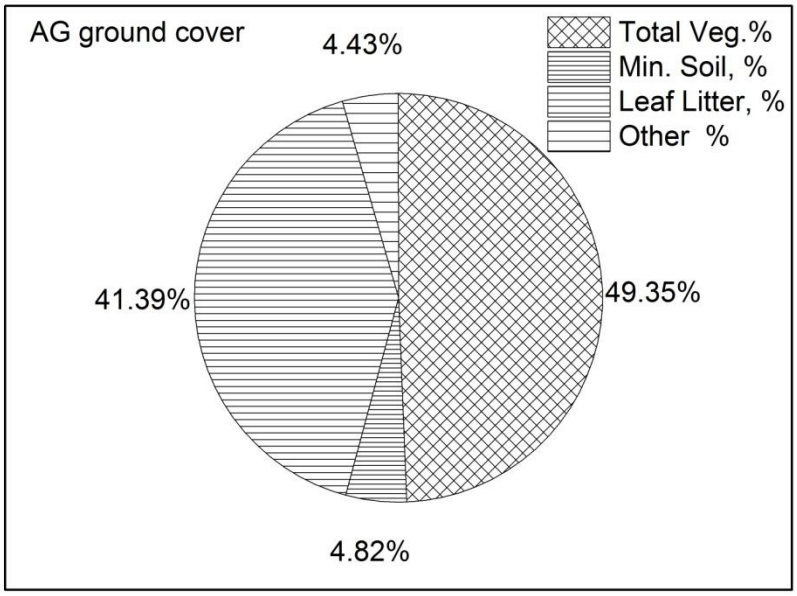

Figure 10. Hinkson Creek Floodplain Agricultural Grassland (AG) site vegetation coverage -July 2011

Grassland vegetation survey species coverage included in descending order, Tall fescue (*Festuca arundinaceae*), June grass (*Koeleria macrantha*), Johnson grass (*Sorghum halepense*), Ground ivy (*Glechoma hederacea*), Japanese hops (*Humulus japonica*) and Missouri goldenrod (*Solidago altissima*) (Table 8). A total of 30 species representing 12 plant families were tallied in the grassland site (Table 6). Of the species surveyed in the grassland 24% were classified as gramminoids, 3% were woody plants (wild grape and Virginia creeper).

Asters (Asteraceae) accounted for 27% of the species found in the grassland (Table 6). Of the total species found in the grassland 13% were members of the fabaceae plant family, thus capable of fixing atmospheric nitrogen for plant use by hosting rhizobial bacterium. Of the grassland vegetation detected in the survey most of the species were native to Missouri (70% native) (Table 6). No tree seedlings were recorded in the grassland site vegetation survey, but potentially invasive Callery pear (*Pyrus spp.)* seedlings were observed in the study area.

Table 8. Hinkson Creek Floodplain grassland vegetation survey results-July, 2011.

Agricultural Grassland- AG		
Species - Common name	**Family**	**% Veg.**
Festuca Arundinacea -Tall fescue	Poaceae	21.1
Koeleria Macrantha -June grass	Poaceae	15.7
Sorghum Halepense -Johnson grass	Poaceae	13.5
Glechoma Hederacea -Ground ivy	Lamiaceae	12.8
Humulus Japonicus -Japanese hops	Canabaceae	11.4
Solidago Altissima -Missouri goldenrod	Asteraceae	7.9
Carex Frankii or *Carex Spp.*-Sedges	Cyperaceae	5.0
Rudbeckia Laciniata -Cutleaf coneflower	Asteraceae	3.6
Phleum Pratense- Timothy	Poaceae	1.5
Solidago Gigantea -Giant goldenrod	Asteraceae	1.5
Verbesina Alternifolia -Yellow ironweed	Asteraceae	1.3
Juncus Spp. (2)- Sedges	Juncaceae	1.2
Phalaris Arundinacea -Reed canary	Poaceae	1.06
Lotus Corniculatus -Bird's-foot Trefoil	Fabaceae	0.94
Solanum Carolinense -Horse nettle	Solanaceeae	0.69
Ambrosia Trifida -Giant ragweed	Asteraceae	0.61
Cirsium Vulgare -Bull Thistle	Asteraceae	0.56
Desmodium Paniculatum -Tick Trefoil	Fabaceae	0.56
Calystegia Silvatica -Shortstalk false bindweed	Convulvaceae	0.31
Physalis Virginiana -Ground Cherry	Solanaceeae	0.28
Verbesina Altissima –Ironweed	Asteraceae	0.25
Muhlenbergia Spp. -Muhly spp.	Poaceae	0.23
Asclepias –Milkweed	Asclepiadaceae	0.17
Rumex Crispus -Curly dock	Polygonaceae	0.17
Elymus Viginicus -Wild rye	Poaceae	0.11
Teucrium Canadense -American Germander	Lamiaceae	0.11
Lactuca Spp.	Asteraceae	0.06
Vicia Dasycarpa -Smooth vetch	Fabaceae	0.03
Trifolium spp.-Ground clover	Fabaceae	0.02
Vitis Spp. -Wild Grape	Vitaceae	0.01

Grassland vegetation height measurements in the 2012 growing season recorded a maximum live height of 1.2m (averaged across the nine plot locations). Plots with the tallest vegetation measured in 2012 were dominated by Johnson grass (*Sorghum halepense*) and Missouri goldenrod (*Solidago altissima*). The maximum vegetation height occurred in early August when the Johnsongrass began anthesis (Table 9). The live vegetation height declined as the Johnsongrass senesced. During September there was a brief period of recovery of live vegetation height when the Missouri goldenrod flowered, but the increase in height was short-lived (figure11). Live vegetation heights decreased rapidly in autumn with the onset of shorter day-lengths and freezing nighttime temperatures (Table 9).

Table 9. Hinkson Creek Floodplain Grassland vegetation heights, April-November 2012

	Vegetation height (m)												
Date	**plot 1**	**plot 2**	**plot 3**	**plot 4**	**plot 5**	**plot 6**	**plot 7**	**plot 8**	**plot 9**	**Mean**	**Max**	**Min**	**St Dev**
20-Apr-12	0.47	0.40	0.51	0.32	0.31	0.76	0.32	0.30	0.29	0.41	0.76	0.29	0.16
3-May-12	0.64	0.51	0.67	0.43	0.45	0.91	0.40	0.37	0.36	0.53	0.91	0.36	0.18
25-May-12	1.04	0.73	0.63	0.68	0.63	0.67	0.70	0.69	0.56	0.70	1.04	0.56	0.13
9-Jun-12	0.96	0.80	0.79	0.84	0.84	0.92	0.74	0.87	0.98	0.86	0.98	0.74	0.08
22-Jun-12	0.88	0.48	0.58	1.10	1.01	1.34	0.60	0.84	1.22	0.89	1.34	0.48	0.30
5-Jul-12	0.82	0.52	0.60	1.33	1.37	1.17	0.62	1.31	1.78	1.06	1.78	0.52	0.44
20-Jul-12	0.99	0.55	0.43	1.43	1.64	1.06	0.67	1.33	1.89	1.11	1.89	0.43	0.50
2-Aug-12	0.92	0.80	0.56	1.57	1.88	0.99	0.66	1.65	1.76	1.20	1.88	0.56	0.51
16-Aug-12	0.83	0.65	0.57	1.38	1.56	1.11	0.56	1.55	1.81	1.11	1.81	0.56	0.48
3-Sep-12	1.01	0.52	0.52	1.43	1.58	0.69	0.50	1.32	1.70	1.03	1.70	0.50	0.49
14-Sep-12	0.69	0.59	0.64	1.44	1.69	0.70	0.53	1.39	1.68	1.04	1.69	0.53	0.50
26-Sep-12	0.46	0.48	0.61	1.25	1.43	0.62	0.49	1.43	1.48	0.92	1.48	0.46	0.46
9-Nov-12	0.37	0.20	0.15	0.22	0.16	0.43	0.26	0.34	0.35	0.27	0.43	0.15	0.10

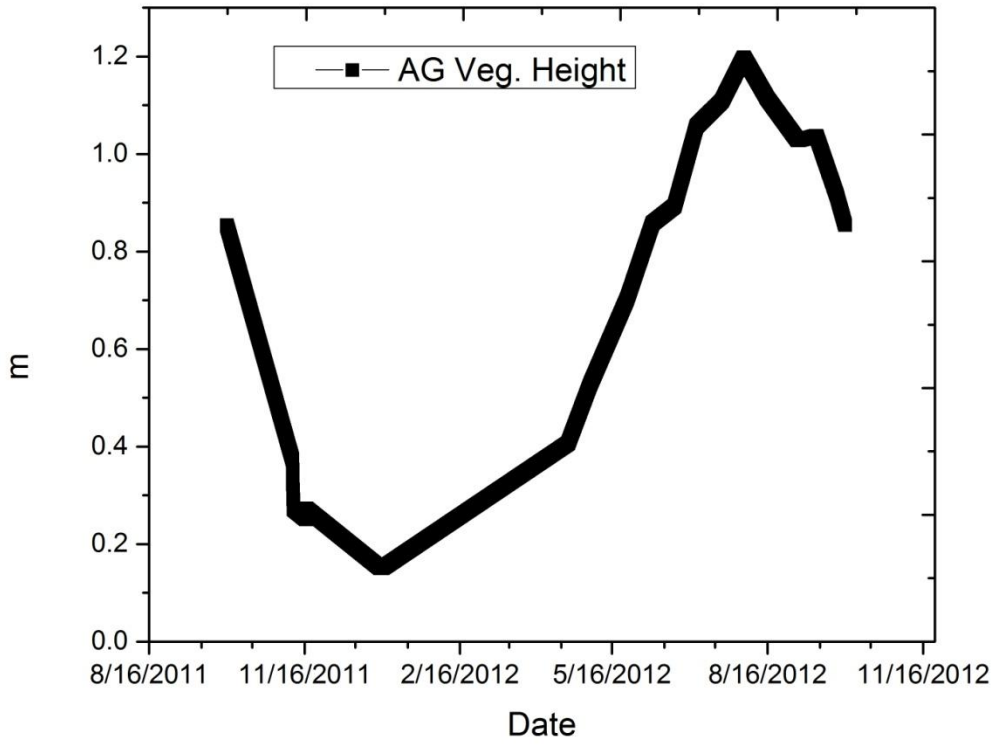

Figure 11. Measured and modeled Hinkson Creek Floodplain Grassland mean vegetation height WY 2012

Bottomland Hardwood Forest Stand Inventory

At the time study bottomland hardwood forest overstory was dominated by Eastern Cottonwood (*Populus deltoides*), Silver maple *(Acer sacharinum*), and Eastern sycamore (*Platanus occidentalis*) trees. The forest mid-story was comprised of Black walnut (*Juglans nigra*) and American elm (*Ulmus Americana*) (Table 10). The forest stand had numerous (16trees hectare^{-1}) Boxelder trees (*Acer negundo*) occupying

intermediate and oppressed canopy positions. Additional tree species observed in the forest (but not tallied as plot trees in the variable radius sampling) include: Honeylocust (*Gleditsia triacanthos*), Hackberry (*Celtis occidentalis*), Green ash (*Fraxinus pennsylvanica*), Osage orange (*maclura pomifera*), River birch (*Betula nigra*), Black willow (*salix nigra*), Black locust (*Robinia psuedoacacia*), Ohio buckeye (*Aesculus glabra*), Paw paw (*Asimina triloba*), Kentucky coffeetree (*Gymnocladus dioicus*) , White mulberry (*Morus alba*) and Black maple (*Acer nigrum*).

The BHF forest mean tree height was 27.99 m, and the basal area was 28.7 m^2 $hectare^{-1}$, with approximately 34 trees $hectare^{-1}$ in the stand (Table 10). The stocking level of the stand was estimated to be 60% (using English units of 124 ft^2 $acre^{-1}$ and 84 trees $acre^{-1}$), from stocking tables developed for bottomland hardwood forests of the Midwest U.S.A. region (Larsen et al., 2010). This stocking percentage exceeds the 'B-line', indicating the forest had a closed canopy, thus satisfying the requirement of uniform and continuous canopy coverage for use of 'big leaf' ET models (Falge et al., 2005, Dai et al., 2004).

Table 10. Tree species and size Hinkson Creek Floodplain BHF -July 2012

	Trees	DBH cm			Height m		
Species	**Hectare^{-1}**	**mean**	**max.**	**min.**	**mean**	**max.**	**min.**
American elm-*Ulmus americana*	5.4	34.4	78.2	18.3	19.7	27.8	11.5
Eastern cottonwood- *Populus deltoides*	1.5	107.5	158.2	72.4	39.4	43.4	30.5
Silver maple- *Acer sacharinum*	8.1	62.4	91.7	24.9	28.9	44.4	4.3
Black walnut - *Juglans nigra*	2.3	46.3	72.4	36.8	29.1	38.9	21.3
Boxelder- *Acer negundo*	16.0	37.0	81.5	12.4	13.9	23.7	3.9
Sycamore- *Platanus occidentalis*	0.6	83.1	108.2	58.4	40.5	49.3	30.3

The frequency distribution of basal area within the forest stand follows a negative exponential curve (Figure 12), indicating an emergent cohort of smaller shade tolerant tree species and a mature overstory of a few large trees (Hubbart et al., 2011). There is no prominent woody understory layer in the forest, although scattered Ohio buckeye (*Aesculus glabra*) and Paw paw (*Asimina triloba*) were observed on the site. Vegetation surveys indicated an abundance of Stinging nettle *(Urtica dioca*), Virginia wild rye *(Elymus virginicus*) and Ground ivy (*Glechoma hederecea*) (Table 7). Woody seedlings detected during vegetation survey include *Acer negundo*, *Platanus occidentalis* and *Quercus rubra* (Table 7). Vegetation survey results do not show advance reproduction of the overstory Cottonwood and Silver maple trees indicating a potential shift to more shade tolerant tree (*Acer negundo*), or mesic (*Quercus rubra*) tree species in the future.

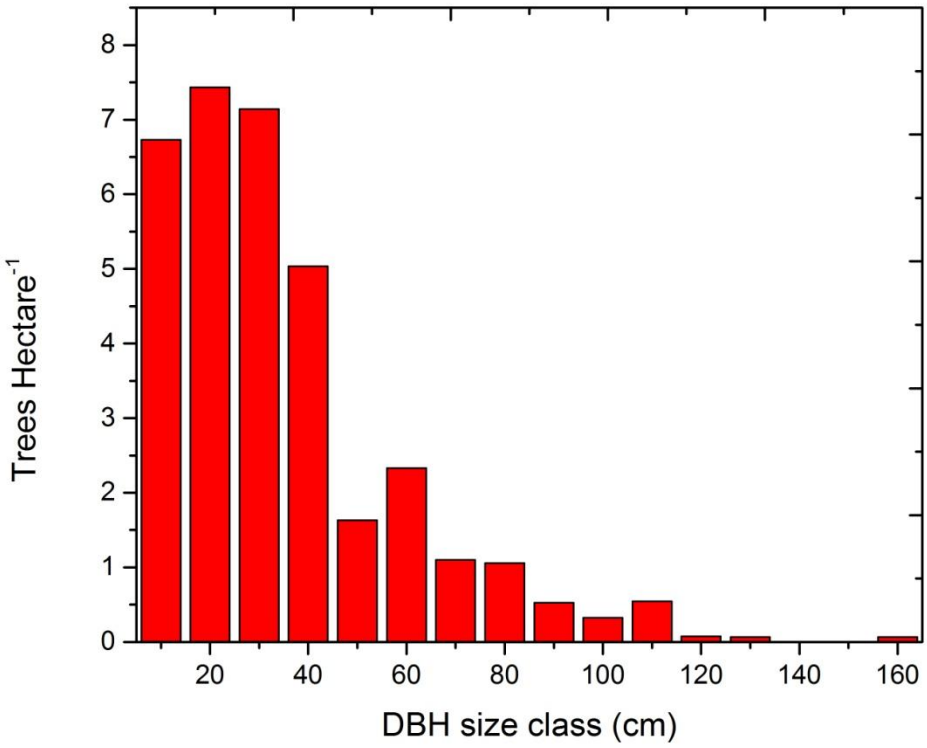

Figure 12. Size class distribution of Hinkson Creek Floodplain Bottomland Hardwood Forest trees

The Average bottomland hardwood forest canopy coverage values ranged from a low value of 55.51% in November to a maximum value of 89.66% in July 2012 (Table 11). Maximum canopy coverage percent occurred in July for most plots (Figure 13), but for plot 1, canopy coverage peaked in June. The early decline of plot 1 canopy coverage is likely the result of observed dieback of the American elm (*Ulmus Americana*) directly above the plot which is presumably infected with Dutch elm disease (*Ophiostoma ulmi*), an introduced old-world pathogen which has been implicated in widespread mortality of

Ulmus spp. in Eastern North America (Hale et al., 2008, Hughes and Cass, 1997). The greatest spatial variability in canopy coverage occurred in the spring and fall, likely because of phenological differences in leaf emergence and senescence across tree species in plots (Table 11). The extent of dormant season canopy coverage was not measured, but it is expected that values dropped below 55% once forest trees were completely defoliated.

Table 11. Hinkson Creek Floodplain Bottomland Hardwood Forest -canopy coverage Measurements (Spherical Densitometer Model-C) April-November 2012.

	Canopy Coverage %												
Date	**plot 1**	**plot 2**	**plot 3**	**plot 4**	**plot 5**	**plot 6**	**plot 7**	**plot 8**	**plot 9**	**Mean**	**Max**	**Min**	**St Dev**
05-Apr-12	69.6	79.2	81.5	83.4	82.1	52.9	69.6	84.1	71.1	74.8	84.1	52.9	10.1
20-Apr-12	83.9	88.0	89.6	82.3	88.0	73.5	80.5	88.0	85.7	84.4	89.6	73.5	5.1
03-May-12	84.7	87.8	91.4	84.1	89.6	75.6	81.5	88.3	84.4	85.3	91.4	75.6	4.8
25-May-12	82.8	88.8	91.7	84.4	89.6	72.2	82.3	89.9	88.8	85.6	91.7	72.2	6.0
09-Jun-12	83.9	91.9	93.8	90.6	93.0	83.9	89.3	91.9	90.9	89.9	93.8	83.9	3.7
22-Jun-12	78.9	91.4	96.4	86.5	94.5	77.6	88.6	94.8	90.9	88.8	96.4	77.6	6.8
05-Jul-12	83.6	93.0	94.5	91.4	92.7	79.2	88.6	94.0	89.9	89.7	94.5	79.2	5.2
20-Jul-12	79.7	91.2	94.5	91.2	95.6	81.8	88.6	94.0	90.1	89.6	95.6	79.7	5.5
02-Aug-12	78.2	89.6	95.3	89.1	90.9	86.5	86.2	92.7	90.4	88.8	95.3	78.2	4.9
16-Aug-12	74.3	90.1	94.8	89.3	93.5	80.8	89.3	92.2	91.2	88.4	94.8	74.3	6.6
03-Sep-12	74.8	87.8	91.7	86.7	92.5	76.9	83.9	89.6	87.5	85.7	92.5	74.8	6.2
14-Sep-12	71.4	80.5	92.2	85.7	88.8	79.2	79.7	86.0	85.7	83.2	92.2	71.4	6.2
26-Sep-12	68.0	81.3	90.1	80.0	87.0	76.9	82.8	83.9	88.8	82.1	90.1	68.0	6.8
26-Oct-12	41.5	50.9	51.6	63.1	69.3	58.9	79.2	78.7	83.4	64.1	83.4	41.5	14.6
09-Nov-12	39.7	53.7	48.0	55.5	68.0	48.8	65.2	57.6	63.1	55.5	68.0	39.7	9.1

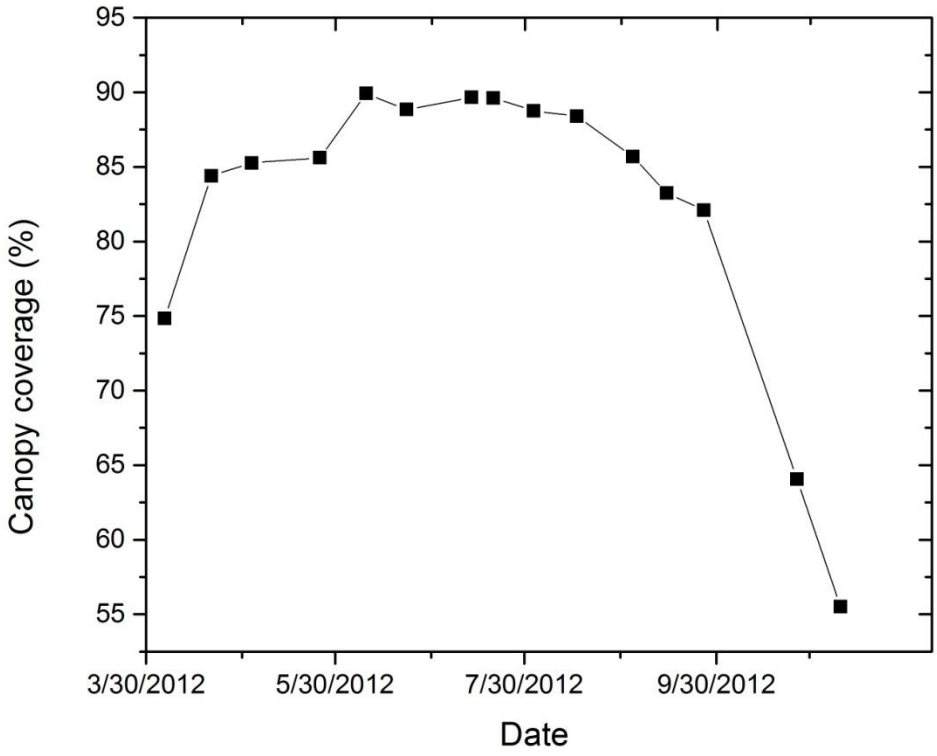

Figure 13. Mean Canopy Coverage percentage (Spherical Densitometer Model-C) measurements, Hinkson Creek Floodplain Bottomland Hardwood Forest, Columbia, Missouri. 2012

EVAPOTRANSPIRATION ESTIMATIONS

Surface Energy Balance

The Surface Energy Balance (SEB) method showed 225mm yr^{-1} greater annual ET within the Hinkson Creek Floodplain forest site than the grassland. Forest evapotranspiration for WY 2012 was estimated as 975mmyr^{-1} and the grassland site modeled 720 mm yr^{-1} of ET (Table 12).

Penman-Monteith

The Penman- Monteith (P-M) method of ET calculation yielded 802 mm yr^{-1} of ET for the BHF site and 719 mm yr^{-1} for the AG site (Table12). The forest site consumed 83mm yr^{-1} more water through transpiration during WY 2012 according to the estimates supplied by the P-M method.

Priestley-Taylor

The Priestley-Taylor (P-T) method estimated 1113 mmyr^{-1} of ET for the forest site and 1034 mm yr^{-1} from the grassland site (Table 12). The forest site lost 79mm yr^{-1} more water than the grassland during WY 2012 according to the estimates calculated by the P-T method.

Easy Penman-Monteith

The easy Penman-Monteith (Easy P-M) method reported 593 $mmyr^{-1}$ of ET from the forest site and 518 mm yr^{-1} for the grassland site (Table 12). Forest ET was greater than grassland ET by a difference of 75 mm yr^{-1} according to the estimates derived by the Easy P-M method.

McNaughton-Black

Annual ET for WY 2012 was higher in the forest than in the grassland according to the estimate calculated using the McNaughton-Black (McN-B) method. Forest ET was estimated at 745mm yr^{-1},using the McN-B method (Table12). Grassland ET was calculated to be 315mm yr^{-1} for WY 2012 using the McN-B method. According to these estimates, forest ET was more than double the grassland ET, with a difference of 430mm yr^{-1} between the two McNaughton-Black estimates.

Bowen Ratio Energy Balance

Forest evapotranspiration was greater than grassland evapotranspiration according to estimates supplied through calculation of the Bowen ratio energy balance (Bowen). Bowen ratio energy balance forest ET was estimated at 1589 $mmyr^{-1}$ for the WY 2012.

Grassland ET was calculated to be less using Bowen, with annual ET totaling 1214 mmyr^{-1} (Table12). The forest Bowen evapotranspiration estimate was 375 mm yr^{-1} higher than the grassland Bowen evapotranspiration estimate.

Shuttleworth-Wallace

The Shuttleworth-Wallace (S-W) equation was the only ET calculation method examined in this study that yielded higher evapotranspiration in the grassland than in the forest site. Using the S-W method forest ET was estimated at 458 mmyr^{-1} for WY 2012 (Table12). Grassland ET for WY 2012 calculated using S-W totaled 722mm yr^{-1}, 224 mm yr^{-1}more than the forest S-W ET estimate.

Table 12..Hinkson Creek Floodplain Bottomland Hardwood Forest (BHF) and Agricultural Grassland (AG) Evapotranspiration Estimates for WY 2012

	SEB mm yr^{-1}	**P-M** mm yr^{-1}	**P-T** mm yr^{-1}	**Esy P-M** mm yr^{-1}	**McN-B** mm yr^{-1}	**Bowen** mm yr^{-1}	**S-W** mm yr^{-1}
BHF	975	802	1113	593	745	1589	458
AG	720	719	1034	518	315	1214	722

EVAPOTRANSPIRATION RESULTS DATA ANALYSIS

Evapotranspiration Results Data Analysis

Annual ET estimates were greater in the BHF than Ag sites for six out of the seven methods examined (Table 12). The estimates range from a minimum value of 315mm yr^{-1} of AG site ET in calculated by the McNaughton-Black method to a high value of 1589mm yr^{-1} in the BHF calculated by the Bowen ratio method.

The methods of ET calculation appear to vary according to season as well as in overall magnitude (Figures 14, 15). The Shuttleworth –Wallace and McNaughton-Black ET calculation methods feature an asymptotic cumulative ET line. The Bowen ratio method provides the largest annual ET value of any method for both the BHF and Ag sites (Table 12). The Surface energy balance, Penman Monteith and Shuttleworth-Wallace equations all yield similar ET estimates for the AG site (Figure 15), but show wide variation in ET values for the BHF (Figure 14).

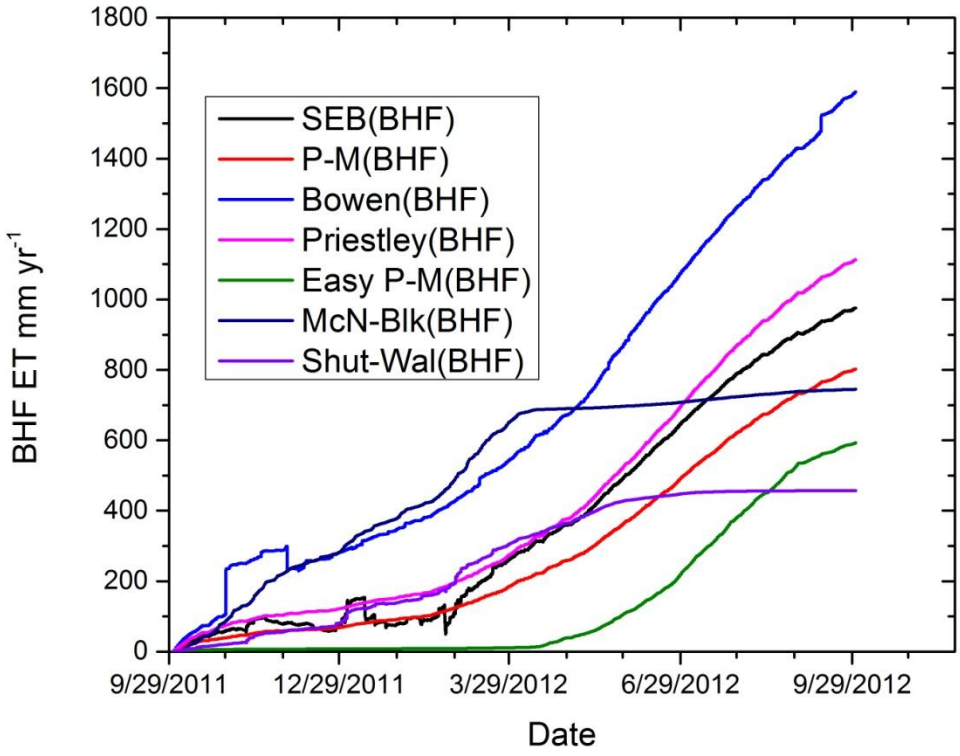

Figure 14. Hinkson Creek Floodplain Bottomland Hardwood Forest (BHF) time series graph of cumulative annual ET for all models examined- Columbia, Missouri-WY 2012

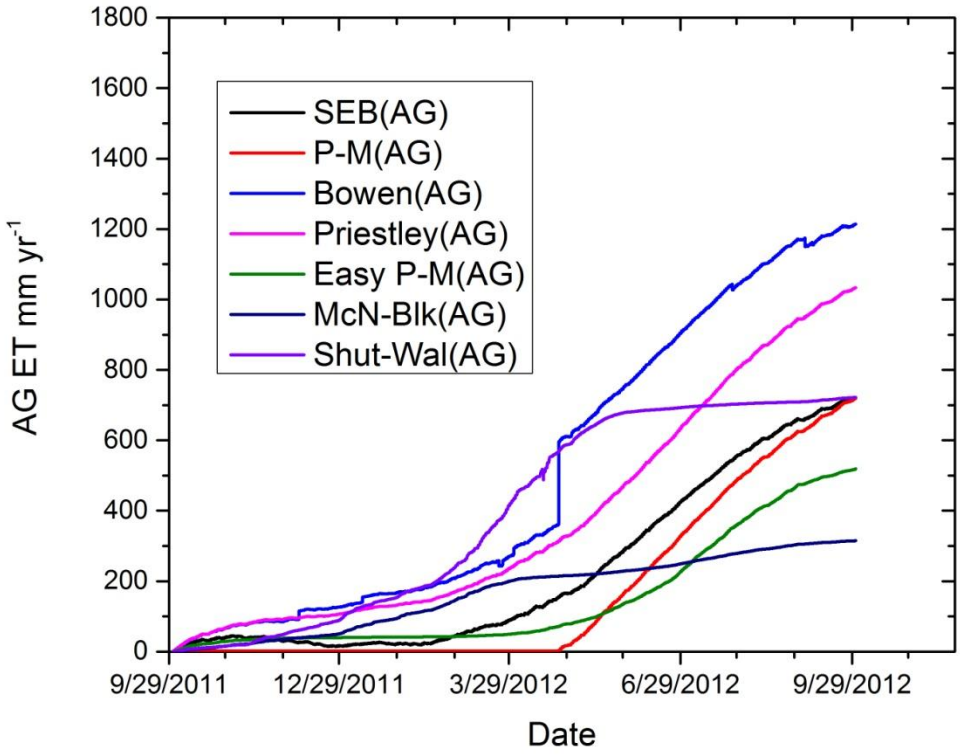

Figure 15. Hinkson Creek Floodplain Agricultural grassland (AG) time series of cumulative annual ET for all models examined Columbia, Missouri- WY 2012 (Penman Monteith negative modeled values zeroed for cumulative sums during the period 10-1-11 to 4-24-12)

Pan Evaporation- Evapotranspiration Model Comparison

Pan evaporation rates were measured at the University of Missouri Horticulture and Agroforestry Research Center (HARC) (New Franklin, MO Lat:39.1, Long:-92.5) during the growing season of the 2012 water year. This mass flux data provided a useful comparison of potential evaporation rates measured during the study period. The Horticulture and Agroforestry Research Center, which is located in New Franklin Missouri (approximately 40km from the Hinkson Floodplain research site) contains a diverse mixture of pastures, forests, orchards and ponds. Pan evaporation measurements were taken at HARC daily during the 2012 growing season and were reported as monthly sums. Comparison of HARC pan evaporation rates to Hinkson floodplain BHF and AG ET show good agreement for all methods except for the Shuttleworth-Wallace and McNaughton-Black models (Tables 13 and 14). Monthly evapotranspiration calculated for the McNaughton-Black and Shuttleworth-Wallace during summer months was statistically different from HARC pan evaporation rates (Table 15). The average summer monthly ET rates of the seven Hinkson Floodplain methods are also statistically different from measured HARC pan evaporation in both the BHF and AG sites, although the average ET for this period is diminished by the inclusion of the lesser McNaughton-Black and Shuttleworth-Wallace data (Table 15).

Table13. Monthly Pan Evaporation (HARC) and Hinkson Creek floodplain grassland evapotranspiration

2012 Month	Pan Evap(HARC) mm E	SEB(AG) mm ET	P-M(AG) mm ET	Bowen(AG) mm ET	P-T(AG) mm ET	Easy P-M(AG) mm ET	McN-B(AG) mm ET	S-W(AG) mm ET
April	119.6	71.0	119.9	317.3	86.2	28.4	12.9	154.6
May	188.2	128.9	154.7	147.9	150.7	62.0	14.0	90.3
June	221.5	138.6	164.3	155.8	164.6	95.5	21.5	13.8
July	242.6	268.8	324.2	291.5	332.9	228.8	51.6	23.4
August	189.7	94.7	126.3	119.4	130.6	104.5	23.6	5.7
September	102.9	61.8	94.2	44.0	89.1	44.3	10.0	12.7
Total (A-S)	1064.5	763.8	983.5	1075.8	954.1	563.5	133.5	300.5

Table14. Monthly Pan Evaporation (HARC) and Hinkson Creek floodplain bottomland hardwood forest evapotranspiration

2012 Month	Pan evap (HARC) mm E	SEB(BHF) mm ET	P-M(BHF) mm ET	Bowen(BHF) mm ET	P-T(BHF) mm ET	Easy P-M(BHF) mm ET	McN-B(BHF) mm ET	S-W(BHF) mm ET
April	119.6	89.7	68.5	121.9	95.8	28.0	27.4	53.8
May	188.2	142.5	110.9	208.3	156.4	73.8	7.3	63.7
June	221.5	152.8	128.8	202.6	172.2	118.7	11.7	19.2
July	242.6	294.3	258.7	390.7	345.9	279.5	27.6	25.7
August	189.7	105.7	102.7	154.2	137.1	142.7	14.1	1.2
September	102.9	71.3	69.5	159.6	94.4	57.9	5.7	0.8
Total (A-S)	1064.5	856.3	739.1	1237.3	1001.7	700.6	94.0	164.3

Table 15. Anova results HARC Pan Evaporation and Hinkson Floodplain ET methods

Anova results HARC Pan evaporation vs Hinkson Floodplain ET			
Statistically different*	**P-value**	**not statistically different***	**P-value**
McNaughton-Black (BHF)	3.52E-05	Surface Energy Balance (BHF)	0.40452
Shuttleworth-Wallace (BHF)	5.98E-05	Penman-Monteith (BHF)	0.16923
BHF mean	0.08947	Bowen ratio (BHF)	0.53862
		Priestley -Taylor (BHF)	0.81776
		Easy Penman-Monteith(BHF)	0.96979
McNaughton -Black (AG)	0.0484	Surface Energy Balance (AG)	0.22003
Shuttleworth-Wallace (AG)	1.34E-04	Penaman-Monteith (AG)	0.74595
AG mean	0.0484	Bowen ratio (AG)	0.81776
		Priestley -Taylor (AG)	0.68099
		Easy Penam-Monteith (AG)	0.68099
*at the 0.05 significance level			

Sanborn Field Reference Evapotranspiration Comparison

Climate measurements are continuously recorded and digitally archived at Sanborn field, a historic crop research site located on the University of Missouri campus in Columbia, Missouri. The plots at Sanborn field have been cropped continuously since 1988 (Jordan et al., 2004) and contain an automated climate station with a service which calculates and publishes (online) reference ET for well watered grass crops. Reference ET calculations from the Sanborn field climate station (Accessed May 15th 2013 aes.missouri.edu/sanborn/weather/sanreal.stm) report a potential evapotranspiration rate of 1176mm for water year 2012 (Figure 16). This is greater than any of the Hinkson

floodplain ET estimates except for the Bowen ratio method for both the BHF and AG (Figure 16). The Sanborn field ET estimates provide a useful comparison to Hinkson floodplain ET because of its' close proximity (approximately 3km away). Sanborn Field WY 2012 reference ET estimates are most closely matched by the BHF Priestley-Taylor and AG Bowen ratio calculation outputs (Figure 16). The Priestley–Taylor method is recognized as an estimate of potential evapotranspiration, so it is fitting that the P-T ET estimate is closest to the Sanborn reference ET which is also a measure of potential ET.

Baskett Area Eddy Covariance- ET Comparison

The Baskett research area located in Ashland, Missouri, has an Ameriflux tower which logs continuous eddy covariance measurements of water vapor flux lost to the atmosphere (Yang et al., 2010). Located within a large tract of upland hardwood forest (Garrett et al. 1985), the Baskett Ameriflux tower flux provides an accurate measurement of annual forest ET in central Missouri (Gu et al., 2012). Baskett area vapor flux data measured 806 mm yr^{-1} of ET for the water year 2012 (Accessed May 15th, 2013. ftp://cdiac.ornl.gov/pub/ameriflux/data/Level1/Sites_ByName/Missouri_Ozark/) (Figure 16).

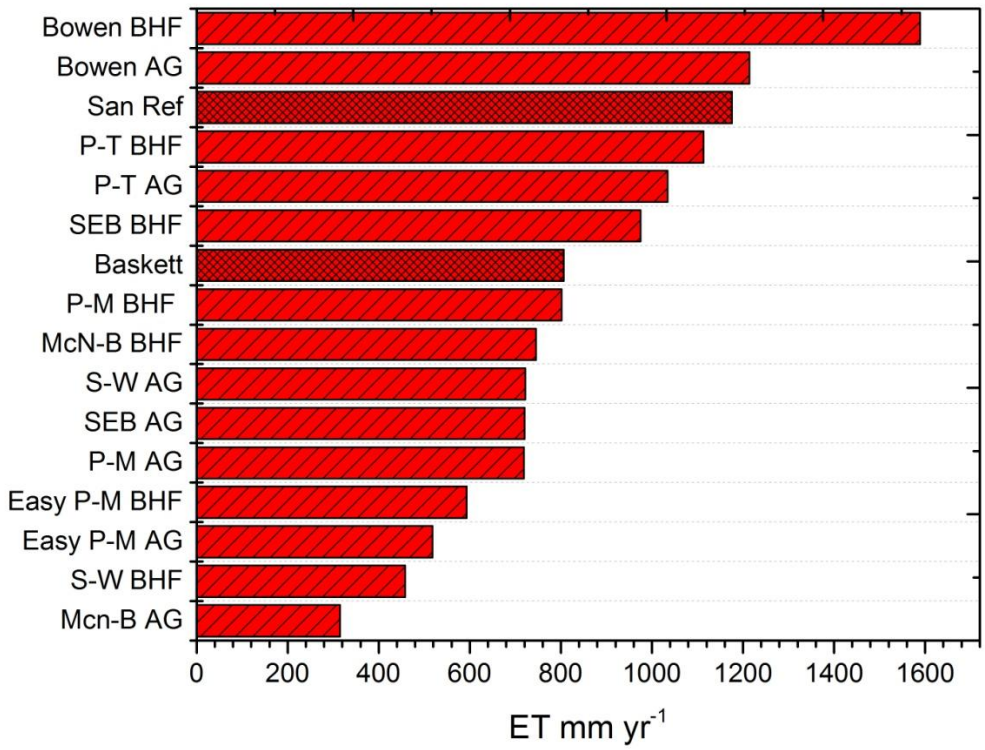

Figure 16.Measured and modeled Evapotranspiration rates for Hinkson Creek Floodplain, with Sanborn Field and Baskett Research Area (in dense cross-hatching)-WY 2012

The Hinkson Floodplain ET estimates that are closest to the WY 2012 measured vapor flux at Baskett research area are the Penman-Monteith and Surface Energy Balance calculations from the bottomland hardwood forest (Figure 16). Although the Penman-Monteith method is widely viewed as highly accurate, it was expected that BHF ET would exceed that of the Baskett area, since the floodplain soils have greater water

holding capacity and effective rooting depths (Young et al., 2001). Therefore, the Surface Energy Balance BHF ET estimate may actually be a more accurate for riparian forests.

EVAPOTRANSPIRATION RESULTS STATISTICAL ANALYSIS

Differences between the BHF and AG site were examined for statistical significance using a one way Anova. There were differences in the mean ET values between the BHF and AG site for the Surface Energy Balance, Penman-Monteith, Easy Penman-Monteith, McNaughton-Black and Shuttleworth-Wallace methods (at the 0.05 significance level). The average hourly ET output of the seven methods were compared for the BHF and AG sites and also were found to be different at the 0.05 significance level (Table 10).

Table 16. Anova results: BHF and AG WY'12 ET

Anova results -BHF vs AG ET			
Statistically different *	**P-value**	**Not statistically different***	**P-value**
Surface Energy Balance	0.00108	Penman-Monteith	0.64187
Priestley-Taylor	0.01219	Bowen Ratio	0.18793
Easy Penman-Monteith	3.64E-07		
McNaughton-Black	0		
Shuttleworth -Wallace	0		
Mean comparison	0.00573		
* at the 0.05 level			

A comparison of mean ET values in Anova showed that there was no statistical difference between the values for the Surface Energy Balance (BHF and AG) and the Sanborn reference ET (Table 12). The AG site Bowen ratio and forest Penman-Monteith ET estimates also were not statistically different from the Sanborn field reference ET values (Table 17). It is not surprising that the Penman-Monteith method is not statistically different than Sanborn field outputs because the reference ET calculation is itself a modified version of the Penman-Monteith equation (ASCE-EWRI) which uses local data inputs and empirical values to estimate potential ET (Lee, 2009, Irmak et al., 2003).

Table 17. Anova results Sanborn reference ET and Hinkson Creek Floodplain ET methods

Anova results: Sanborn Field reference ET vs Hinkson Floodplain ET			
Statistically different*	**P-value**	**not statistically different**	**P-value**
Bowen ratio (BHF)	0.00751	Surface Energy Balance(BHF)	0.7924
Priestley-Taylor(BHF)	0.02887	Penman-Monteith (BHF)	0.5933
Easy Penman-Monteith (BHF)	0		
McNaughton-Black (BHF)	0		
Shuttleworth- Wallace(BHF)	0		
BHF Mean	2.22E-16		
Penman-Monteith (AG)	0.01105	Surface Energy Balance(AG)	0.5087
Priestley-Taylor (AG)	7.90E-07	Bowen ratio (AG)	0.87705
Easy Penman-Monteith (AG)	0		
McNaughton-Black(AG)	0		
Shuttleworth- Wallace (AG)	0		
AG mean	0		
*at the 0.05 significance level			

The BHF and AG Penman-Monteith WY 2012 ET estimates were not statistically different from measured Baskett ET (Table 18). The AG site Bowen ratio ET estimate was also not statistically different from Baskett area ET (Table 18).

Table 18. Anova results: Baskett area ET vs. Hinkson Creek Floodplain ET modeling methods

Anova results: Hinkson ET vs Baskett			
Statistically different *	**P-value**	**not statistically different**	**P-value**
Surface Energy Balance (BHF)	0.02304	Penman-Monteith (BHF)	0.85556
Bowen ratio(BHF)	3.60E-07		
Priestley-Taylor(BHF)	0		
Easy Penman-Monteith(BHF)	0		
McNaughton-Black(BHF)	0.00219		
Shuttleworth-Wallace(BHF)	0		
BHF mean	0.00493		
Surface Energy Balance(AG)	0.00528	Penman-Monteith (AG)	0.62985
Priestley-Taylor (AG)	0	Bowen ratio(AG)	0.09013
Easy Penman-Monteith(AG)	0	AG mean	0.23187
McNaughton-Black(AG)	0		
Shuttleworth-Wallace (AG)	0.00366		
*at the 0.05 significance level			

Anova comparison of HARC Pan Evaporation and Hinkson Creek Floodplain ET models only showed statistical differences for the McNaughton-Black and Shuttleworth - Wallace methods (Table 19).

Table 19. Anova comparison of measured Pan Evaporation (HARC) New Franklin, Missouri and Hinkson Creek ET models, April to November 2012.

Anova results HARC Pan evaporation vs Hinkson Floodplain ET			
Statistically different*	**P-value**	**not statistically different***	**P-value**
McNaughton-Black (BHF)	3.52E-05	Surface Energy Balance (BHF)	0.40452
Shuttleworth-Wallace (BHF)	5.98E-05	Penman-Monteith (BHF)	0.16923
BHF mean	0.08947	Bowen ratio (BHF)	0.53862
		Priestley -Taylor (BHF)	0.81776
		Easy Penman-Monteith(BHF)	0.96979
McNaughton -Black (AG)	0.0484	Surface Energy Balance (AG)	0.22003
Shuttleworth-Wallace (AG)	1.34E-04	Penaman-Monteith (AG)	0.74595
AG mean	0.0484	Bowen ratio (AG)	0.81776
		Priestley -Taylor (AG)	0.68099
		Easy Penam-Monteith (AG)	0.68099
*at the 0.05 significance level			

A Tukey means comparison of the seven ET methods show statistical differences at the 0.05 significance level (Table 20). Mean ET values of the seven models were examined for the BHF and AG sites respectively. Therefore the null hypothesis that all of the ET calculation methods would produce equivalent results is not supported (Table 20).

Table 20 .Tukey comparison of mean ET values for Hinkson Creek AG and BHF sites.

Tukey	MeanDiff	SEM	q Value	Prob	Alpha	Sig	LCL	UCL
P-M(AG) SEB(AG)	-1.76E-04	0.01843	0.01348	1	0.05	0	-0.05452	0.05417
Bowen(AG) SEB(AG)	0.05614	0.01843	4.30732	0.03754	0.05	1	0.0018	0.11049
Bowen(AG) P-M(AG)	0.05632	0.01843	4.3208	0.03648	0.05	1	0.00197	0.11067
Priestley(AG) SEB(AG)	0.03564	0.01843	2.73431	0.45794	0.05	0	-0.01871	0.08999
Priestley(AG) P-M(AG)	0.03582	0.01843	2.74779	0.45164	0.05	0	-0.01853	0.09017
Priestley(AG) Bowen(AG)	-0.0205	0.01843	1.573	0.92462	0.05	0	-0.07485	0.03385
easy p-m(AG) SEB(AG)	-0.02297	0.01843	1.76193	0.87611	0.05	0	-0.07732	0.03138
easy p-m(AG) P-M(AG)	-0.02279	0.01843	1.74845	0.88006	0.05	0	-0.07714	0.03156
easy p-m(AG) Bowen(AG)	-0.07911	0.01843	6.06925	3.56E-04	0.05	1	-0.13346	-0.02476
easy p-m(AG) Priestley(AG)	-0.05861	0.01843	4.49624	0.02485	0.05	1	-0.11296	-0.00426
McN-Blk(AG) SEB(AG)	-0.04616	0.01843	3.54142	0.15761	0.05	0	-0.10051	0.00819
McN-Blk(AG) P-M(AG)	-0.04599	0.01843	3.52794	0.16106	0.05	0	-0.10033	0.00836
McN-Blk(AG) Bowen(AG)	-0.10231	0.01843	7.84874	5.97E-07	0.05	1	-0.15665	-0.04796
McN-Blk(AG) Priestley(AG)	-0.0818	0.01843	6.27573	1.84E-04	0.05	1	-0.13615	-0.02745
McN-Blk(AG) easy p-m(AG)	-0.0232	0.01843	1.77949	0.87084	0.05	0	-0.07754	0.03115
Shut-Wal(AG) SEB(AG)	1.79E-04	0.01843	0.01372	1	0.05	0	-0.05417	0.05453
Shut-Wal(AG) P-M(AG)	3.55E-04	0.01843	0.02721	1	0.05	0	-0.05399	0.0547
Shut-Wal(AG) Bowen(AG)	-0.05597	0.01843	4.29359	0.03865	0.05	1	-0.11031	-0.00162
Shut-Wal(AG) Priestley(AG)	-0.03546	0.01843	2.72059	0.46437	0.05	0	-0.08981	0.01889
Shut-Wal(AG) easy p-m(AG)	0.02315	0.01843	1.77565	0.872	0.05	0	-0.0312	0.07749
Shut-Wal(AG) McN-Blk(AG)	0.04634	0.01843	3.55514	0.15415	0.05	0	-0.00801	0.10069
At the 0.05 significance level the population means are statistically different								

Tukey	MeanDiff	SEM	q Value	Prob	Alpha	Sig	LCL	UCL
P-M(BHF) SEB(BHF)	-0.01965	0.01058	2.62629	0.50917	0.05	0	-0.05084	0.01155
Bowen(BHF) SEB(BHF)	0.06987	0.01058	9.33935	8.40E-10	0.05	1	0.03868	0.10107
Bowen(BHF) P-M(BHF)	0.08952	0.01058	11.96564	1.11E-15	0.05	1	0.05833	0.12072
Priestley(BHF) SEB(BHF)	0.01569	0.01058	2.09684	0.75534	0.05	0	-0.01551	0.04688
Priestley(BHF) P-M(BHF)	0.03534	0.01058	4.72313	0.01471	0.05	1	0.00414	0.06653
Priestley(BHF) Bowen(BHF)	-0.05419	0.01058	7.24251	6.30E-06	0.05	1	-0.08538	-0.02299
easy p-m(BHF) SEB(BHF)	-0.04348	0.01058	5.81145	7.84E-04	0.05	1	-0.07468	-0.01228
easy p-m(BHF) P-M(BHF)	-0.02383	0.01058	3.18517	0.26767	0.05	0	-0.05503	0.00736
easy p-m(BHF) Bowen(BHF)	-0.11335	0.01058	15.1508	4.44E-16	0.05	1	-0.14455	-0.08216
easy p-m(BHF) Priestley(BHF)	-0.05917	0.01058	7.90829	4.69E-07	0.05	1	-0.09036	-0.02797
McN-Blk(BHF) SEB(BHF)	-0.02621	0.01058	3.50339	0.1675	0.05	0	-0.05741	0.00498
McN-Blk(BHF) P-M(BHF)	-0.00656	0.01058	0.87711	0.9962	0.05	0	-0.03776	0.02463
McN-Blk(BHF) Bowen(BHF)	-0.09609	0.01058	12.84274	4.44E-16	0.05	1	-0.12728	-0.06489
McN-Blk(BHF) Priestley(BHF)	-0.0419	0.01058	5.60024	0.00146	0.05	1	-0.07309	-0.0107
McN-Blk(BHF) easy p-m(BHF)	0.01727	0.01058	2.30806	0.66145	0.05	0	-0.01393	0.04846
Shut-Wal(BHF) SEB(BHF)	-0.05892	0.01058	7.87571	5.36E-07	0.05	1	-0.09012	-0.02773
Shut-Wal(BHF) P-M(BHF)	-0.03927	0.01058	5.24943	0.00388	0.05	1	-0.07047	-0.00808
Shut-Wal(BHF) Bowen(BHF)	-0.1288	0.01058	17.21507	4.44E-16	0.05	1	-0.15999	-0.0976
Shut-Wal(BHF) Priestley(BHF)	-0.07461	0.01058	9.97256	3.71E-11	0.05	1	-0.10581	-0.04342
Shut-Wal(BHF) easy p-m(BHF)	-0.01544	0.01058	2.06426	0.76881	0.05	0	-0.04664	0.01575
Shut-Wal(BHF) McN-Blk(BHF)	-0.03271	0.01058	4.37232	0.03266	0.05	1	-0.06391	-0.00152
At the 0.05 significance level the population means are statistically different								

Regression Analysis of Explanatory Variables

Incoming solar radiation has been proposed as a primary driving force for ET in natural systems. The intensity of incident solar radiation impacts the output of various ET models differently. While the Penman-Monteith and Priestley-Taylor methods respond with a positive linear increase to additions of solar radiation (Figure 17), ET models such as the SEB and Easy P-M exhibit a less predictable response (Figure 18).

ET models which are not responsive to changes in incoming solar radiation may be plotted against other explanatory variables to examine the source of variation. For instance, the Easy Penman-Monteith model increases linearly with larger vapor pressure deficits, while the SEB is only weakly correlated to increases of vapor pressure deficit

(Figure 19). Overall, ET methods that depend primarily on net radiation (SEB, P-M, Bowen, P-T) appear to be more reliable than those which rely on other stomatal conductance (Easy P-M), vapor pressure deficits and stomatal conductance (McN-B) or a combination of inputs (S-W).

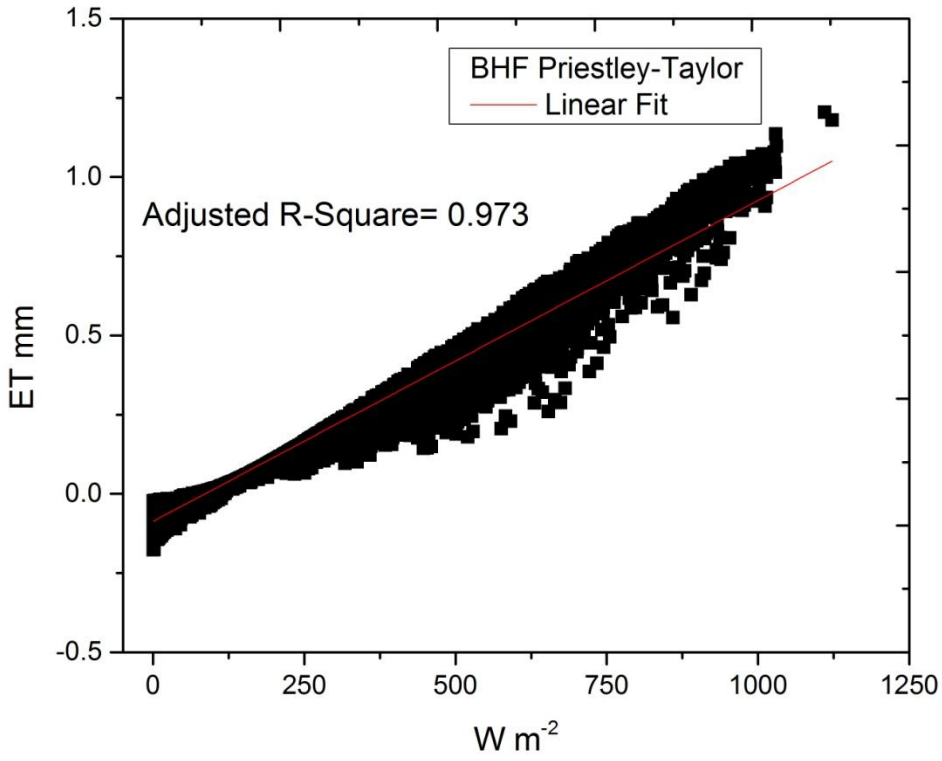

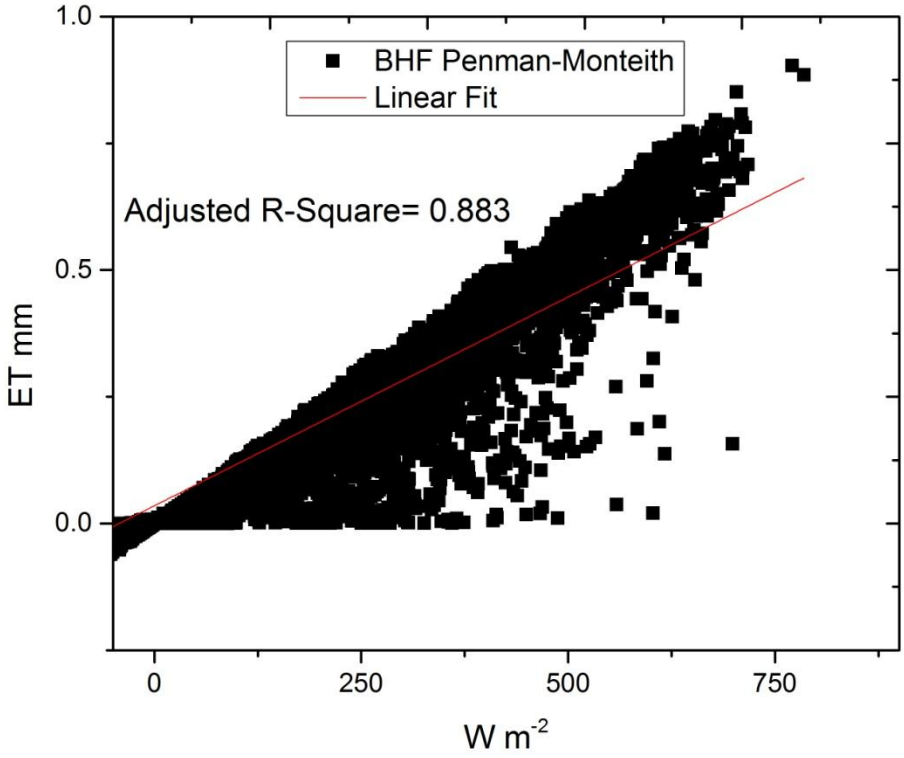

Figure 17.Modeled ET as a response variable of incoming solar radiation using Priestley-Taylor and Penman-Monteith Hinkson Creek Floodplain Bottomland Hardwood Forest (BHF)- WY 2012.

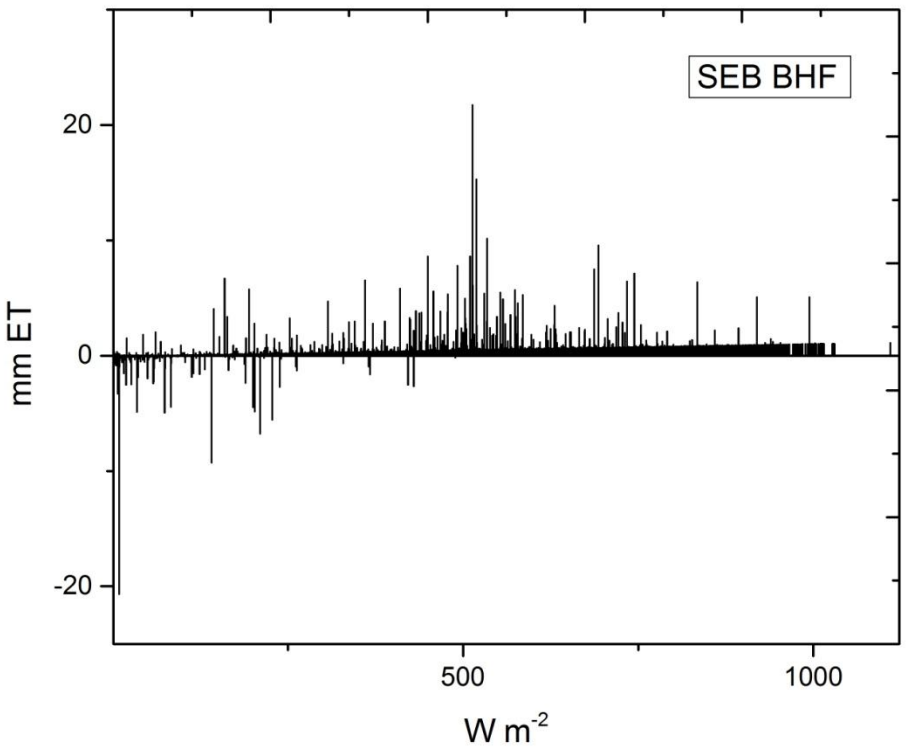
SEB BHF
20
0
-20
mm ET
500
1000
W m-2

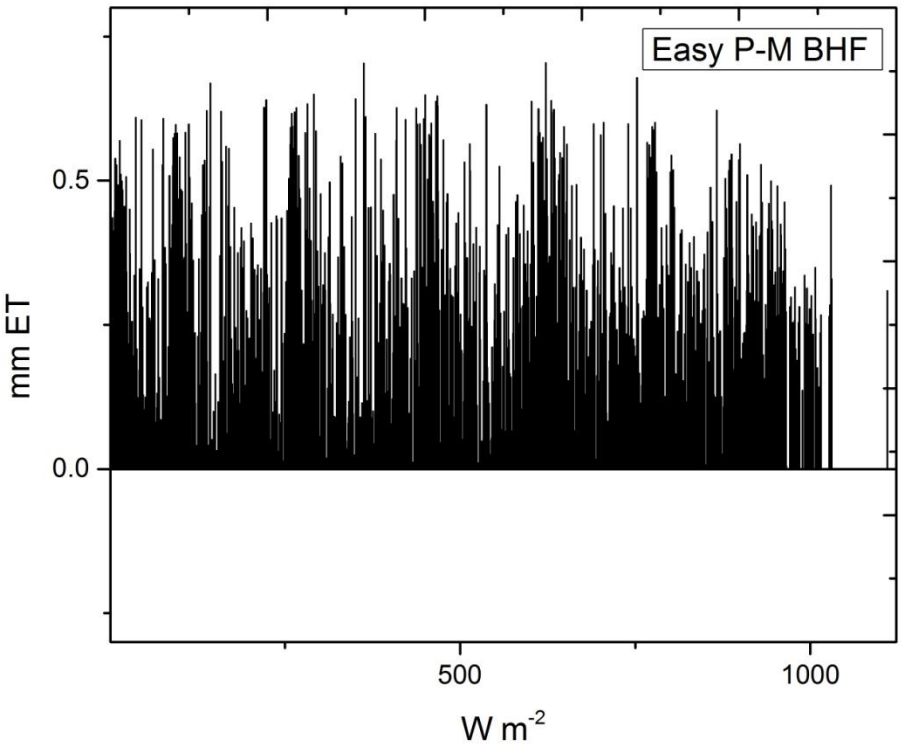

Figure 18. Modeled ET as a response variable of incoming solar radiation using Surface Energy Balance and Easy Penman-Monteith methods, Hinkson Creek Floodplain Bottomland Hardwood Forest (BHF) – WY 2012

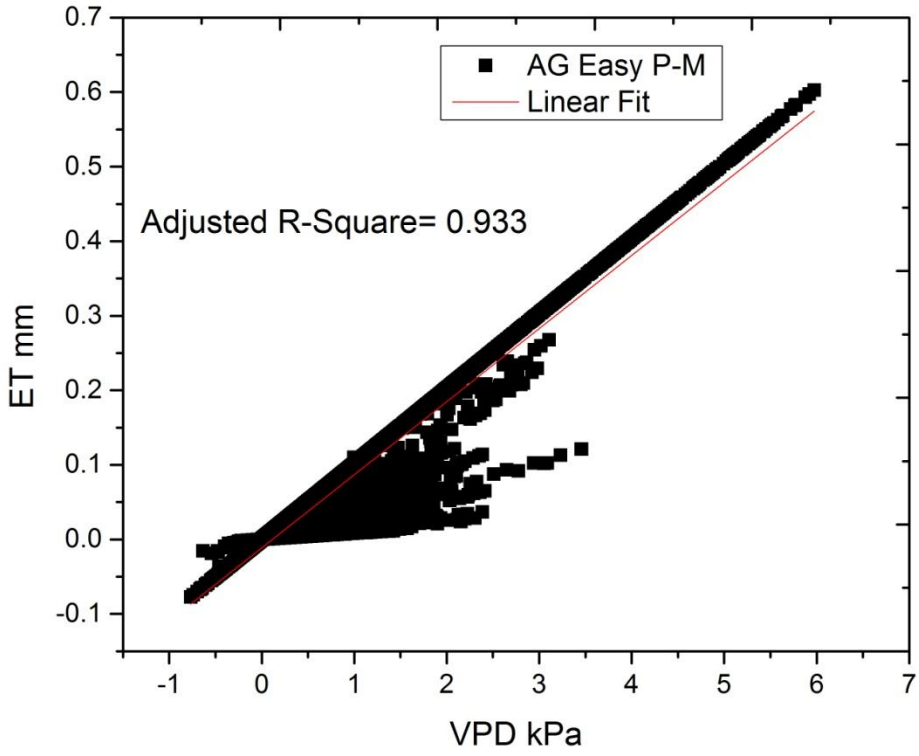
AG Easy P-M
Linear Fit
Adjusted R-Square= 0.933
ET mm
VPD kPa
0.7
0.6
0.5
0.4
0.3
0.2
0.1
0.0
-0.1
-1
0
1
2
3
4
5
6
7

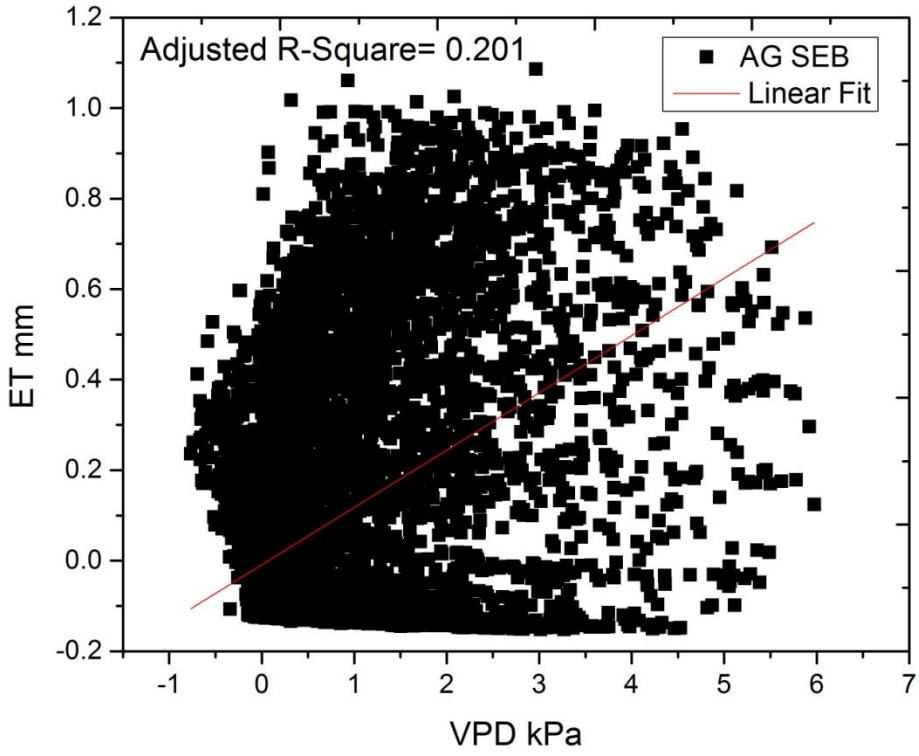

Figure19. Modeled ET as a response variable to vapor pressure deficit using the Easy Penman-Monteith and Surface Energy Balance methods, Hinkson Creek Floodplain Agricultural Grassland (AG)- WY 2012.

CHAPTER V:

DISCUSSION

GENERAL CLIMATE WY 2012

The Water Year 2012 weather was warmer and drier than average in Mid-Missouri. Persistent high pressure air masses aloft prevented entry of moist air masses from the Gulf of Mexico and there were fewer than average summer thunderstorms. Soil Moisture declined to critical levels and large swathes of the central US were under severe drought (Al-Kaisi et al., 2013, Smith, 2013). These conditions resulted in elevated mean air temperatures and vapor pressure deficits in Mid-Missouri.

FOREST AND GRASSLAND MICROCLIMATE

The bottomland hardwood forest and agricultural grassland exhibited measurable differences of several key climate variables recorded during the 2012 growing season (Table 5.). For instance, the mean soil moisture was higher within the Ag site throughout the majority of the water year 2012 (Figure 20).

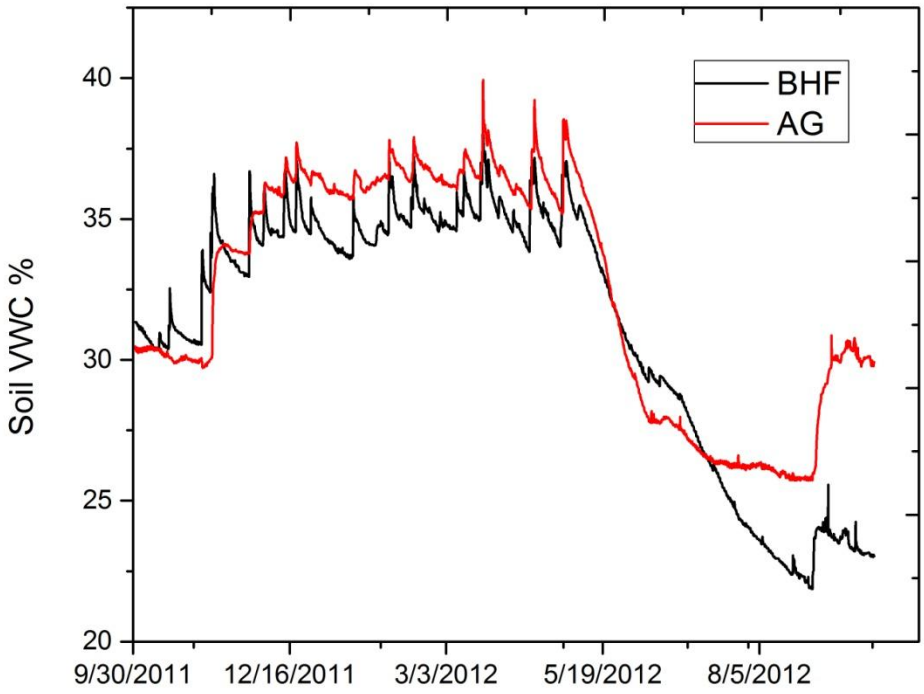

Figure 20. Average Hinkson Creek Floodplain soil Volumetric Water Content (VWC) to 30cm depth WY 2012.

Grassland site soils had greater differences between maximum and minimum moisture values, although the BHF site recorded higher standard deviation of soil moisture values (Table 5). Soil and air temperatures were higher overall in the AG site and displayed greater standard deviation, suggesting a possible buffering effect from the presence of the BHF forest canopy.

Watershed mass balance equations (Eq. 1.3) may be used to estimate basin-wide evapotranspiration, provided that precipitation and discharge are known. The total precipitation minus runoff yields evapotranspiration (assuming there was no change in storage within the watershed). USGS measurements of Hinkson Creek (USGS 06910230) discharge report a total of 24,784,699m^3 water flowed out of the basin during WY 2012 (http://waterdata.usgs.gov/usa/nwis/uv?06910230) (Figure 21). Total discharge divided by approximate watershed area (180,000,000m^2) and multiplied by 1000 (converting meters to mm) gives a total runoff of 137mm yr^{-1}. Climate records from Sanborn Field (Lat: 38.943201°,Long:-92.320395) indicate 739.2 mm yr^{-1} precipitation fell in Columbia, Missouri during WY 2012. A basin wide evapotranspiration rate of 601mm yr^{-1} is estimated from yearly precipitation minus runoff for WY 2012. The effects of drier antecedent soil moisture conditions on stream runoff may be observed in the combined precipitation log and hydrograph (Figure 21), where rainfall events during the latter part of the water year do not elicit a proportional response in stream discharge compared to precipitation events in the spring. Presumably, evapotranspiration of soil moisture during the growing season allowed for greater storage of infiltrated rainfall later in the year, reducing storm runoff and subsequent stream discharge.

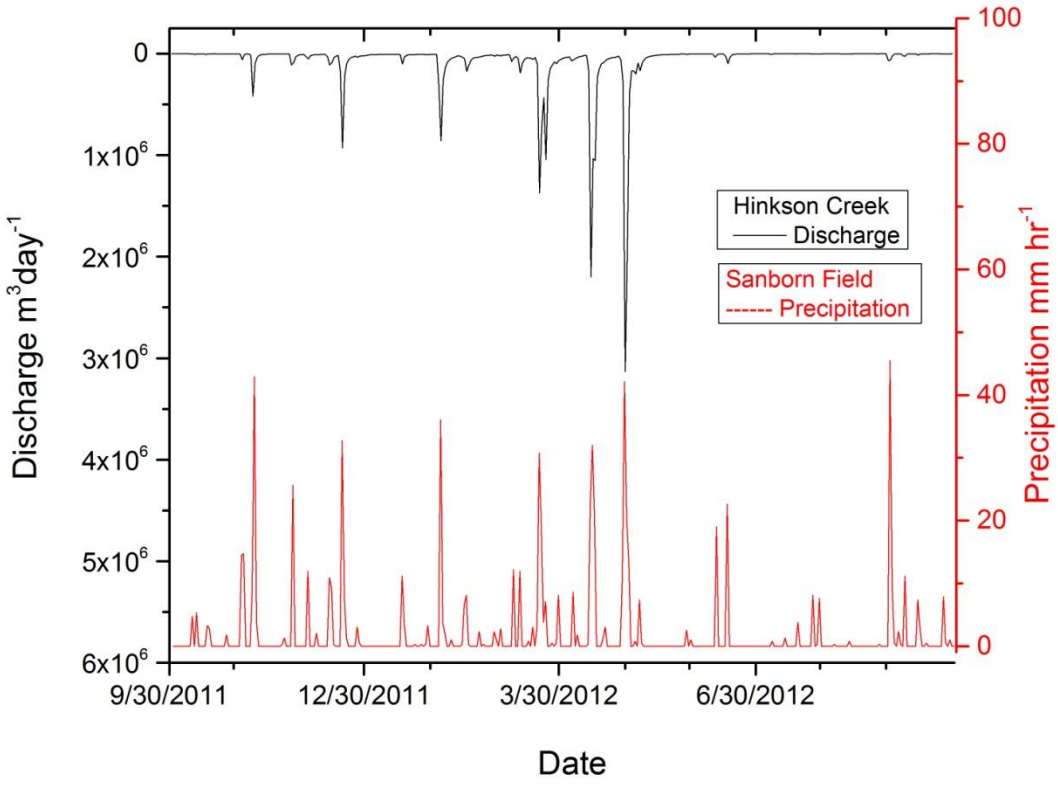

Figure 21.. Daily precipitation (Sanborn Field) and Hinkson Creek discharge (USGS 06910230) -WY 2012, Columbia, Missouri.

FOREST AND GRASSLAND VEGETATION

Vegetation survey results show a greater number of species were found in the AG site, although the BHF site features a higher proportion of native species and more plant families represented (Table 6). Ground coverage within the AG site had a high proportion of leaf litter (AG leaf litter =41.39%, BHF leaf litter =10.81%), (Figures 9 and 10), but the site had been mowed several weeks prior to the survey date and these conditions are not necessarily representative of the site in WY 2012. The AG site was mowed again in September 2011, prior to the beginning of WY 2012 (Oct 1st 2011-Sept 30th 2012) and subsequently the vegetation was allowed to grow freely during the remainder of 2011 and all of 2012.

EVAPOTRANSPIRATION MODEL PERFORMANCE

Surface Energy Balance

The surface energy balance produced plausible ET estimates for both the BHF (975mm yr^{-1}) and AG sites (720mm yr^{-1}) of the Hinkson Creek Floodplain (Table 12). The surface energy balance calculated greater ET in the forest site, likely as a result of receiving more net radiation. The SEB ET estimates were close to the Sanborn Field

reference ET and Baskett area eddy covariance ET measurements (Figure 16). The SEB also tracked well with the HARC pan evaporation rates during summer months (Tables 14 and 15). The SEB is widely recognized as a reliable method for estimating ecosystem ET (Rosenberry et al 2004). The forcings driving the SEB are the most physically based of all of the methods examined (Lenters et al. 2011). Therefore, the ET calculations made using this model are likely highly accurate and the Bottomland hardwood forest may actually transpire greater amounts of soil water annually than the grassland site.

Penman-Monteith

The Penman-Monteith (P-M) method of ET calculation resulted in higher annual ET in the Hinkson Creek Bottomland Hardwood Forest (802mm yr^{-1}) than the grassland site (719mm yr^{-1}) (Table 12). These results were consistent with ET calculated by other means (Figure 17). For instance, grassland ET was estimated at 720mm yr^{-1} using the SEB method and as 722mm yr^{-1} using the Shuttleworth-Wallace method. Likewise, the P-M annual forest ET was close to the Baskett area eddy covariance measured ET (806 mm yr^{-1}). Given that the P-M ET is driven by many physical parameters (Akinbile and Sangodoyn, 2011), it is likely that the observed difference in forest and grassland ET reflect actual differences in ecosystem level water use.

Priestley-Taylor

The Priestley Taylor (P-T) ET calculation method appears to be a viable method for estimating potential evapotranspiration, but use of this method for modeling actual evapotranspiration may be limited without further data manipulation to account for soil moisture limitations (Fisher et al., 2005). The P-T ET method reported greater annual ET in the forest (1113mm yr^{-1}), than in the grassland site (1034mm yr^{-1}) (Table 12). The P-T forest annual ET estimate is close to the Sanborn field reference ET estimate (1176mm yr^{-1}), which is also an estimation of potential ET (i.e. ET rate of vegetation which is not water limited) (Figure 16). Further refinement of the P-T equation could include adjustments to the coefficient term (α), which was set at 1.26 by common convention (Rosenberry et al., 2004), but could be reduced to represent greater resistance to atmospheric conductance of water vapor from the surface boundary layer, or limitations of soil moisture (Fisher et al., 2005).

Easy Penman-Monteith

The Easy Penman-Monteith (Easy P-M) method of ET yielded annual Hinkson Creek Floodplain ET estimates, which were smaller than those produced using the conventional Penman-Monteith equation. Easy P-M did show greater ET in the forest (593mm yr^{-1}) than in the grassland (518 mm yr^{-1}), (Table 12), but both of these estimates fall below those produced by measured mass flux of water (Baskett eddy covariance ET)

or more reliable models (SEB, P-M). However, the Bottomland hardwood forest Easy P-M estimate is very close to that produced by Hinkson Creek watershed mass balance analysis (601 mm yr^{-1}). The Easy P-M method performed well during the growing season, with both the forest and grassland ET rates nearly matching those observed from HARC pan evaporation measurements. However, the easy P-M method may not have accurately modeled dormant season ET. The Easy P-M method is highly dependent on accurate stomatal conductance terms (Komatsu et al. 2006), and the modeled values for winter-time stomatal conductance may not have been adequate for successful implementation of this model on an annual basis. The conductance rates of water vapor through bare twigs is not well reported for the Midwestern USA in the literature, and in the future on-site measurement of these parameters could produce more accurate Easy P-M annual ET estimates.

McNaughton-Black

The McNaughton-Black (McN-B) ET method produced widely divergent ET estimates for the forest (745mm yr^{-1}) and grassland (315mm yr^{-1}) portions of the Hinkson Creek Floodplain (Table 12). Greater forest ET is consistent with the results of other ET models (SEB, P-M, P-T, Easy P-M, Bowen), but the magnitude of the difference calculated by the McN-B method is surprising. The BHF site transpired more than twice as much water vapor as the AG site according to the output modeled by the McN-B calculations. The McN-B model may have enhanced sensitivity to variations of stomatal

resistance, which could have caused under-estimation of grassland ET, due to the greater modeled growing season stomatal resistance of the grasses. For successful implementation of the McN-B model in estimating annual ET, direct measurement of biological parameters such as stomatal resistance would be highly desirable.

Bowen Ratio Energy Balance

The Bowen Ratio Energy Balance (Bowen) method of ET calculation produced the largest annual ET estimates for both the forest (1589mm yr^{-1}) and the grassland site (1214mm yr^{-1}) (Table 12). The Bowen ratio ET estimates are closest to those supplied by the Priestley-Taylor ET model (P-T: BHF 111mm yr^{-1}, AG 1034mm yr^{-1}) and the annual reference ET reported by Sanborn Field (1176mm yr^{-1}) (Figure 16). The large annual ET estimated by the Bowen method may be due to post-processing of the ET which removed nighttime ET values from consideration (hourly ET data points which had net radiation values less than 3 Wm^{-2}, were set to 0mm in the cumulative totals). The nighttime ET values removed were mostly negative, and the post processing resulted in greater annual ET sums. Prior to post-processing, the AG Bowen ET estimate was around 100mm yr^{-1} (a result that was deemed highly unlikely), and the post-processed figure of 1214mm yr^{-1} appears more plausible. The Bowen ET estimate in the AG site was highly sensitive to temperature inversions during night and removing these values improved the model overall. The forest site nighttime ET values were also zeroed for consistency and this post-processing may have inflated the BHF Bowen ET estimates (prior to removal of

nighttime, Bowen estimate of annual ET was ~ 1000mm yr^{-1}). The sensitivity of this model to temperature inversions may make it undesirable for use in annual ET studies, where such conditions are common.

Shuttleworth-Wallace

The Shuttleworth-Wallace (S-W) method of ET calculation is notable as the only model examined which produced greater grassland (722mm yr^{-1}) than forest (458mm yr^{-1}) annual ET (Table 12). The grassland S-W ET estimate was comparable to those produced by the P-M and SEB methods (Figure 16). Unfortunately, the S-W may have under-estimated forest ET during the growing season, due to interaction of the multiple resistances to vapor diffusion present from soil to canopy, resulting in a lower annual ET rate than that found in the simpler model of grassland ET. Apparently, the S-W model models the abundant layers of forest vegetation as cumulative (series) resistances to vapor diffusion rather than as potential sources (parallel resistances) of transpiration. This soil-focused approach to ET estimation may be more applicable to the agrarian settings of agricultural crops and pastures rather than forests (at least without extensive parameterization of the forest resource in both spatial and temporal dimensions). Due to the operational complexity and inflexibility of this model I do not recommend its use in comparisons of ecosystem level ET.

VARIABLILTY IN EVAPOTRANSPIRATION ESTIMATES

Forest and Grassland Evapotranspiration Differences

The observed variation in annual estimates of Hinkson Creek floodplain ET may be explained through differences in site (AG vs. BHF), or differences in data inputs (empirical estimates vs. measured climate variables) required for the individual models. Overall, the Bottomland hardwood forest had greater annual modeled ET. All methods of ET estimation showed statistically significant differences between the BHF and AG sites except the Penman-Monteith and Bowen ratio methods (Table 10). The larger annual ET modeled for the forest site may have been caused by differences in forest albedo and stomatal conductance.

The lower albedo (α) of the forest vegetation (BHF α was modeled as 0.22 as opposed to α of 0.30 to0.25 for AG site) allowed for greater receipt of solar radiation and higher net radiation overall. The BHF net radiation was 42.7 MJ hour^{-1} greater than the AG site on average over the course of WY 2012. A portion of the additional solar energy absorbed by the BHF vegetation was dispersed as latent heat of evaporated water and reported here as greater modeled ET. The Surface Energy Balance, Bowen ratio, Penman-Monteith and Priestley-Taylor ET models are sensitive to variations in net radiation and the reported larger forest ET rates from these models may be due in part to greater net radiation in the BHF.

Higher stomatal conductance rates were modeled for the bottomland hardwood forest site, resulting in lower resistance to vapor diffusion from the vegetation canopy compared to the AG site. Although the modeled BHF stomatal conductance was much lower than that of the AG site during the dormant season to account for loss of forest leaves (figure 10), there was little ET during this period, due to the cool temperatures and moderate vapor pressure deficits of winter. With the onset of spring the BHF and AG site stomatal resistances were modeled to previously published values, with greater resistance modeled for the grassland site. The growing season differences in stomatal resistance to vapor diffusion between the forest and grassland had an apparent impact on the modeled ET totals, particularly for the Easy Penman-Monteith model which showed greater ET overall in the BHF. The Easy Penman-Monteith ET calculation outputs are determined by stomatal conductance and vapor pressure deficits (eq 2.9) and considering that the forest had on average lower measured vapor pressure deficits (mean hourly VPD: AG= 0.719kPa, BHF =0.623kPa), the increase in modeled ET may be attributed to differences in stomatal conductance (Table 5). Similarly, the McNaughton-Black ET calculation method is also highly sensitive to variations in both stomatal resistance and vapor pressure deficits (eq. 3.0) and it also yielded greater annual ET for the BHF site. Unfortunately reliance on empirical and modeled data for stomatal conductance values introduces error into ET estimates and models could be improved through direct measurement of the stomatal conductance term.

The AG site vegetation is comprised of warm season grasses (C_4) which are able to conduct photosynthesis at a greater water use efficiency than cool season plants (C_3)

(Lin et al., 2008, Lin et al., 2007) which include most trees. While C_3 plants commonly fix one molecule of CO_2 for 500 water molecules transpired, C_4 plants are capable of much more efficient photosynthesis. Many C_4 plants are able to fix one molecule of CO_2 for every 250 molecules of water lost, operating at twice the water use efficiency of C_3 plants (Taiz and Zeiger, 2006). The conservative water use strategy of C_4 plants indicates that the smaller stomatal conductances assigned to the AG site may reflect actual physiological differences between warm season grasses and trees. Warm season grasses are able to maintain high productivity with reduced stomatal aperture by reducing photorespiration, through enhanced primary carboxylation of CO_2 catalyzed by phosphoenolpyruvate carboxylase (Chollet et al, 1996), rather than Rubisco, and by use of CO_2 stored in bundle sheath structures (Maroco et al., 1998). Scott (2008) examined woody plant (C_3) and warm season grass (C_4) evapotranspiration in riparian areas of the southwest US and found that the Mesquite (*Prosopis spp.*) trees maintained greater transpiration rates compared to the C_4 grasses.

Growing season ET is primarily comprised of transpiration from plant leaf stomata, and vegetation density can affect annual ET rates. Forests typically have a higher leaf area index (LAI) than grasses, indicating that there is more area available for transpiration to occur (Ryu et al., 2012, Lenters et al., 2011, Zhu et al., 2011, Jenerette et al., 2009). The elevated canopy structure of the forest provides a vertical component to leaf distribution, allowing for a greater leaf surface area than grasses (Federer et al., 1996). Using ceptometer and hemispherical methods, Hubbart et al. (2011) measured mean canopy LAI rates of 2.98 and 3.06 within the BHF stand in August 2010. Also, the

riparian forest in this study has a ground layer of grasses and forbs that contribute to overall LAI and are also capable of transpiring water vapor, adding to the vapor flux lost from the forest canopy. Mean vegetation height measurements from August 16th 2012 indicate that the BHF groundcover at that time was actually taller than that measured in the AG site (BHF mean veg. height=1.19m, AG mean veg. height=1.13m) and considerable ET may occur from the ground layer of the forest before canopy leaf emergence in spring.

Other physiological differences between grasses and trees may account for some of the modeled differences in ET between the BHF and AG sites. The higher ET rates reported in the BHF site could be explained in part by the deeper effective rooting depth of floodplain trees. Many floodplain tree species have large underground root structures that are capable of accessing shallow groundwater (Gazal et al., 2006, Naiman and Decamps, 1997). Grasses and annual plants typically have much smaller root systems than trees (Schenk and Jackson, 2002, Stone and Kalisz, 1991). Deep roots enable trees to continue transpiring when surface soils are dried below the permanent wilting point, resulting in higher forest ET during dry periods when grasses are unable to reach shallow groundwater sources (Jobbagy and Jackson, 2004).

The riparian tree species found within the BHF site are considered facultive phreatophytes capable of accessing shallow groundwater when soil restrictive layers are not present. A list of published tree root depths (Stone and Kalisz, 1991) for the tree species encountered in the BHF forest inventory is provided below (Table 21). The Hinkson Creek Floodplain study site soils are comprised of the Haymond soil series

which is described as a very deep soil with more than 2m to restrictive layers (Young et al., 2001), and therefore some of the tree root depths described in Table 15 may have been realized within the BHF. Although tree roots may not be able to grow all the way down to water table depth, the roots can extract additional water from the capillary fringe directly above the saturated zone. Deep tree roots are also located below the winter freeze layer allowing for uptake of water from the forest soil to occur earlier in the spring and later in the fall. This ability trees to extract soil water over a longer period could also contribute to the larger evapotranspiration modeled in the forest site.

Table 21. Reported rooting depths for tree species found in the Hinkson Creek Floodplain BHF .

Species	Rooting depth m	Reporting Author
American elm-*Ulmus americana*	6.1	Hayes and Stoeckler 1935
Eastern cottonwood- *Populus deltoides*	3.6	Sprackling and Read 1979
Silver maple- *Acer sacharinum*	3.3	Sprackling and Read 1979
Black walnut - *Juglans nigra*	2.2	Pham et al 1978
Boxelder- *Acer negundo*	4	Biswell 1935
Sycamore- *Platanus occidentalis*	2.1	Biswell 1935

Differences in Model Evapotranspiration Estimates

Overall the Surface Energy Balance (SEB) and Penman-Monteith (P-M) equations appear to perform well under both forest and grassland conditions. These equations also matched up well against other measured (Baskett Ameriflux, HARC Pan Evaporation) and modeled (Sanborn reference ET) ET rates from mid Missouri. The SEB equation was not statistically different from HARC pan evaporation (Table 19) or the Sanborn reference ET rate (Table 17), but it was statistically different from the Baskett ET rate (Table 18). Statistical differences were observed between the P-M AG modeled ET and Sanborn reference ET (Table 12), but none were found between P-M and HARC pan evaporation data (Table 19) or Baskett ET (Table 18). The close correspondence of annual ET rate between modeled P-M and the Baskett Ameriflux ET data is notable (Figure 16). However, just because the P-M equation correlates well with other reported regional ET data it does not mean that it necessarily provided the most accurate estimate for Hinkson Creek Floodplain evapotranspiration.

While the Baskett Ameriflux ET measurements are highly accurate they must be considered as actual ET for an upland Oak-Hickory forest and may not be representative of forest or grassland ET occurring on alluvial soils. The upland hardwood forest at Baskett is rooted in shallower soils (Young et al., 2001) and is comprised of tree species which have lower stomatal conductance than bottomland hardwoods (Yang et al., 2010). Considering these site differences, I propose that the SEB estimate is likely the most accurate model for annual BHF evapotranspiration and the 975mm total represents actual

ET for the site. Of the models examined, the SEB equation uses several critical climate data inputs, but it is not hindered by many empirically derived parameters. Considering this, the 720mm estimate of AG site ET computed by the SEB is the most accurate estimate and the forest site did indeed transpire more water than the grassland in 2012. The Shuttleworth-Wallace (AG) and P-M (AG) methods also produced estimates within several mm of the SEB modeled AG ET rate, potentially confirming the efficacy of this method. However, the Shuttleworth-Wallace method performed poorly in the BHF site, producing the only estimate which was lower than for the AG site out of any of the equations examined, but this method is difficult to parameritize (Fisher et al., 2005) and is unlikely to be versatile enough for use in a wide variety of ecosystems.

Both the McNaughton-Black (McN-B) and Shuttleworth-Wallace (S-W) models performed poorly compared to the HARC growing season pan evaporation rates and were the only models which appeared to have diminishing ET rates during the warm part of the year (Figures 22,23). Furthermore the ET estimates for the McN-B and S-W equations were drastically different for the BHF and AG sites (Table 12), an unlikely result considering that most other methods showed reasonably close agreement between Hinkson Creek floodplain sites. For these reasons I would not recommend using the McN-B or S-W methods for ET modeling in mid –Missouri.

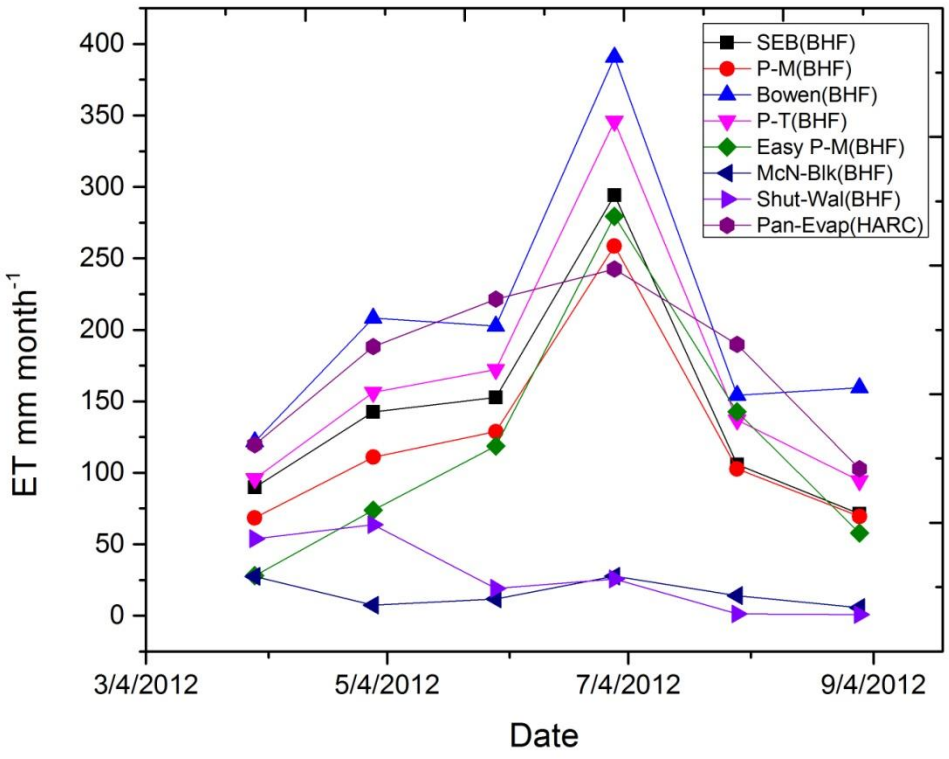

Figure 22. Growing season 2012 Hinkson Creek Floodplain BHF (Columbia, MO) Evapotranspiration and regional monthly Pan Evaporation monthly (HARC, New Franklin MO)

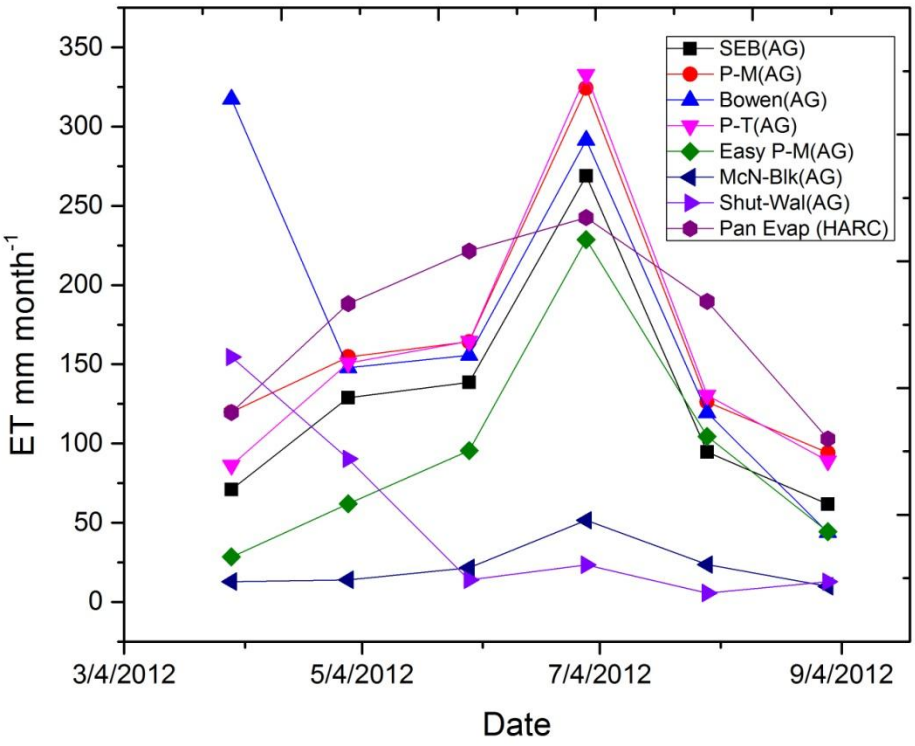

Figure 23.Growing season 2012 Hinkson Creek Floodplain Agricultural Grassland (AG) Evapotranspiration (Columbia, MO) and regional monthly Pan Evaporation monthly (HARC, New Franklin, MO)

Other methods performed surprisingly well considering their modest data input requirements. The Priestley-Taylor (P-T) equation yielded plausible values for BHF and AG potential evapotranspiration and with proper adjustments for soil-water limitations they could be successfully used to model actual ET. The close correlation of the P-T modeled ET to HARC pan evaporation shows how this model performs well at supplying the potential evapotranspiration locations based on incoming radiation and temperature

data alone (Figures 15, 16). One possible approach for improvement of the P-T equation accuracy is to calibrate the dimensionless stabilization coefficient (α) to better fit conditions observed on the site (in this case it could be reduced from 1.26 to a smaller value to reduce the overall ET output to more closely reflect actual ET).

The Easy Penman-Monteith (Easy P-M) model appeared to under-estimate ET for both the AG and BHF sites compared to the majority of the other models. However, considering the modest data requirements and ease of calculation, the Easy P-M model performed better than expected. The modeled variations of stomatal resistance may have limited the output of this model. A more accurate annual ET estimate could be achieved by using summertime stomatal conductance values year-round for ET calculations in Mid-Missouri.

The Bowen ratio method performed fairly well, although prior to elimination of nighttime latent heat values, the AG site model was reporting very small annual ET values (~100mm yr^{-1}). The original small AG Bowen ratio ET values were the result of numerous negative latent heat values, (well beyond those expected by occasional condensation), possibly caused by nighttime temperature inversions on the site. Following removal of said nighttime values, the AG Bowen ratio ET estimate was modeled to a plausible level, but the BHF Bowen ratio ET rate was increased to the largest modeled value of all of the methods examined (1588mm yr^{-1}),(Table 12). Possibly the original BHF Bowen ratio of 1168mm yr^{-1} may have been a more accurate estimate, but the nighttime values were removed from both the BHF and AG sites to ensure consistency when comparing methods. Considering the sensitivity of the Bowen ratio

method to temperature inversions it appears that this method is not reliable without performing additional data manipulation.

Overall, ET models with more empirical parameters (McN-B, Easy P-M, S-W, P-T) performed more poorly than those which had more robust site recorded data requirements (SEB, P-M, Bowen). Models such as P-M and S-W contain a combination of empirical and field measured forcings and are more difficult to place in a distinct physical/empirical model category. While the P-M ET model performed very well the S-W ET estimates appear to be somewhat unreliable (at least for forest ET estimation).

DIFFICULTIES WITH THE CURRENT RESEARCH

The evapotranspiration models examined here could provide more accurate forest ET estimates with direct measurements of climate variables from above forest canopy level rather than using modeled values for wind speed velocity and substitution of incoming solar radiation values from the grassland site to approximate conditions above the canopy. However, canopy towers are costly, difficult to maintain, and impractical to construct for short term studies. Use of a net radiometer, rather than calculating net radiation from incoming solar, could also improve ET estimates. Modeling vegetation albedo from published sources instead of direct measurement also may have introduced error into the calculation of net radiation in the forest and grassland ET estimates.

Both forest and grassland ET estimates could also be improved by direct measurement of vegetation stomatal conductance rather than relying on published values

for these parameters for use in models including the P-M , Easy P-M , McN-B and S-W. The uncertainties of dormant season stomatal conductance also may have introduced error into ET models which are sensitive to this parameter (Easy P-M, McN-B and S-W).

The ET models in this study were all equipped with equal input values with the same time-step (hourly). It is possible that individual models could perform better on a different temporal scale (i.e. daily rather than hourly calculation time step). Seasonal adjustments to key variables such as albedo, stomatal conductance and vegetation height may have affected certain models more than others. However, the aim of the study was to compare ET models with equivalent forcings rather than optimize performance of individual models. Therefore, when parameters such as stomatal conductance were varied seasonally, the changes were applied across all models utilizing the given parameter. It is possible that ET models such as Easy P-M and McN-B could produce more accurate annual ET estimates with static values of stomatal conductance fixed for the duration of the Water Year.

IMPLICATIONS FOR MANAGEMENT

Based on the findings of this study it is recommended that bottomland hardwood forests in urban areas be protected from development. These floodplain forest stands may serve an important role in reducing overland flooding through drying of floodplain soils by forest transpiration. Urban floodplain locations which are not currently forested should be planted with trees to counteract runoff from impervious surfaces such as pavement and buildings in the watershed.

In floodplain locations where maintaining a grass cover is preferred, it is recommended that cool season grasses be established and mowed regularly to maximize consumptive water use and provide the most effective storage location for local flood attenuation. Where early-successional native plant habitat is desired, planting native warm season grasses and flowering forbs is acceptable, considering that the wildlife habitat value may exceed the value of a nominal increase in water consumption afforded by establishing rapidly transpiring forest cover.

FUTURE DIRECTIONS

The role of Bottomland hardwood forest in floodplain management could be further explored. Examining the increased hydraulic resistance by floodplain forests on overbank flows during flood events could further quantify the benefits of these forests for flood amelioration. The affects of flooding on forest succession in floodplain forests should be further studied, especially since many of the mature overstory trees currently do not appear to be reproducing successfully (Hubbart et al., 2011). Flooding of riparian forests are known to be causes of both mortality and reproduction within forest ecosystems (Naiman and Decamps, 1997) and long term studies could be initiated to examine this phenomena. Further studies could also examine the relative ability of young forests and biomass plantations to transpire soil water and provide roughness in opposition to floodwaters.

The evapotranspiration conducted by riparian forests also has implications for local cooling in urban areas, since radiant energy used for latent heat is not available for conversion into sensible heat (Maes et al., 2011). The effects of evaporative cooling and shading from trees on urban centers should be investigated to counteract urban heat island effects. Forest transpiration is also correlated with carbon sequestration (Kochendorfer et al., 2011, Domec et al., 2010, Fisher et al., 2007) and attention should be given to quantify the capacity of these ecosystems to capture and store atmospheric carbon.

The relative value of floodplain forests and grasslands as sites for native plant conservation and preservation is an important area of consideration that remains undetermined. Although grasslands were not found to transpire as much soil water annually, there may be benefits to maintaining some locations as seed sources for rare grasses and forbs. The role of bottomland forests and riparian grasslands as wildlife refugia and migration corridors within urban settings could also be explored within the context of riparian habitat preservation.

Additional research could be done to characterize the role of soil biota of floodplain forests and grasslands, with particular attention given to the relative abundance of bacteria and fungi found in these ecosystems. Other below-ground research such as examination of floodplain forest tree roots in the spatial and temporal accessibility of shallow groundwater resources could further explain the mechanisms behind the greater evapotranspiration rates detected in bottomland hardwood forests.

Although the land use practices examined in this research are labeled distinctly grassland or forest, combining features of both ecosystems may also be a feasible management strategy in some cases. Such agroforestry practices may be applied to combine tree and grassland attributes in select urban floodplain locations. Multiple benefits may be accrued by planting of valuable native floodplain tree species such as Black walnut (*Juglans nigra*) (Noweg and Kurtz, 1987) and Pecan (*Carya illinoisensis*) (Allen et al., 2005), which produce both timber and nuts for human consumption (Thompson and Madden, 2003). The ecological and economic feasibility of agroforestry plantations could be a focus of future research in urban floodplain land use dynamics

CHAPTER VI:

CONCLUSIONS AND SYNTHESIS

Characterizing the role of bottomland hardwood forests in floodplain hydrology is critical for making informed land use decisions in urban areas. It is proposed that floodplain forests attenuate flood events by transpiring greater quantities of soil water than adjacent grasslands. In order to confirm that floodplain forests ecosystems have greater annual evapotranspiration seven ET models were tested in the Hinkson Creek Floodplain forest and grassland sites. Model performance was examined in addition to quantitative assessment of forest and grassland ET.

The bottomland hardwood forests (BHF) in this study was found to have greater evapotranspiration rates than adjacent agricultural grassland (AG). There were statistically significant differences (at the 0.05 significance level) between BHF and AG ET for five out of the seven methods examined. Six out of seven methods of ET calculation showed higher rates of ET in BHF than AG, within the Hinkson Creek Floodplain. Modeled WY 2012 ET rates in BHF range from 458mm yr^{-1} (S-W) to 1589mm yr^{-1} (Bowen), with estimates from reliable methods ranging from 802mm yr^{-1} (P-M) to 975mm yr^{-1} (SEB). The modeled ET for the AG site ranges from a low estimate of 315mm yr^{-1} (McN-B), to a high value of 1214mm yr^{-1}. Plausible AG yearly ET values include 720mm yr^{-1} (SEB) and 719mm yr^{-1}(P-M). The difference of the more reliable ET

estimates from the BHF and AG site respectively represent an additional 83mm yr^{-1} to 255mm yr^{-1} of soil moisture removed from the forest floodplain soil. Coupled with the increased infiltration capacity of forest soils, the enhanced evapotranspiration of bottomland forests could ameliorate flood events through absorption and storage of overland flows.

The ET methods which performed the best in comparison to reference sites in Mid-Missouri include the Surface Energy Balance, Penman-Monteith and the Bowen ratio. Reference ET from nearby Sanborn field was greater than estimates produced by all ET models except the Bowen ratio (with nighttime values removed). Baskett area eddy covariance ET measurements closely match the Penman-Monteith BHF modeled ET. The BHF Surface Energy Balance ET estimate is greater than that reported from the Baskett Ameriflux tower, but it is likely a more accurate model than the P-M equation, because of known site features of the BHF floodplain (deep soils, riparian tree species) compared to the upland forests of the Baskett area. Pan evaporation data closely matches Priestley-Taylor ET growing season estimates, presumably because both model potential rather than actual ET. Models including Shuttleworth-Wallace and McNaughton-Black perform erratically and produce wide variations of ET outputs depending on site inputs (BHF or AG) and are not recommended for annual ET modeling in Mid-Missouri.

Floodplain grassland locations were found to support greater numbers of plant species than bottomland hardwood forests, but when overstory tree species are included, both sites have nearly identical species counts (BHF-29spp., AG-30spp.). The Bottomland hardwood forest site had greater understory ground coverage (with live

vegetation and leaf litter) and may be more suited for erosion control than frequently mowed grassland. The cool humid microclimate conditions and provision of coarse woody debris by riparian forests directly benefit adjacent streams and any quantitative loss of water input is likely outweighed by a qualitative improvement of water quality in forested watersheds.

The results of this study show that bottomland hardwood forests transpire greater amounts of soil water than riparian grasslands. Therefore, it is desirable to expand the land area of this forest resource, where possible. Bottomland hardwood forests historically covered floodplains in the Central and Southern US (Romano, 2010, MacDonald, 1979). Riparian tree species are adapted to survive and even reproduce during flooding (Naiman and Decamps 1997). Floodplain forests are examples of resilient plant communities (Naiman et al, 2010, Tabbachi et al., 2000) and although they may contain fewer plant species than grasslands overall, a greater percentage of native species were found growing under forest canopies. The stability and resilience of floodplain forests make them desirable vegetation communities to occupy sensitive regions such as urban riparian corridors. The potential for these forests to ameliorate potential flood events makes riparian forest conservation a critical feature urban floodplain management planning.

It is therefore it is recommended that floodplain forests be preserved or re-established to ensure maximum absorption of potential flood events within urban areas. Multiple ecosystem services will be provided by such forests including; flood mitigation, local cooling, carbon sequestration, enhanced nutrient and sediment filtration, wildlife

habitat preservation, stream shading, potential biomass or timber harvest and provision of aesthetically pleasing sites for recreational activities.

LITERATURE CITED

Abdel-Wahed, M., and Snyder, R. 2008. "Simple Equation to Estimate Reference Evapotranspiration from Evaporation Pans Surrounded by Fallow Soil." *Journal Of Irrigation & Drainage Engineering* 134, no. 4: 425-429

Abernathy Y., Turner R.1987 " US Forest Wetlands: 1940-1980" *Bioscience*. No 37:721-727

Abtew W. Obeysekera J., Iricanin N., 2010. "Pan Evaporation and potential evapotranspiration trends in South Florida." *Hydrologic Processes* 25, no.6: 958-969

Akinbile, C., and Sangodoyin, A. 2011. "Evapotranspiration, Soil and Water Quality Implications on Upland Rice Production." *Asian Journal Of Crop Science* 3, no. 4: 169-178

Allen, S., Jose, S., Brecke,B., Nair,V., Graetz, D. and Ramsey, C. 2005. " Nitrogen mineralization in a Pecan (*Carya illinoensis* K, Koch) – cotton (*Gossypium hirsutum* L.) alley cropping system in the Southern United States" *Biol. Fertil. Soils.* No. 41: 28-37.

Al-Kaisi, M., Elmore,R., Guzman, J., Hanna,H.,Hart,C., Helmers,M., Sawyer,J.2013. "Drought impact on crop production and the soil environment: 2012 experiences from lowa." *Journal Of Soil & Water Conservation* 68, no. 1: 19A-24A.

Allen, R.2005.”Penman-Monteith Equation.” Elsevier Ltd.

Almquist, E., Jack S., Messina M. 2002. “Variation of the treefall gap regime in a bottomland hardwood forest: relationships with microtopography.” *Forest Ecology and Management.* No.157. 155-163

Amiro, B. 2009.”Measuring boreal forest evapotranspiration using the energy balance residual” *Journal of Hydrology*.No.366. 112-118

Attarod, P., V. Bayiamzadeh, A. Tajdini, and M. Roohnia. 2009. "Annual Trends in Evapotranspiration from Major Vegetations of Thailand." *American Journal of Plant Physiology* 4, no. 3: 100-108.

Barros, R., D. Isidoro, and R. Aragüés. 2011. "Long-term water balances in La Violada irrigation district (Spain): I. Sequential assessment and minimization of closing errors." *Agricultural Water Management* 102, no. 1: 35-45.

Biswell,H.1935. “Effects of environment upon rooting habits of certain deciduous forest trees.” *Botany Gazette*.no.96:140-142

Berretta, C., Gnecco, L., Lanza, and P. La Barbera. 2007. "Hydrologic influence on stormwater pollution at two urban monitoring sites." *Urban Water Journal* 4, no. 2: 107-117.

Bond, B., and K, Kavanagh. 1999. "Stomatal behavior of four woody species in relation to leaf-specific hydraulic conductance and threshold water potential." *Tree Physiology* 19, no. 8: 503-510

Borders, B., Pushnik J., and Wood D. 2006. "Comparison of Leaf Litter Decomposition Rates in Restored and Mature Riparian Forests on the Sacramento River, California." *Restoration Ecology* 14, no. 2: 308-315.

Bowen, I. 1926. “The ratio of heat losses by conduction and by evaporation from any water surface” *Physical Review*. Vol 27. 779-787.

Brodribb, T., and Holbrook,N. 2003. "Changes in leaf hydraulic conductance during leaf shedding in seasonally dry tropical forest." *New Phytologist* 158, no. 2: 295-303.

Cavalcanti, G., and B., Lockaby. 2005. "Effects of Sediment Deposition on Fine Root Dynamics in Riparian Forests." *Soil Science Society Of America Journal* 69, no. 3: 729-737

Cea, L., Garrido, M., Puertas, J., Jácome, A., Del Río, H., and Suárez, J. 2010. "Overland flow computations in urban and industrial catchments from direct precipitation data Using a two-dimensional shallow water model." *Water Science & Technology* 62, no. 9: 1998-2008

Chahouki M., Khojasteh, F.,and Tavili, A. 2012. "Distribution of Vegetation Type according to Edaphic Properties and Topography in Iran." *Polish Journal Of Environmental Studies* 21, no. 4: 1071-1077

Chaney, E., Elmore, W., Platts, w. S.1990.”Livestock grazing and on western riparian areas.” *USEPA*, Washington, DC.

Chollet,R., Vidal, J.,O’Leary, M.1996. “Phosphoenolpyruvate carboxylase: A ubiquitous , highly regulated enzyme in plants.” *Annual Review. Plant Physiology Plant Molecular Biology* no. 42: 273-298

Chuanguo Y., Zhaohui L., Zhongbo Y., Zhenchun H., Shaofeng L. 2010. "Analysis and Simulation of Human Activity Impact on Streamflow in the Huaihe River Basin with a Large-Scale Hydrologic Model." *Journal Of Hydrometeorology* 11, no. 3: 810-821.

Cionco, R.1972. "A wind profile index for canopy flow." *Boundary Layer Meteorology*. No.3: 255-263

Cole, D., and Marion, J. 1988. "Recreation impacts in some riparian forests of the eastern United States." *Environmental Management* 12, no. 1: 99-107.

Cope, M., McLafferty, S., Rhoads, B. 2011. "Farmer Attitudes Toward Production of Perennial Energy Grasses in East Central Illinois: Implications for Community-Based Decision Making." *Annals Of The Association Of American Geographers* 101, no. 4: 852-862

Corenblit, D., Steiger, J., Gurnell,A., Naiman, R. 2009. "Plants intertwine fluvial landform dynamics with ecological succession and natural selection: a niche construction perspective for riparian systems." *Global Ecology & Biogeography* 18, no. 4: 507-520.

Cosenza, P. and Tabbagh, R. 2003. "Relationship between thermal conductivity and water content of soils using numerical modeling." *European Journal of Soil Science* 54: 581-587.

Dai,Y., Dickinson, R., and Ying-Ping, W. 2004. "A Two-Big-Leaf Model for Canopy Temperature, Photosynthesis, and Stomatal Conductance." *Journal Of Climate* 17, no. 12: 2281-2299

Delpierre, N., Dufrêne, E, Soudani, K., Ulrich, E., Cecchini, S., Boé, J. and C. François. 2009. "Modelling interannual and spatial variability of leaf senescence for three deciduous tree species in France." *Agricultural & Forest Meteorology* 149, no. 6/7: 938-948.

Devore J. 2012. Statistics: The exploration and analysis of data. Seventh Edition. Cengage. Boston MA

DeWalle, D. 2010. "Modeling Stream Shade: Riparian Buffer Height and Density as Important as Buffer Width." *Journal Of The American Water Resources Association* 46, no. 2: 323-333.

Dingman S. 2002.Physical Hydrology Second Edition. Waveland Press. Long Grove, IL.Pgs.11-12.

Domec, J., King J. , Noormets A. , Treasure E. , Gavazzi M. , Ge, S. , and McNulty S . 2010. "Hydraulic redistribution of soil water by roots affects whole-stand evapotranspiration and net ecosystem carbon exchange." *New Phytologist* 187, no. 1: 171-183.

Dosskey, M.., Vidon, P., Gurwick, N., Allan, C., Duval, T., and Lowrance, R. 2010. "The Role of Riparian Vegetation in Protecting and Improving Chemical Water Quality in Streams." *Journal Of The American Water Resources Association* 46, no. 2: 261-277.

Drozdov, S. V., and Vostrikov, A. 2000. "Structural Features and Energy of Small Water Clusters." *Technical Physics Letters* 26, no. 5: 397

Eccel, E. , Toller, G. , Ghielmi, L. 2004. " The soil water balance of a mixed oak stand in the southern Alps." *Studi Trent. Sci. Nat. Acta. Biol.*no.81 : 137-149

El –Baroudy, I. 2010. "Comparison of three data-driven techniques in modelling the evapotranspiration process." *Journal of Hydroinformatics* 12, no. 4: 365-379.

Falge, E., Reth, S., Brüggemann, N., Butterbach-Bahl, K., Goldberg,V., Oltchev,A., and Bernhofer, C. 2005. "Comparison of surface energy exchange models with eddy flux data in forest and grassland ecosystems of Germany." *Ecological Modelling* 188, no. 2-4: 174-216.

Federer, C.,Vorosmarty, C., Fekete, B. 1996. "Intercomparison of methods for methods for calculating evaporation in regional and global water balance models. *Water Resources Research.*no.32 2315-2321.

Fisher, J., DeBiase, T., Qi, Y., Xu, M., and Goldstein, A. 2005. "Evapotranspiration models compared on a Sierra Nevada forest ecosystem." *Environmental Modelling & Software* 20, no. 6: 783-796.

Fisher, J., Baldocchi, D., Misson, L., Dawson, T., and Goldstein, A. 2007. "What the towers don't see at night: nocturnal sap flow in trees and shrubs at two AmeriFlux sites in California." *Tree Physiology* 27, no. 4: 597-610

Fisher, R. and Binkley, D. 2000. Ecology and management of forest soils. Third Edition Wiley and Sons. New York, NY.

Foote, R., Grogan, P.2010."Soil Carbon Accumulation During Temperate Forest Succession on Abandoned Low productivity Agricultural Lands."*Ecosystems.*13: 795-812

Freni, G., and Oliveri, E. 2005. "Mitigation of urban flooding: A simplified approach for distributed stormwater management practices selection and planning." *Urban Water Journal* 2, no. 4: 215-226.

Garrett, H., Pallardy, S., and Nigh, T. 1985. "Sugar maple-environment relationships in the River Hills and central Ozark Mountains of Missouri." *American Midland Naturalist* 114, no. 2: 235.

Gazal, R., Scott, R., Goodrich, D., and Williams, D. 2006. "Controls on transpiration in a semiarid riparian cottonwood forest." *Agricultural & Forest Meteorology* 137, no. 1/2: 56-67.

Ghavasieh, A., Poulard,C. and Paquier, A.2006."Effect of roughened strips on flood propagation: Assessment on representative virtual cases and validation." *Journal Of Hydrology* 318, no. 1-4 (March 2006): 121-137

Ghandhari, A., and Moghaddam, S. 2011. "Water Balance Principles: A Review of Studies on Five Watersheds in Iran." *Journal Of Environmental Science & Technology* 4, no. 5: 456-479

Giese L., Aust, W. , Kolka, R., Trettin, C. 2003. "Biomass and carbon pools of disturbed riparian forests."*Forest Ecology and Management.* No. 180: 493-508

Githinji, L. , Dane, J., Walker, R. 2009 "water use patterns of tall fescue and hybrid bluegrass cultivars subjected to ET-based irrigation scheduling." Irrigation Science. 27:377-391

Goodrich D. , Scott, R., Qi, J., Goff, B., Unkrich, C., Moran,M., Williams D., Schaeffer,S., Snyder,K., MacNish, R., Madock, T., Poole D., Chebounif, A.,

Cooperg D., Eichingerh,I., Shuttleworth, W., Kerri, W., Marsetta, Y., Ni,W. 2000. “Seasonal estimates of riparian evapotranspirationusing remote and in situ measurements.” *Agriculture and Forest Meteorology*.no.105:281-309.

Gregory, S., Swanson, F., McKee,W. and Cummins, K. 1991. "Ecosystem Perspective of Riparian Zones: Focus on Links between Land and Water." *Bioscience BISNAS* 41, no. 8: 540-5

Gribovszki, Z., Kucsara M., Szilágyi J., and Kalicz, P. 2008. "Riparian zone evapotranspiration estimation from diurnal groundwater level fluctuations” *Journal Of Hydrology* 349, no. 1-2: 6-17.

Groninger J. 2005.”Increasing the impacts of bottomland hardwood afforestation.”*Journal of Forestry*, no.103, 4:184-188

Gu, L., Massman,W., Leuning, R., Pallardy, S., Meyers,T., Hanson,P., Riggs, J., Hosman, K., andYang,B. 2012. "The fundamental equation of eddy covariance and its application in flux measurements." *Agricultural & Forest Meteorology* 152, 135-148.

Gwaze, D., Elliott, A. 2011. “Cavity Trees, Snags, and Overstory Density in a Riparian Forest in Northeastern Missouri.” *Northern Journal of Applied Forestry.* No. 28: 105-109

Hale, B., Alsum, E., Adams, M. 2008. “Changes in floodplain forest vegetation of the lower wisconsin river over the last fifty years” *The American Midland Naturalist.* 160:454-476

Harding, J., Claassen, K., and Evers, N. 2006. "Can forest fragments reset physical and water quality conditions in agricultural catchments and act as refugia for forest stream invertebrates?." *Hydrobiologia* 568, no. 1: 391-402.

Hardison, E., O'Driscoll, M., DeLoatch, J., Howard, R., & Brinson, M. 2009, "Urban Land Use, Channel Incision, and Water Table Decline Along Coastal Plain Streams, North Carolina" *Journal Of The American Water Resources Association*, No.45, 4, 1032-1046

Hayes,F., Stoeckler J. 1935. "Soil and Forest relationships of the shelterbelt zone." Possibilities of shelterbelt planting in the plains region. US Government Printing office. Washington D.C. Sept 12th. Pp 111-153

Healey, N., Irmak, A., Arkebauer, T., Billesbach, D., Lenters, J., Hubbard, K., & . Kjaersgaard, J. 2011. "Remote sensing and in situ-based estimates of evapotranspiration for subirrigated meadow, dry valley, and upland dune ecosystems in the semi-arid sand hills of Nebraska, USA." *Irrigation & Drainage Systems* 25, no. 3: 151-178.

Herbst, M., 1995. "Stomatal behavior in a beech canopy: an analysis of Bowen ratio measurements compared with porometer data."*Plant Cell and Environment.*18. 1010-1018

Hodges, J. 1997. "Development and ecology of bottomland hardwood sites." *Forest Ecology and Management.* No. 90: 117-125

Hubbart, J., Muzika, R.-M., Huang,D. and Robinson, A. 2011. Improving Quantitative Understanding of Bottomland Hardwood Forest Influence on Soil Water Consumption in an Urban Floodplain. *The Watershed Science Bulletin*, 3:34-43.

Hubbart, J., Holmes,J. and Bowman,G.. 2010. TMDLs: Improving stakeholder acceptance with science-based allocations. *The Watershed Science Bulletin*, Fall: 19–24

Huggett, R. 2007 "A History of the Systems Approach in Geomorphology" *Géomorphologie : relief, processus, environnement.* 145-158

Hughes, J. and Cass, W. 1997. "Pattern and process of a floodplain forest, Vermont, USA: Predicted response of vegetation to perturbation" *Journal of Applied Ecology*. No. 34:594-612

Husch, B., Beers,T. and Kershaw, J. 2003. Forest Mensuration. Fourth Edition. Krieger Publishing Co., Malabar, Florida 443 p.

Huxman, T., Wilcox B., Breshears D. , Scott R., Snyder K., Smal, E., Hultine, K., Pockman, W., and Jackson, R. 2005. "Ecohydrological Implications of Woody Plant Encroachment." *Ecology* 86, no. 2: 308-319.

Ibañez, M., Pérez,P., Caselles,V. and Castellvi,F. 1998. "A simple method for estimating the latent heat flux over grass from radiative Bowen ratio."*American Meteorological Society*. No.37. 387- latent heat flux over grass 392.

Irmak, S., Irmak,A., Allen, G. and Jones, J. 2003. "Solar and Net Radiation-Based Equations used to Estimate Reference Evapotranspiration in Humid Climates." *Journal of Irrigation & Drainage Engineering* 129, no. 5: 336-347.

Irmak, A., Irmak,S. and Martin,D. 2008. "Reference and Crop Evapotranspiration in South Central Nebraska. I: Comparison and Analysis of Grass and Alfalfa-Reference Evapotranspiration." *Journal of Irrigation & Drainage Engineering* 134, no. 6: 690-699

Irmak, S., Kabenge, I., Skaggs, K., & Mutiibwa, D. 2012. "Trend and magnitude of changes in climate variables and reference evapotranspiration over 116-yr period in the Platte River Basin, central Nebraska–USA." *Journal Of Hydrology* 420-421, 228-244.

Jacobs,J. , Mergelsberg,S., Lopera, A. ,and Myers, D. 2002. "Evapotranspiration From a Wet Prairie Wetland Under Drought Conditions: Paynes Prairie Preserve, Florida, USA." *The Society of Wetland Scientists*22 no. 2 : 374-385

Jenerette, G., Scott, R., Barron-Gafford,G. , Huxman, T. 2009. "Gross primary production variability associated with meteorology, physiology, leaf area, and water supply in contrasting woodland and grassland semiarid riparian ecosystems."*Journal of geophysical research.*Vol. 114: G04010

Jennings, S., Brown, N., Sheil, D. 1999. "Assessing forest canopies and understory illumination : canopy closure ,canopy cover and other mneasures." *Journal of Forestry* No 72. (1) : 59-74

Jeng-Lin, T., Ben-Jei, T., Po-Sheng, L., Ming-Hwi, Y., and Yuan, S. 2007. "Surface Energy Components and Land Characteristics of a Rice Paddy." *Journal Of Applied Meteorology & Climatology* 46, no. 11: 1879-1900. *Environment Complete*

Jobbágy, E., and Jackson, R. 2004. "Groundwater use and salinization with grassland afforestation." *Global Change Biology* 10, no. 8: 1299-1312.

Jordan, D., Miles, R., Hubbard, V. and Lorenz, T. 2004. "Effect of management practices and cropping systems on earthworm abundance and microbial activity in Sanborn Field: a 115-year-old agricultural field." *Pedobiologia* 48, no. 2: 9

Kaplan, D., Munoz-Carpena,R. 2010. "Complementary effects of Surface water and groundwater on soil moisture dynamics in a degraded coastal floodplain forest." *Journal of Hydrology.* No. 398: 221-234

Kershner, J., Archer, E., Coles-Ritchie,M., Crowley, E., Henderson,R., Kratz,K., Quimby,C., Turner, D., Ulmer,L., Vinson,M. 2004."Guide to effective monitoring of aquatic and riparian resources" *Gen. Tech. Rep.*RMS-GTR-121. Fort Collins, CO: US Department of Agriculture, Rocky MountainResearch Station.57 p..

Kim, N., Won,Y., Lee, J., and Jeong,J. 2011. "Hydrological impacts of urban imperviousness in White Rock Creek watershed." *Transactions Of The ASABE* 54, no. 5: 1759-1771

King S., Antrobus T. 2001. "Canopy disturbance patterns in a bottomland hardwood forest in northeast Arkansas."*The Society of Wetland Scientists,* Vol.21 No.4: 543-553

Knight, K., Schultz, R. , Mabry, C. and Isenhart, T.. 2010. "Ability of Remnant Riparian Forests, With and Without Grass Filters, to Buffer Concentrated Surface Runoff." *Journal of the American Water Resources Association* 46, no. 2: 311-322

Koch, K., Ensikat, H. 2008 “The hydrophobic coatings of plant surfaces: Epicuticular wax crystals and their morphologies, crystallinity and molecular self-assembly.” *Micron* 39:759-772.

Kochendorfer, J., Castillo,E., Haas, E., Oechel, W., Paw, U. 2011. “Net ecosystem exchange, evapotranspiration and canopy conductance in a riparian forest.” Agriculture and Forest Meteorology.151. 544-553,

Koehle, J., and Adelman,I. 2007. "The effects of temperature, dissolved oxygen, and Asian tapeworm infection on growth and survival of the Topeka shiner." *American Fisheries Society. Transactions* 136, no. 6: 1607-1613

Komatsu, H., Kang, Y., Kume, T., Yoshifuji, N., Hotta,N. 2006 “Transpiration from a *Cryptomeria japonica* plantation, part 1: aerodynamic control of transpiration.”Hydrological Processes. No. 20 1309-1320.

Krebs, C. 1989. Ecological Methodology. Harper and Row, Publishers. New York. 654 pp.

Larsen, D., Dey, D., Faust, T. 2010. “A stocking diagram for Midwestern Eastern Cottonwood –Silver Maple-American Sycamore Bottomland Forests.” *Northern Journal of Applied Forestry*.no.27(4) 132-139

La Torre,T., Ileana, B., Devendra, M. Amatya, Ge, S., and Callahan, T. 2011. "Seasonal rainfall-runoff relationships in a lowland forested watershed in the southeastern USA." *Hydrological Processes* 25, no. 13: 2032-2045.

Lee, K. 2009. "Predicting Incoming Solar Radiation and Its Application to Radiation-Based Equation for Estimating Reference Evapotranspiration." *Journal of Irrigation & Drainage Engineering* 135, no. 5: 609-619.

Lenters J., Cutrell G., Istanbulluoglu, E., Scott D., Herrman, K., Irmak A., Eisenhauer, D. 2011. "Seasonal energy and water balance of a *phragmites australis*-dominated wetland in the Republican River basin of south-central Nebraska (USA)."*Journal of Hydrology.*408: 19-34

Lim, W., Roderick,M., Hobbins,M., Wong,S., Groeneveld,P., Sun,F., and Farquhar,G. 2012. "The aerodynamics of pan evaporation." *Agricultural & Forest Meteorology* 152, 31-43.

Lin, C., Lerch, R., Garrett, H., Jordan, D.,George,M. 2007. "Ability of forage grasses exposed to atrazine isofluxulate to reduce nutrient levels in soils and shallow graoundwater" *Communications in Soil Science and Plant Analysis,*38:1119-1136

Lin, C., Lerch, R., Garrett, H., George,M. 2008. "Bioremediation of atrazine-contaminated soil by forage grasses: Transformation, uptake and detoxification" *Journal of Environmental Quality.*37:196-206

Macdonald, J., MacIsaac,E., and Herunter,H. 2003. "The effect of variable-retention riparian buffer zones on water temperatures in small headwater streams in sub-boreal forest ecosystems of British Columbia." *Canadian Journal Of Forest Research* 33, no. 8: 1371-1382

MacDonald P., Frayer W. and Clauser J. 1979 “Documentation, chronology and future projections of bottomland hardwood habitat losses in the lower Mississippi alluvial plain. USFWS, Washington, DC, 427 pp.

Maes, W., Pashuysen,T., Trabucco,A., Veroustraete,F. and Muys,B. 2011. "Does energy dissipation increase with ecosystem succession? Testing the ecosystem exergy theory combining theoretical simulations and thermal remote sensing observations." *Ecological Modelling* 222, no. 23/24: 3917-3941

Marian,M., Tymkow,P., and Wezyk, P. 2009. "Identification of flow resistance coefficients in floodplain forests using terrestrial laser scanning ." *Studia Geotechnica Et Mechanica* 31, no. 1: 39-50.

Maroco, J., Ku,M., Lea,P, Dever,L., Leegood, R., Furbank,R., Edwards,G. 1998. “Oxygen requirements and inhibition of C_4 photosynthesis: An analysis of C_4 plants deficient in the C_3 and C_4 cycles.” *Plant Physiology.* no. 116 : 823-832.

Masoner, J., Stannard,D., Christenson, S. 2008. "Differences in Evaporation Between a Floating Pan and Class A Pan on Land." *Journal Of The American Water Resources Association* 44, no. 3: 552-561

Matteo, M., Randhir,B. 2006. “Watershed-Scale Impacts of Forest Buffers on Water Quality and Runoff in Urbanizing Environment.” Journal of Water Resources Planning and Management.Vol.132, No. 3. 144-152

McNaughton,K., Black, T. 1973. “A study of evapotranspiration from a douglas fir forest using the energy balance” *Water Resources Research.*Vol 9. No.6

Medeiros, P., Marcuzzo,F., Youlton,C. and Wendland,E. 2012. "Error Autocorrelation and Linear Regression for Temperature-Based Evapotranspiration Estimates Improvement1." *Journal Of The American Water Resources Association* 48, no. 2: 297-305.

Monteith, J. 1965. "Evaporation and the environment" *Symposium. Society of Experimental Biology*. 19: 205-234

Monteith, J. 1970. "Solar radiation and productivity in tropical ecosystems" *Opening paper read at IBP/UNESCO Meeting on Productivity of Tropical Ecosystems.* Makere University, Uganda

Morison,J., Piedade,M., Müller,E., Long,S., Junk,W. and Jones,M. 2000. "Very high productivity of the C4 aquatic grass Echinochloa polystachya in the Amazon floodplain confirmed by net ecosystem CO2 flux measurements." *Oecologia* 125, no. 3: 400-411.

Muerth, M., and Mauser, W. 2012. "Rigorous evaluation of a soil heat transfer model for mesoscale climate change impact studies." *Environmental Modelling & Software* 35, 149-162.

Naiman, J., Decamps, H. 1997. "The ecology of interfaces: Riparian zones" *Annu. Rev. Ecol. Syst.* 28: 621-658

Naiman, J., Bechtold,S., Beechie,T., Latterell,J., and Van Pelt,R. 2010. "A Process-Based View of Floodplain Forest Patterns in Coastal River Valleys of the Pacific Northwest." *Ecosystems* 13, no. 1: 1-31.

Navjot S., Sodhi, et al., "Flooding Policy Makers with Evidence to Save Forests." *AMBIO - A Journal Of The Human Environment* 38, no. 2 (March 2009): 125-126.

Neary, D., Ice G., and Jackson C. 2009. "Linkages between forest soils and water quality and quantity." *Forest Ecology & Management* 258, no. 10: 2269-2281.

Newbold, J., Herbert, S., Bernard, W., Sweeney, B., Kiry, P., and Alberts, S. 2010. "Water Quality Functions of a 15-Year-Old Riparian Forest Buffer System." *Journal Of The American Water Resources Association* 46, no. 2: 299-310.

Newell P., King, S., Kaller, M. 2009. "Foraging behavior of pileated woodpeckers in partial cut and uncut bottomland hardwood forest." *Forest Ecology and Management.* No. 258 : 1456-146

Nicotra, A., Cosgrove,M., Cowling,A., Schlichting,C., Jones,C. and Hikosaka, K. 2007. "Leaf shape linked to photosynthetic rates and temperature optima in South African Pelargonium species." *Oecologia* 154, no. 4: 625-635.

Nigh, T., Schroeder, W. 2002. "Atlas of Missouri ecological sections." *Missouri Department of Conservation.*

Nilsson, C., Svedmark, M. 2002. "Basic Principles and Ecological Consequences of Changing Water Regimes: Riparian Plant Communities." *Environmenal Management.* No. 4: 468-480

Noweg,T., Kurtz,W. 1987. " Eastern black walnut plantations: An economically viable option for conservation reserve lands in the corn belt" *Northern Jurtanl of applied Forestry.* No. 4: 158-160

Odhiambo, G. and Savage, M. 2009.” Sensible Heat Flux by Surface Layer Scintillometry and Eddy Covariance over a Mixed Grassland Community as Affected by Bowen Ration and MOST Formulations for Unstable conditions.” *American MeteorologicalSociety.*No 10:479-472

Ochsner,T., Horton,R. et al.,. (2001). "A New Perspective on Soil Thermal Properties." Soil Sci. Soc. Am. J. 65: 1641-1647.

Oswalt, S., and King,S. 2005. "Channelization and floodplain forests: Impacts of accelerated sedimentation and valley plug formation on floodplain forests of the Middle Fork Forked Deer River, Tennessee, USA [electronic resource]." *Forest Ecology And Management* 215, no. 1-3: 69-83.

Otles Z., Gutowski W. 2005. “Atmospheric Stability Effects on Penman-Monteith Evapotranspiration Estimates.”*Pure and Applied Geophysics.*No.162: 2239-2254

Pan, M., Sahoo, A., Troy, T., Vinukollu, R., Sheffield, J., and Wood, E. 2012. "Multisource Estimation of Long-Term Terrestrial Water Budget for Major Global River Basins." *Journal Of Climate* 25, no. 9: 3191-3206.

Pataki, D., Boone C., Hogue, T., Jenerette,G. , McFadden, J , Pincetl, S. 2011. “Ecohydrology Bearings- Invited Commentary Socio-ecohydrology and the urban water challenge.”*Ecohydrology.*No.4. 341-347

Penman, H.1948. “Natural evaporation from open water, bare soil and grass.” *Proceeds Royal Society London.* Series A, 193: 120-148

Peters-Lidard, C. 1998. "The Effect of Soil Thermal Conductivity Parameterization on Surface Energy Fluxes and Temperatures." Journal of the Atmospheric Sciences 55: 1209-1224

Pham,C., Yen,C., Cox,G., Garrett,H. 1978. "Slope position, soil-water storage capacity and black walnut root development." *Proc. Symp. Soil moisture…Site Productivity*. U.S. Dept. Agric. For. Serv., Southeastern area. Atlanta GA. Pp.326-335.

Planty-Tabacchi, A., Tabacchi, E., Decamps, H., Lambs, L., Guilloy, H., and Muller, E. 2000. "Impacts of riparian vegetation on hydrological processes." *Hydrological Processes* 14, no. 16/17: 2959.

Popham, T.and Baker, R. 1987. "Ocular and Densimeter Estimates of Understory Foliar Cover in Forests of Alabama*." Res. Note SO-334*. New Orleans, LA: U.S. Department of Agriculture, Forest Service, Southern Forest Experiment Station. 4 p..

Popovska,C., Jovanovski,M., Ivanoski, D., and Peševski, I. 2010. "Storm sewer system analysis in urban areas and flood risk assessment." *Mathematical Modeling In Civil Engineering* no. 4: 56-62.

Pouyat, R., Groffman P., Yesilonus I., Hernandez, L. 2002."Soil carbon pools and fluxes in urban ecosystems."*Environmental Pollution.*116.S107-S118, Supplement 1

Priestley,C., Taylor,R. 1972. "On the assessment of surface heat flux and evaporation using large-scale parameters" *Mon. Weather Rec.*100, 81-92

Puckett, L. 2004. "Hydrogeologic controls on the transport and fate of nitrate in ground water beneath riparian buffer zones: results from thirteen studies across the United States." *Water Science & Technology* 49, no. 3: 47-53.

Qiuhong,T., Taikan,O., Kanae,S. and Heping,H. 2007. "The Influence of Precipitation Variability and Partial Irrigation within Grid Cells on a Hydrological Simulation." *Journal Of Hydrometeorology* 8, no. 3: 499-512.

Ramsay, P., Martin,K., Reid, C., and Duckworth, J. 2006. "Taxonomic, morphological and structural surrogates for the rapid assessment of vegetation." *Journal Of Vegetation Science* 17, no. 6: 747-754

Rauner J. 1976. " Deciduous Forests." *Vegetation and the Atmosphere.*No.2:241-264

Reichold, L., Zechman, E., Brill,E, and Holmes,H. 2010. "Simulation-Optimization Framework to Support Sustainable Watershed Development by Mimicking the Predevelopment Flow Regime." *Journal Of Water Resources Planning & Management* 136, no. 3: 366-375.

Romano, S. 2010. "Our current understanding of the Upper Mississippi River System floodplain forest." *Hydrobiologia* 640, no. 1: 115-124.

Rosenberry D., Stannard, D., Winter,T., Martinez, M. 2004. "Comparison of 13 equations for determining evapotranspiration from a prairie wetland, Cottonwood lake area, North Dakota, USA."*Wetlands.* No. 3: 483-497

Rossi, L., Chèvre, N., Fankhauser,R., Margot,J., Curdy, R., Babut, M., and Barry, D. 2013. "Sediment contamination assessment in urban areas based on total suspended solids." *Water Research* 47, no. 1: 339-350

Ryu,Y., Verfaillie,J., Macfarlane,C., Kobayashi,H., Sonnentag,O., Vargas,R., Ma,S., and Baldocchi, D. 2012. "Continuous observation of tree leaf area index at ecosystem scale using upward-pointing digital cameras." *Remote Sensing Of Environment* 126, 116-125

Schenk, H., Jackson, R. 2002. "Rooting depths, lateral root spreads and below-ground/above-ground allometries of plants in water-limited ecosystems." *Journal Of Ecology* 90, no. 3: 480-494. *Academic Search Complete*, EBSCO*host*

Shuttleworth,W., Wallace, J. 1985. "Evaporation from sparse crops- an energy combination theory" *Quarterly Journal of the Royal Meteorological Society.* No. 111: 839-855

Scott, R., Cable,W., Huxman,T., Nagler,P., Hernandez,M., Goodrich,D. 2008. "Multiyear riparian evapotranspiration and groundwater use for a semiarid watershed." *Journal of Arid Environments.* 72. 1232-1246

Scott, R., Huxman, T., Williams,D., Goodrich,D. 2005 " Ecohydrological impacts of woody-plant encroachment : seasonal patterns of water and carbon dioxide exchange within a semiarid riparian environment." *Global Change Biology*.12, 311-324

Senay,G., Leake,S., Nagler,P., Artan,G., Dickinson,J., Cordova,J. and Glenn,E. 2011. "Estimating basin scale evapotranspiration (ET) by water balance and remote sensing methods." *Hydrological Processes* 25, no. 26: 4037-4049.

Šír, M., Čermák, J., Nadezhdina, N., Pražák,J. and Tesař,M. 2008. “Measuring and modeling forest transpiration” *IOP Conference Series: Earth and Environmental Science.* Vol. 4, No. 1

Smith,A. 2013. “Sidebar7.1: Billion-dollar weather and climate disasters: 2012 in context" *Bulletin Of The American Meteorological Society* S15

Song, I., Ik-Jae ,K., Dae, H., Myeong-Seop, B., Jae-Kwan, L., and Moon-Seong, K. 2012. "Prioritizing locations for the riparian establishment based on spatiotemporal change of riparian forest area at a watershed scale." *Paddy & Water Environment* 10, no. 1: 49-58.

Sprackling,J., Read,R. 1979. “tree root systems in eastern Nebraska.” *Nebraska Conservation Bulletin.*No.37

Stannard, D., Paul, W., Laws, R., and Poeter, E. 2010. "Consumptive use and resulting leach-field water budget of a mountain residence." *Journal Of Hydrology* 388, no. 3/4: 335-349.

Stanturf, J., Schoenholtz, S., Schweitzer, C., Shepard, J. 2001. “Achieving restoration success : Myths in bottomland hardwood forests” *Society for Ecological Restoration.* Vol 9. No.2 : 189-200

Stella, J., Hayden,M., Battles,J., Piégay,H., Dufour,S. and Fremier,A. 2011. "The Role of Abandoned Channels as Refugia for Sustaining Pioneer Riparian Forest Ecosystems." *Ecosystems* 14, no. 5: 776-790.

Steppe, K., & Lemeur, R. 2007. "Effects of ring-porous and diffuse-porous stem wood anatomy on the hydraulic parameters used in a water flow and storage model." *Tree Physiology* 27, no. 1: 43-52

Steyermark, J. 1963. *Flora of Missouri*.15th edition. Ames, Iowa: Iowa State University Press

Stone, E., Kalisz,P. 1991. "On the maximum extent of Tree Roots." *Forest Ecology and Management.* No.46: 59-102

Suyker, A., and Verma, S. 2001. "Year-round observations of the net ecosystem exchange of carbon dioxide in a native tallgrass prairie." *Global Change Biology* 7, no. 3: 279-289.

Sweeney B., Bott T., Jackson J., Kaplan L., Newbold, D., Standley, L., Hession, W., Horwitz, R. 2004. "Riparian deforestation, stream narrowing, and loss of ecosystem services." Proceedings of the National Academy of Sciences of the United States of America.Vol.101 no.39 14132-14137

Sypka,P., Starzak,R. 2013. "Simplified, empirical model of wind speed profile under canopy of Istebna spruce stand in mountain valley." *Agricultural & Forest Meteorology* 171-172, 220-233

Tabacchi,E., Lambs,L., Guilloy,H., Planty-Tabacchi,A., Muller,E., Decamps, H. 2000. "Impacts of riparian vegetation on hydrological processes."*Hydrologic Processes* 14, 2959-2976

Taiz,L., Zeiger,E. 2006. Plant Physiology fourth Edition.*Sinauer associates ,Inc.* Sunderland,MA 01375 U.S.A. pp 68-69, 173-178.

Temesgen,B., Eching, S., and Frame,K. 2007. "Comparing Net Radiation Estimation Methods: CIMIS versus Penman–Monteith." *Journal Of Irrigation & Drainage Engineering* 133, no. 3: 265-271.

Thomas,H. and Nisbet,T. 2007.” An assessment of the impact of floodplain woodland on flood flows.” *Water and Environment Journal*, 1747-6585

Thom,R. and Wilson, J. 1980 “ The Natural Division of Missouri” Transactions *Missouri Academy of Sciences* 14:1-23

Thompson,T. and Madden,G.2003. “ A guide to nut tree culture in North America” *Northern Nut Growers Association.* No.1 : 395

Tillinghast,E., Hunt,W. and Jennings,G. 2011. "Stormwater control measure (SCM) design standards to limit stream erosion for Piedmont North Carolina." *Journal Of Hydrology* 411, no. 3/4: 185-196.

Twedt,D., Uihlein,W., Elliott,A. 2006. "A Spatially Explicit Decision Support Model for Restoration of Forest Bird Habitat." *Conservation Biology* 20, no. 1: 100-110.

Twine,T., Kucharik,C. and Foley,J. 2004. "Effects of Land Cover Change on the Energy and Water Balance of the Mississippi River Basin." *Journal of Hydrometeorology* 5, no. 4: 640-655.

Tyree,M., Sperry,J. 1988 “Do plants operate near the Point of Catastrophic Xylem Dysfunction Caused by Dynamic Water Stress? Answers From a Model” *Plant Physiology* Volume 88, 574-580.

Ullah,S., Breitenbeck, G. and Faulkner, S. 2005. “Denitrification and N_2O emission from forested and cultivated alluvial soil.” *Biogeochemistry* .No. 73: 499-513

U.S. Census. 2011. United States Census Bureau: Missouri 2010 census. http://2010.census.gov/news/releases/operations/cb11-cn49.html

USDA NRCS.2012. Web Soil Series. Accessed January 22, 2012 https://soilseries.sc.egov.usda.gov/OSD_Docs/H/HAYMOND.html

Vidon,P., Allan,C., Burns,D., Duval,T., Gurwick,N., Inamdar,S., Lowrance, R., Okay, J., Scott, D. and Sebestyen,S. 2010. "Hot Spots and Hot Moments in Riparian Zones: Potential for Improved Water Quality Management."

Vitasse,Y., Porté,A., Kremer,A., Michalet,R., and Delzon,S. 2009. "Responses of canopy duration to temperature changes in four temperate tree species: relative contributions of spring and autumn leaf phenology." *Oecologia* 161, no. 1: 187-1989

Volpi,E., Di Lazzaro,M., and Fiori,A. 2012. "A simplified framework for assessing the impact of rainfall spatial variability on the hydrologic response." *Advances In Water Resources* 46, 1-10.

Wagner,P., Fiener,P., Wilken,F., Kumar,S., and Schneider, K. 2012. "Comparison and evaluation of spatial interpolation schemes for daily rainfall in data scarce regions." *Journal Of Hydrology* 464-465, 388-400.

Wang, J., Endreny,T., and Nowak,D. 2008. "Mechanistic Simulation of Tree Effects in an Urban Water Balance Model." *Journal Of The American Water Resources Association* 44, no. 1: 75-85.

Wang,W. 2012. "An Analytical Model for Mean Wind Profiles in Sparse Canopies." *Boundary-Layer Meteorology* 142, no. 3: 383-399

Warring,R. and Running,S. 1978. “Sapwood water storage: its contribution to transpiration and effect upon the water conductance through the stems of old-growth Douglas-fir.” *Plant, Cell and Environment* 1, 131-140.

Weber,S., Graf,A. and Heusinkveld,B. 2007. "Accuracy of soil heat flux plate measurements in coarse substrates – Field measurements versus a laboratory test." *Theoretical & Applied Climatology* 89, no. 1/2: 109-114.

Wilcox,B., Huang,Y. and Walker, J. 2008. "Long-term trends in streamflow from semiarid rangelands: uncovering drivers of change." *Global Change Biology* 14, no. 7: 1676-1689

Wine, M., and Zou, C. 2012. "Long-term streamflow relations with riparian gallery forest expansion into tallgrass prairie in the Southern Great Plains, USA." *Forest Ecology & Management* 266, 170-179

Wipfli, M. 2005. "Trophic linkages between headwater forests and downstream fish habitats: implications for forest and fish management." *Landscape & Urban Planning* 72, no. 1-3: 205-213.

Wohl, E., Polvi, L., Cadol, D. 2010. “Wood distribution along streams draining old-growth floodplain forests in Congaree National Park, South Carolina, USA.” *Geomorphology* 126: 108-120

Woodrow, I., Ball,T. and Berry,J. 1990. "Control of photosynthetic carbon dioxide fixation by the boundary layer, stomata and ribulose 1,5-biphosphate carboxylase/oxygenase." *Plant, Cell & Environment* 13, no. 4: 339-347

Xiao-Bing, L., Yun-Hao,C., Hua,Y., and Yun-Xia,Z. 2005. "Improvement, Comparison, and Application of Field Measurement Methods for Grassland Vegetation Fractional Coverage." *Journal Of Integrative Plant Biology* 47, no. 9: 1074-1083

Xixi,W., Melesse,A., McClain,M., and Wanhong,Y. 2007. "Water quality changes as a result of coalbed methane development in a rocky mountain watershed." *Journal Of The American Water Resources Association* 43, no. 6: 1383-1399.

Yang, B., Pallardy,S., Meyers,P., Gu, L., Hanson, P., Wullschleger,S., Huer, M., Hosman,K., Riggs,J., Sluss,D. 2010. "Environmental controls on water use efficiency during severe drought in an Ozark Forest in Missouri, USA." *Global Change Biology* 16, no. 8: 2252-2271.

Yeh, P. and Famiglietti,J. 2009. "Regional Groundwater Evapotranspiration in Illinois." *Journal of Hydrometeorology* 10, no. 2: 464-478.

Young, F., Radatz, C., Marshall, C. 2001. Soil survey for Boone County, Missouri In *NRCS, Washington, DC.*

Yu, K., Faulkner, S. and Baldwin, M. 2008. "Effect of hydrological conditions on nitrous oxide, methane, and carbon dioxide dynamics in a bottomland hardwood forest and its implication for soil carbon sequestration." *Global Change Biology.* No. 14: 798-812

Zhang,Y., Shen,Y., Sun, H., Gates J. 2011." Evapotranspiration and its partitioning in an irrigated winter wheat field: A combined isotopic and micrometeorologic approach."*Journal of Hydrology.* 408: 203-211.

Zhu,J., Young, M., Healy, J., Jasoni,R., Osterberg,J. 2011. “Interference of river level changes on riparian zone evapotranspiration estimates from diurnal groundwater fluctuations.” *Journal of Hydrology.*403: 381-389

APPENDIX A:

Monthly Hinkson Creek Floodplain Evapotranspiration Totals, WY 2012

Hinkson Creek Floodplain Grassland site Columbia, Missouri

Monthly Evapotranspiration mm										
	SEB(BHF)	P-M(BHF)	P-T(BHF)	Easy P-M(BHF)	McN-B(BHF)	Bowen(BHF)	S-W(BHF)	San Ref ET	Baskett ET	Pan Evap
Oct-11	63.2	41.2	79.6	6.1	100.0	243.1	22.3	82.5	38.3	-
Nov-11	17.8	18.8	26.8	1.1	127.7	55.4	36.2	42.2	20.8	-
Dec-11	8.4	10.7	18.5	0.5	71.4	-12.2	31.1	27.3	16.9	-
Jan-12	-10.2	23.1	30.8	0.7	95.2	65.1	53.4	36.7	11.6	-
Feb-12	44.4	32.3	42.7	0.7	102.3	79.5	70.3	45.9	19.0	-
Mar-12	147.3	66.2	85.1	2.3	166.3	123.3	99.4	90.7	49.6	-
Apr-12	89.7	68.5	95.8	28.0	27.4	121.9	53.8	96.0	101.0	119.6
May-12	142.5	110.9	156.4	73.8	7.3	208.3	63.7	150.8	194.2	188.2
Jun-12	152.8	128.8	172.2	118.7	11.7	202.6	19.2	177.7	149.0	221.5
Jul-12	294.3	258.7	345.9	279.5	27.6	390.7	25.7	360.7	224.2	242.6
Aug-12	105.7	102.7	137.1	142.7	14.1	154.2	1.2	146.3	52.3	189.7
Sep-12	71.3	69.5	94.4	57.9	5.7	159.6	0.8	97.3	72.4	102.9
Total	1064.0	890.2	1205.6	705.9	656.8	1548.4	454.5	1271.6	910.9	N/A

Hinkson Creek floodplain forest site Columbia, Missouri

Monthly Evapotranspiration mm										
	SEB(AG)	P-M(AG)	P-T(AG)	Easy P-M(AG)	McN-B(AG)	Bowen(AG)	S-W(AG)	San Ref ET	Baskett ET	Pan Evap
Oct-11	43.5	67.8	72.6	30.2	17.5	71.5	17.1	82.5	38.3	-
Nov-11	-12.0	-136.2	21.4	7.8	18.3	16.6	34.9	42.2	20.8	-
Dec-11	-15.4	-1.6	15.0	1.9	21.0	40.9	50.9	27.3	16.9	-
Jan-12	5.3	-0.4	25.3	1.5	45.2	39.9	61.5	36.7	11.6	-
Feb-12	24.0	-0.5	37.2	1.7	46.3	42.2	80.9	45.9	19.0	-
Mar-12	49.0	-29.3	72.5	7.6	54.8	82.5	190.2	90.7	49.6	-
Apr-12	71.0	119.9	86.2	28.4	12.9	317.3	154.6	96.0	101.0	119.6
May-12	128.9	154.7	150.7	62.0	14.0	147.9	90.3	150.8	194.2	188.2
Jun-12	138.6	164.3	164.6	95.5	21.5	155.8	13.8	177.7	149.0	221.5
Jul-12	268.8	324.2	332.9	228.8	51.6	291.5	23.4	360.7	224.2	242.6
Aug-12	94.7	126.3	130.6	104.5	23.6	119.4	5.7	146.3	52.3	189.7
Sep-12	61.8	94.2	89.1	44.3	10.0	44.0	12.7	97.3	72.4	102.9
Total	814.8	815.4	1125.5	584.0	319.0	1297.9	718.9	1271.6	910.9	N/A

Species Lists From BHF and AG Vegetation Surveys

species	family	monocot	native	woody	graminoid	fabaceae	Asteraceae	BHF %Co
Acer Negundo (Boxelder)	Aceraceae	dicot	1	1	0	0	0	0.15
Ammannia Coccinea (Scarlet Toothcup)	Lythraceae	dicot	1	1	0	0	0	0.10
Amphicarpaea Bracteata (American hogpeanut)	Fabaceae	dicot	1	0	0	1	0	8.56
Bidens Bipinnata (Spanish needles)	asteraceae	dicot	1	0	0	0	1	0.06
Boehmeria Cylindrica (Smallspike false nettle)	Urticaceae	dicot	1	0	0	0	0	0.25
Carex Frankii or Carex Spp.	Cyperaceae	monocot	1	0	1	0	0	0.01
Dioscorea Villosa (Wild yam)	Dioscoraceae	monocot	1	0	0	0	0	0.10
Elymus Viginicus (Wild rye)	Poaceae	monocot	1	0	1	0	0	14.11
Euonymus Fortunei (Winter creeper)	Celestraceae	dicot	0	0	0	0	0	0.08
Glechoma Hederacea (Ground ivy)	Lamiaceae	dicot	0	0	0	0	0	31.61
Humulus Japonicus (Japanese hop)	Canabaceae	dicot	0	0	0	0	0	1.78
Impatiens Capensis (Jewelweed)	Balsaminaceae	dicot	1	0	0	0	0	2.85
Lycopus Spp. (Bugle weed)	Lamiaceae	dicot	1	0	0	0	0	0.08
Parthenocissus Quinquefolia (Virginia creeper)	Vitaceae	dicot	1	1	0	0	0	0.35
Pilea Pumila (Clear weed)	Urticaceae	dicot	1	0	0	0	0	3.03
Platanus Occidentalis (American sycamore)	Platanaceae	dicot	1	1	0	0	0	0.03
Poa spp.	Poaceae	monocot	0	0	1	0	0	0.83
Polygonum Hydropiperoides (Swamp smartweed)	Polygonaceae	dicot	1	0	0	0	0	5.34
Polygonum Virginianum (Jumpseed)	Polygonaceae	dicot	1	0	0	0	0	1.42
Quercus Rubra (Red oak)	Fagaceae	dicot	1	1	0	0	0	0.03
Rudbeckia Laciniata (Cutleaf coneflower)	Asteraceae	dicot	1	0	0	0	1	1.81
Smilax Spp. (Green briar)	Smilaceae	monocot	1	0	0	0	0	0.14
Symphyotrichum Cordifolium (Blue Wood Aster)	Asteraceae	dicot	1	0	0	0	1	0.03
Urtica Dioica (Stinging nettle)	Urticaceae	dicot	1	0	0	0	0	35.17
Verbesina Alternifolia (Yellow ironweed)	Asteraceae	dicot	1	0	0	0	1	3.69

species	family		native	woody	graminoid	fabaceae	Asteraceae	Ag%of veg
Ambrosia Trifida (Giant ragweed)	asteraceae	dicot	1	0	0	0	1	0.6
Asclepias (Milkweed)	Asclepiadaceae	dicot	1	0	0	0	0	0.2
Calystegia Silvatica (Shortstalk false bindweed)	Convulvaceae	dicot	1	0	0	0	0	0.3
Carex Frankii or Carex Spp.	Cyperaceae	monocot	1	0	1	0	0	5.0
Cirsium Vulgare (Bull Thistle)-	asteraceae	dicot	0	0	0	0	1	0.6
Desmodium Paniculatum (Tick Trefoil)	Fabaceae	dicot	1	0	0	1	0	0.6
Elymus Viginicus (Wild rye)	Poaceae	monocot	1	0	1	0	0	0.1
Festuca Arundinacea (Tall fescue)	Poaceae	monocot	0	0	1	0	0	21.1
Glechoma Hederacea (Ground ivy)	Lamiaceae	dicot	0	0	0	0	0	12.8
Humulus Japonicus (Japanese hop)	Canabaceae	dicot	0	0	0	0	0	11.4
Juncus Spp. (2)	Juncaceae	monocot	1	0	1	0	0	1.2
Koeleria Macrantha (June grass)	Poaceae	monocot	1	0	0	0	0	15.7
Lactuca Spp.	Asteraceae	dicot	1	0	0	0	1	0.1
Lotus Corniculatus (Bird's-foot Trefoil)	Fabaceae	dicot	0	0	0	1	0	0.9
Muhlenbergia Spp. (Muhly spp.)	Poaceae	monocot	1	0	1	0	0	0.2
Phalaris Arundinacea (Reed canary)	Poaceae	monocot	1	0	1	0	0	1.1
Phleum Pratense(Timothy)	Poaceae	monocot	0	0	0	0	0	1.5
Physalis Virginiana (Ground Cherry)	Solanaceeae	dicot	1	0	0	0	0	0.3
Rudbeckia Laciniata (Cutleaf coneflower)	Asteraceae	dicot	1	0	0	0	1	3.6
Rumex Crispus (Curly dock)	Polygonaceae	dicot	0	0	0	0	0	0.2
Solanum Carolinense (Horse nettle)	Solanaceeae	dicot	1	0	0	0	0	0.7
Solidago Altissima (Missouri goldenrod)	Asteraceae	dicot	1	0	0	0	1	7.9
Solidago Gigantea (Giant goldenrod)	Asteraceae	dicot	1	0	0	0	1	1.5
Sorghum Halepense (Johnson grass)	Poaceae	monocot	0	0	1	0	0	13.5
Teucrium Canadense (American Germander)	Lamiaceae	dicot	1	0	0	0	0	0.1
Trifolium (Ground clover)	Fabaceae	dicot	0	0	0	1	0	0.0
Verbesina Alternifolia (Yellow ironweed)	Asteraceae	dicot	1	0	0	0	1	1.3
Verbesina Altissima (Ironweed)	Asteraceae	dicot	1	0	0	0	1	0.3
Vicia Dasycarpa (Smooth vetch)	Fabaceae	dicot	0	0	0	1	0	0.0
Vitis Spp. (Wild Grape)	Vitaceae	dicot	1	1	0	0	0	0.0

Bottomland Hardwood Forest Stand Inventory

plot	tree #	plot tree	species	DBH(in)	DBH (cm)	height (m)	merch (m)
1	1	1	American elm	30.8	78.2	27.8	10
1	2	2	Eastern cottonwood	47.2	119.9	40.1	10.5
1	3	3	Silver maple	24	61.0	18.3	10.6
1	4	4	Black walnut	14.5	36.8	26.8	9.1
1	5	5	Silver maple	13.8	35.1	16.1	8.5
1	6	6	Eastern cottonwood	62.3	158.2	39.8	9.3
1	7	7	Silver maple	27.4	69.6	15.3	3
1	8	8	Black walnut	16.4	41.7	21.3	8.1
2	9	1	Black walnut	28.5	72.4	35.5	11.7
2	10	2	Boxelder	15.5	39.4	20	5.1
2	11	3	American elm	13.2	33.5	18	2.9
2	12	5	Boxelder	25.1	63.8	23.7	4.5
2	13	6	Silver maple	22.3	56.6	15.1	3.5
2	14	7	Eastern cottonwood	40.4	102.6	38.8	16.5
2	15	8	Black walnut	17.8	45.2	26.6	10.7
2	16	9	American elm	7.2	18.3	11.5	1.5
3	17	1	Boxelder	25	63.5	7.4	1.2
3	18	2	Boxelder	24.7	62.7	13.1	2.6
3	19	3	Boxelder	13.9	35.3	9.1	1.3
3	20	4	Silver maple	24.2	61.5	13.7	5.6
3	21	5	Boxelder	9.5	24.1	8.3	1.7
3	22	6	American elm	13	33.0	18.9	6.4
3	23	7	Eastern cottonwood	29	73.7	35.6	11.1
3	24	8	Silver maple	31	78.7	8.6	4.1
3	25	9	Eastern cottonwood	37.3	94.7	37.3	16.4
3	26	10	Boxelder	14.7	37.3	12.2	2.1
3	27	11	Eastern cottonwood	50.5	128.3	40.7	16.5
3	28	12	Eastern cottonwood	42	106.7	42.1	12.4
3	29	13	Silver maple	20	50.8	19.3	7
4	30	1	Eastern cottonwood	47.2	119.9	40.1	10.5
4	31	2	Black walnut	14.7	37.3	31.8	10
4	32	3	Eastern cottonwood	32.3	82.0	40.9	23.7
4	33	4	Boxelder	13.2	33.5	16.6	2.4
4	34	5	Eastern cottonwood	42.2	107.2	37.6	12.4
4	35	6	Eastern cottonwood	41.8	106.2	30.5	20.2
4	36	7	Eastern cottonwood	42.9	109.0	43.4	7.7

4	37	8	Black walnut	17.1	43.4	29.4	9.3
4	38	9	Eastern cottonwood	32.8	83.3	34.2	19.4
4	39	10	Silver maple	24.2	61.5	30.4	9.3
4	40	11	Silver maple	12.7	32.3	21.1	4.9
4	41	12	Boxelder	11.1	28.2	23.1	6.3
4	42	13	Silver maple	9.8	24.9	4.3	3.5
5	43	2	Silver maple	17.8	45.2	25.2	8
5	44	4	Eastern cottonwood	33.9	86.1	37.5	16.4
5	45	5	Silver maple	16.1	40.9	23.3	5.7
5	46	6	Silver maple	18.2	46.2	30.8	9.9
5	47	8	Silver maple	34.1	86.6	37.8	9.9
5	48	9	Boxelder	16.8	42.7	21	2.2
5	49	10	Eastern cottonwood	37.9	96.3	41.7	12.3
5	50	11	Eastern cottonwood	42.8	108.7	36.2	8.6
5	51	12	Silver maple	14.3	36.3	27.8	8.9
5	52	13	Eastern cottonwood	43.8	111.3	41.9	10.4
5	53	14	Black walnut	22.3	56.6	38.9	14.5
6	54	4	Boxelder	4.9	12.4	3.9	1
6	55	5	Boxelder	12.8	32.5	17	5.7
6	56	7	Eastern cottonwood	28.5	72.4	42.2	21.2
6	57	8	Eastern cottonwood	32.1	81.5	39.4	18.7
6	58	9	Eastern cottonwood	38.5	97.8	41.9	9.8
6	59	10	Sycamore	38.6	98.0	38.1	10.8
6	60	11	Silver maple	23.2	58.9	43.2	9.9
6	61	12	Silver maple	27.1	68.8	30.7	13.5
6	62	13	Black walnut	14.6	37.1	22.5	9.3
6	63	14	Silver maple	24	61.0	25.3	9.3
6	64	15	Silver maple	32.8	83.3	39	14.3
7	65	1	Silver maple	32.4	82.3	41.7	15.8
7	66	2	Boxelder	32.1	81.5	19.1	8.9
7	67	3	Silver maple	18.6	47.2	26.8	8.1
7	68	4	Silver maple	28.1	71.4	40.3	14.7
7	69	5	Silver maple	36.1	91.7	36.3	17.6
7	70	6	Silver maple	14.1	35.8	32.7	15.7
7	71	7	Silver maple	18.8	47.8	20.6	11.2
7	72	8	Silver maple	21.2	53.8	28.2	9.9
7	73	9	SYcamore	26.3	66.8	39.8	17.8
8	74	1	American elm	11.1	28.2	24	7
8	75	2	American elm	10.5	26.7	19.6	5.8
8	76	3	Silver maple	25.3	64.3	36.1	7.4

8	77	4	Silver maple	32.5	82.6	39.9	10.9
8	78	5	American elm	10.7	27.2	16.6	4.3
8	79	7	Silver maple	17.1	43.4	13.7	3.6
8	80	8	Silver maple	30.9	78.5	35.7	19.4
8	81	9	Sycamore	42.6	108.2	49.3	19.4
8	82	10	Silver maple	26.1	66.3	31	8.3
8	83	11	American elm	11.7	29.7	21.3	7.5
8	84	12	Silver maple	34.9	88.6	33.4	7.5
8	85	13	Silver maple	35.1	89.2	36.8	10.9
8	86	14	Sycamore	23	58.4	30.3	21.7
8	87	15	Sycamore	23.3	59.2	36.1	20.1
9	88	2	Silver maple	35.5	90.2	44.4	9.9
9	89	3	Boxelder	6.8	17.3	7.3	1.4
9	90	4	Boxelder	10.4	26.4	20.7	6.5
9	91	5	Silver maple	25.4	64.5	33	10
9	92	7	Silver maple	23.6	59.9	43.4	12.9
9	93	8	Silver maple	13.9	35.3	21.6	8.4
9	94	9	Boxelder	6	15.2	6.2	1
9	95	10	Silver maple	22.2	56.4	14.9	7.7
9	96	11	Silver maple	31.1	79.0	30.72	8.64
9	97	12	Boxelder	5	12.7	7.4	4.8
9	98	13	Silver maple	26.7	67.8	41.2	14.3
9	99	14	Silver maple	26.7	67.8	41.2	14.3